

REPUBLIQUE ALGERIENNE DEMOCRATIQUE ET POPULAIRE  
MINISTRE DE L'ENSEIGNEMENT SUPERIEUR ET DE LA RECHERCHE

UNIVERSITE FERHAT ABBAS, SETIF  
FACULTE DES SCIENCES DE L'INGENIEUR  
DEPARTEMENT DE "GENIE DES PROCEDES"



## THESE

Présentée pour l'obtention du diplôme de

### DOCTORAT D'ETAT

Option : Génie des polymères

Par

**Abdelmalek DOUIBI**

*Thème:*

***"EXTRUSION OF FOAMED PVC:***

***EFFECTS OF A COMBINATION OF TWO CHEMICAL BLOWING  
AGENTS (ABFA AND SBC) ON RHEOLOGICAL, MECHANICAL  
AND MORPHOLOGICAL PROPERTIES"***

Soutenue le 11/04/2007

Devant le Jury :

Président	Pr. N. HADDAOUI	Professeur	Université Ferhat ABBAS, SETIF
Rapporteur	Pr. D. BENACHOUR	Professeur	Université Ferhat ABBAS, SETIF
Examineurs	Pr. B. DJELLOULI	Professeur	Université Ferhat ABBAS, SETIF
	Dr. A. LALLAM	M.C.	Université H. A., MULHOUSE
	Dr. H. DJIDJELLI	M.C.	Université A. M., BEJAIA

## DEDICATION

*I would like to dedicate this thesis to:*

- *The memory of my dear father;*
- *My dear mother who has supported me all the way since the beginning of my studies ;*
- *My wife who has been of a great motivation and inspiration and for the countless ways she ensured that I finished this study this year;*
- *My sons HAMDOUN, TEKTOUK, TAROU and especially ICHOU;*
- *All my brothers and sisters;*
- *My best friends HAMMOUDI, ABDELHAK, FARID, SAID, AZEDINNE, NORI, HAKIM, YACINE, FAKHRI, TAHAR and MONCEF; there are many friends and other family members who need to be listed for their part in this thesis.*

*Finally, this thesis is dedicated to all those who believe in the richness of learning*

## ACKNOWLEDGEMENTS

*I would like to express my gratitude and my deep appreciation to my supervisor Pr. D. BENACHOUR for his constructive and scientific guidance, kindness, helpful suggestions and criticisms given during the course of this study. I am much indebted to him for helping me formulate these ideas. Without his generous, careful supervision over so many years (including those of my master thesis), continued belief in my ability, and friendship, this thesis would not have been completed. He is my inspiration for what academic life should be about.*

*I am also grateful to polymer engineering department staff who helped me to carry out the experimental work as well as my best friends for their help and encouragement.*

*I would like also to thank the president and all the members of the jury who accepted to evaluate this work.*

## **ABSTRACT**

The present study deals with the behavior of two chemical blowing agents (BA) in a rigid Poly (Vinyl Chloride) (PVC) compound under processing conditions.

The first part of the work discusses the effect of the addition of a combination of two chemical BA; AzoBisFormAmide (ABFA) and/or Sodium BiCarbonate (SBC), on the processability of rigid PVC compound, using a Brabender torque rheometer. This apparatus simulates the conditions of temperature and shear that occur during processing. This technique was previously used under conditions bearing no relation to real polymer processing. Our contribution is to overcome this problem and to provide a complimentary comprehension. It was found that addition of BA separately, leads to the appearance of a new peak following that of the fusion (fluxing) one on the Brabender torque rheometer process curve. On the other hand, two distinct peaks were shown when both BA are added together. These peaks correspond to the decomposition of the BA and the expansion of the resulting cells. From this study, the Brabender torque rheometer has proven to be a valuable new technique to follow the stages of decomposition of the BA and the cell expansion within an environmental polymeric resin under real processing conditions.

The second part of the work deals with the effect of the addition of a combination of two chemical BA; ABFA and SBC, on the foaming efficiency of rigid PVC compound using a laboratory scale extruder. It was found that foaming efficiency increased with BA loading to an optimum value, which is characterized by a critical concentration (CC) of BA. This CC was noticed to be higher in the case of SBC compared to that of ABFA. On the other hand, the foaming efficiency showed a synergistic effect according to some mixing ratios of two BA (70% ABFA). These mixing ratios were based on the CC of each BA.

## TABLE OF CONTENTS

<b><u>Contents</u></b>	<b><u>Pages</u></b>
<b>Dedication</b> .....	i
<b>Acknowledgements</b> .....	ii
<b>Abstract</b> .....	iii
<b>Table of contents</b> .....	iv
<b>List of Tables</b> .....	v
<b>List of Figures</b> .....	x
<b>INTRODUCTION</b> .....	1
<b>CHAPTER I: THEORITICAL BACKGROUND</b>	
I.1. Poly (vinyl chloride) .....	3
I.2. Compounding P.V.C ingredients.....	3
I.2.1. Stabilizers.....	3
I.2.2. Lubricants.....	3
I.3. Additives used in the expansion processes.....	4
I.3.1. Physical blowing agents.....	4
I.3.2. Chemical blowing agents.....	4
I.3.2.1. Inorganic blowing agents.....	5
I.3.2.1.1. Sodium bicarbonate (SBC).....	5
I.3.2.2. Organic blowing agents.....	6
I.3.2.2.1. Azobisformamide (ABFA).....	7
I.3.2.3. Chemical blowing agent activators .....	9
I.3.3. Methods of incorporation.....	10
I.3.3.1. Evaluation of blowing agent efficiency.....	11
I.4. Foaming and expansion process.....	11
I.4.1. Expansion stages.....	11
I.4.1.1 Initiation of cell nucleation.....	12
I.4.1.2. Growth or expansion of cells.....	12
I.4.1.3. Stabilization of cells.....	12

I.4.2. Cell structure.....	13
I.4.3.2. Die.....	13
I.4.3.2. Sizing die (calibrator).....	14
I.4.4. Techniques for foam extrusion.....	14
I.4.4.1. Free foaming extrusion (F.F.E).....	14
I.4.4.2. Controlled foaming extrusion (C.F.E).....	14
<b>CHAPTER II: ADVANCES IN DEVELOPMENT OF EXTRUSION OF FOAMED RIGID PVC</b>	
II.1. Formulation of foamed rigid PVC.....	16
II.2. Techniques used for evaluation of chemical blowing agents.....	16
II.3. Expansion with a combined use of chemical blowing agents.....	18
<b>CHAPTER III: EXPERIMENTAL</b>	
III.1 Raw material.....	23
III.1.1. Poly (Vinyl Chloride).....	23
III.1.2 Thermal stabilizer (Kickers).....	23
III.1.3 Lubricants.....	23
III.1.3.1 Internal lubricant.....	23
III.1.3.2 External lubricant.....	23
III.1.4 Chemical blowing (BA) agents.....	23
III.1.4.1 Azobisformamide (ABFA).....	23
III.1.4.2 Sodium bicarbonate (SBC).....	24
III.2 Formulation and mixing.....	24
III.2.1 Formulation .....	24
III.2.2 Mixing step.....	25
III.3 Tests.....	25
III.3.1 Brabender Study.....	25
III.3.2 Specific gravity.....	25
III.3.3 Foaming efficiency (extrusion).....	26
III.3.4 Micrography.....	26
III.3.4.1 Optical Microscope.....	26
III.3.4.2 Liquid nitrogen break.....	26
III.3.4.3 Microtoming.....	26
III.3.5 Mechanical tests.....	26

III.3.5.1 Tensile tests.....	27
III.3.5.1 Tensile tests.....	27
III.3.5.2 Impact tests.....	28
III.3.5.3 Hardness tests.....	28
III.3.5 Thermal tests (DSC).....	28
<b>CHAPTER IV: PROCESSABILITY OF FOAMED RIGID PVC USING BRABENDER</b>	
IV. 1. Introduction.....	29
IV.2 Processability on foamed rigid PVC.....	30
IV.2.1 Effect of the addition of ABFA on the plastograph of rigid PVC.....	30
IV.2.2 Effect of ABFA concentration on the rigid PVC plastograph.....	33
IV.2.3 Effect of the addition of SBC on the plastograph of rigid PVC.....	37
IV.2.4 Effect of SBC concentration on the rigid PVC plastograph. ....	39
IV.2.5 Effect of a mixture of ABFA and SBC on the rigid PVC plastograph.....	42
IV.2.6 Effect of a concentration of BA mixture on the rigid PVC plastograph.....	45
IV.3. Differential Scanning Calorimetry (DSC).....	49
IV-3-1. DSC thermograms of ABFA.....	49
IV-3-2. DSC thermograms of SBC.....	48
IV-3-3. DSC thermograms of the mixture (ABFA+SBC).....	51
<b>CHAPTER V: RHEOLOGICAL, MECHANICAL AND MORPHOLOGICAL PROPERTIES</b>	
V.1 Rheological and morphological properties (using BA separately).....	53
V.1.1 Extent of expansion.....	53
V.1.1.1 Variation of the extrudate diameter with ABFA concentration.....	53
V.1.1.2 Variation of extent of expansion with ABFA concentration.....	57
V.1.1.3 Variation of the extrudate diameter with SBC concentration.....	59
V.1.1.4 Variation of the percentage expansion with SBC concentration.....	61

V.1.1.5 Comparison between ABFA and SBC.....	61
V.2. Mechanical properties (using BA separately).....	63
V.2.1 Tensile properties.....	63
V.2.1.1- Variation of elastic modulus.....	63
V.2.1.2 Variation of tensile stress at break.....	65
V.2.1.3 Variation of strain at break.....	68
V.2.1.4 Variation of energy at rupture.....	70
V.2.2 Variation of unnotched Izod impact.....	72
V.2.3 Variation of hardness.....	74
V.3. Rheological and morphological properties (using a mixture of BA) .....	77
V.3.1 Extent of expansion.....	78
V.3.1.1 Variation of the extrudate diameter with ABFA percentage within a mixture of BA.. .....	78
V.3.1.2 Variation of the percentage expansion.....	79
V.4. Mechanical properties (using a mixture of BA).....	83
V.4.1 Tensile properties.....	83
V.4.1.1- Variation of elastic modulus.....	83
V.4.1.2 Variation of tensile stress at break.....	84
V.4.1.3 Variation of strain at break.....	84
V.4.1.4 Variation of energy at rupture.....	84
V.4.2 Variation of unnotched Izod impact .....	85
V.4.3 Variation of Hardness.....	85
<b>General Conclusions .....</b>	<b>89</b>
<b>Recommendations .....</b>	<b>90</b>
<b>References .....</b>	<b>91</b>



## **List of Tables**

<b><u>Title</u></b>	<b><u>Pages</u></b>
Table I.1: Functional groups of organic foaming agents.....	6
Table I.2: Properties of commercial available BA.....	7
Table III.1: Formulations.....	25
Table III.2: Temperature profile.....	27
Table V.1: Extent of expansion (diameter versus surface area).....	84

## **List of Tables in appendices**

Table 1: Variation of the extrudate diameter as a function of ABFA concentrations
Table 2: Variation of the extrudate diameter as a function of SBC concentrations
Table 3: Variation of the expansion (%) as a function of ABFA concentrations
Table 4: Variation of the expansion (%) as a function of SBC concentrations
Table 5: Variation of the elastic Modulus as a function of ABFA concentrations
Table 6: Variation of the stress at break as a function of ABFA concentrations
Table 7: Variation of the elongation at break as a function of ABFA concentrations
Table 8: Variation of the energy at rupture as a function of ABFA concentrations
Table 9: Variation of the elastic Modulus as a function of SBC concentrations
Table 10: Variation of the stress at break as a function of SBC concentrations
Table 11: Variation of the strain at break as a function of SBC concentrations
Table 12: Variation of the energy at rupture as a function of SBC concentrations
Table 13: Variation of the resilience as a function of ABFA concentrations
Table 14: Variation of the resilience as a function of SBC concentrations
Table 15: Variation of the hardness Shore D (first lecture) as a function of ABFA concentrations
Table 16: Variation of the hardness Shore D (Second lecture) as a function of ABFA concentrations
Table 17: Variation of the hardness Shore D (First lecture) as a function of SBC concentrations

Table 18: Variation of the hardness Shore D (Second lecture) as a function of SBC concentrations

Table 19: Variation of the extrudate diameter as a function of (ABFA/SBC: 0.4/0.6) concentrations

Table 20: Variation of the expansion (%) as a function of (ABFA/SBC: 0.4/0.6) concentrations

Table 21: Variation of the elastic modulus as a function of (ABFA/SBC: 0.4/0.6) concentrations

Table 22: Variation of the stress at break as a function of (ABFA/SBC: 0.4/0.6) concentrations.

Table 23: Variation of strain at break as a function of (ABFA/SBC: 0.4/0.6) concentrations

Table 24: Variation energy at rupture as a function of (ABFA/SBC: 0.4/0.6) concentrations

Table 25: Variation of the resilience as a function of (ABFA/SBC: 0.4/0.6) concentrations

Table 26: Variation of the hardness Shore D (first lecture) as a function of (ABFA/SBC: 0.4/0.6) concentrations at various extrusion speeds

Table 27: Variation of the hardness Shore D (Second lecture) as a function of (ABFA/SBC: 0.4/0.6) concentrations

## List of Figures

<u>Title</u>	<u>Pages</u>
Figure I.1: Schematic diagram of free foaming extrusion.....	14
Figure I.2: Schematic diagram of controlled foaming extrusion.....	15
Figure II.1: Torque evolution as a function of time.....	18
Figure II.2: Foam density as a function of volumetric flow rate ABFA/SBC ratios..	20
Figure II.3: Three dimensional plot of foam density as a function of ABFA and SBC concentration.....	21
Figure IV.1: The brabender torque rheometer process curve for an unfoamed rigid PVC compound.....	30
Figure IV.2: Torque evolution as a function of time.....	32
Figure IV.3: Torque and density evolution as a function of time (0.6phr ABFA).....	33
Figure IV.4: Torque evolution as function of time (0.6 phr ABFA, 0.2 phr ABFA and without ABFA).....	35
Figure IV.5: Torque evolution as function of time (0.6 phr ABFA, 0.2 phr ABFA and without ABFA).....	36
Figure IV.6: Torque evolution as function of time (PVC, PVC+ABFA residue).36	
Figure IV.7: Thermal stability time as function ABFA residue concentration.....	37
Figure IV.8: Torque evolution as function of time (0.6 phr SBC and without SBC)...39	
Figure IV.9: Torque and density evolution as a function of time (0.6 phr SBC).39	
Figure IV.10: Torque evolution as function of time (0.4, 0.6, 1.2 phr SBC and without SBC).....	41
Figure IV.11: Torque evolution as function of time (0.6, 1.2 phr SBC and without SBC).....	41
Figure IV.12: Torque evolution as function of time (0.6 phr SBC and 0.6 phr ABFA).....	42
Figure IV.13: Thermal stability time as function ABFA residue concentration.....	43
Figure IV.14: Torque evolution as function of time (0.3 phr SBC + 0.3 phr ABFA)....	44
Figure IV.15: Torque evolution as function of time (concentration mixture of BA).....	45

Figure VI.16: Torque and density evolution as function of time (concentration of BA mixture).....	46
Figure.IV.17: Torque evolution as function of time (concentration of BA mixture)....	48
Figure IV.18: Torque evolution as function of time (0.6 phr BA mixture and 1.2 phr BA mixture).....	48
Figure IV.19: Thermal stability time as function BA mixture residue concentration.....	49
Figure IV.20: DSC thermogram of ABFA.....	50
Figure IV.21: DSC thermogram of ABFA and PVC.....	50
Figure IV.22: DSC thermogram of SBC.....	51
Figure IV.23: DSC thermogram of SBC and PVC.....	51
Figure IV.24: DSC thermogram of the mixture (ABFA+SBC) and PVC.....	52
Figure V.1 : Extrudate diameter as a function of ABFA concentration.....	54
Figure V.2: Optical micrograph of unfoamed rigid PVC extrudate.....	55
Figure V.3: Optical micrograph of foamed rigid PVC extrudate (0.2 phr ABFA).....	55
Figure V.4: Optical micrograph of foamed rigid PVC extrudate (0.4 phr ABFA).....	56
Figure V.5: Optical micrograph of foamed rigid PVC extrudate (0.5 phr ABFA).....	56
Figure V.6: Optical micrograph of foamed rigid PVC extrudate (0.4 phr ABFA).....	57
Figure V.7: Optical micrograph of foamed rigid PVC extrudate (0.4 phr ABFA).....	58
Figure V.8: Percentage of expansion as function of ABFA concentration.....	59
Figure V.9: Foaming efficiency as function of SBC concentration at 20 and 40 rpm.....	60
Figure V.10: Optical micrograph of foamed rigid PVC extrudate (0.2 phr SBC).....	61
Figure V.11: Optical micrograph of foamed rigid PVC extrudate (0.6 phr SBC).....	61
Figure V.12: Optical micrograph of foamed rigid PVC extrudate (0.8 phr SBC).....	62
Figure V.13: Percentage of expansion as function of SBC concentration.....	63
Figure V.14: Elastic modulus as function of ABFA concentration.....	64
Figure V.15: Elastic modulus as function of SBC concentration.....	65
Figure V.16: Elastic modulus as function of BA concentration at 40 rpm.....	66
Figure V.17: Stress at break as function of ABFA concentration.....	67
Figure V.18: Stress at break as function of SBC concentration.....	68
Figure V.19: Stress at break as function of BA concentration at 40 rpm.....	68
Figure V.20: Strain at break as function of ABFA concentration.....	70
Figure V.21: Strain at break as function of SBC concentration.....	70

Figure V.22: Strain at break as a function of BA concentration at 40 and 50 rpm...	71
Figure V.23: Energy at break as function of ABFA concentration.....	72
Figure V.24: Energy at rupture as function of SBC concentration.....	72
Figure V.25: Energy at rupture as function of BA concentration at 40 rpm.....	73
Figure V.26: Resilience as a function of ABFA concentration.....	74
Figure V.27: Resilience as a function of SBC concentration.....	74
Figure V.28: Hardness as a function of ABFA concentration (First lecture).....	76
Figure V.29: Hardness as a function of ABFA concentration (Second lecture).....	76
Figure V.30: Hardness as a function of SBC concentration (First lecture).....	77
Figure V.31: Hardness as a function of SBC concentration (Second lecture).....	77
Figure V.32: Extrudate diameter as a function of percent ABFA.....	79
Figure V.33: Percentage expansion as a function of percent ABFA.....	80
Figure V.34: % of expansion as a function of percent ABFA at 40 and 50 rpm.....	80
Figure V.35: Optical micrograph of foamed rigid PVC extrudate (30% ABFA of BA mixture based on their optimum concentrations) at 50rpm.....	81
Figure V.36: Optical micrograph of foamed rigid PVC extrudate (70% ABFA of BA mixture based on their optimum concentrations) at 50rpm.....	82
Figure V.37: Optical micrograph of foamed rigid PVC extrudate (70% ABFA of BA mixture based on their optimum concentrations) at 40rpm.....	82
Figure V.38: Elastic modulus as a function of ABFA percentage .....	85
Figure V.39: Stress at break as a function of ABFA percentage.....	86
Figure V.40: Strain at break as a function of ABFA percentage.....	87
Figure V.41: Energy at break as a function of ABFA percentage.....	87
Figure V.42: Resilience as a function of ABFA percentage.....	88
Figure V.43: Hardness as a function of ABFA percentage (First lecture).....	88
Figure V.44: Hardness as a function of ABFA percentage (Second lecture).....	89

## INTRODUCTION

As plastic materials go up in cost, the idea of using less material to do the same task becomes more and more attracting [1]. One of the fastest growing markets in the vinyl industry is rigid vinyl foam profiles. Enthusiasm among processors has been sparked by newly developed compounds and manufacturing techniques. The rigid one holds a unique place in the field of structural thermoplastic foams and in wood replacement market [2].

Such cellular products have the look, feel and handling characteristics of wood. To that effect, these products possess several adequate properties, which can not be achieved neither by other ways nor by traditional compact products [3]. The price of wood per unit is less than cellular rigid vinyl, but the overall cost of producing small, finished, complicated shapes in wood is usually more expensive. Also, it is possible to make many difficult shapes, (by direct extrusion) which are impossible or impractical to make out of wood [2].

Many techniques have been reported as satisfactory for evaluation of solid chemical blowing agent systems [4-7], but they mainly refer to decomposition temperature and gas volume in the pure state. Work on the effect of formulated compound ingredients refer essentially to plastisol technology [8], and little information is available on decomposition under pressure [9-10]. Many studies have been reported using Brabender torque rheometer on cellular PVC, for instance the evaluation of the hot melt properties of cellular plastisol [11], the dynamic heat stability of expanded semi rigid PVC [12], and the decomposition behavior of ABFA in rigid PVC compound [13]. With the continual improvement in PVC compound and the requirement for improved performance, the need for better laboratory techniques for evaluating PVC compounds is necessary. In practice, the processability of PVC compounds is generally evaluated on a Brabender torque rheometer, since this apparatus simulates the conditions of temperature and shear that occur during processing [14]. For that reason, this tool was

chosen in our study, which deals with the behavior of two chemical blowing agents in a rigid PVC compound under processing conditions.

Foaming in cellular PVC is usually accomplished by adding a chemical blowing agent to the formulation in a sufficient concentration to give a desired product. The degree of foaming depends on the viscosity and melt elasticity of the PVC formulation, the gas pressure involved and the degree of solvation of the gas in the melt. Ideally, the blowing agent will not produce any gas until the PVC blend has fused and can form a melt seal. This prevents gas escape out the extruder hopper [15]. During processing, the blowing agent will decompose quickly but a small percentage will remain un-reacted at the die exit to provide nucleation sites for bubble formation. After exiting from the die, the super saturated gas-resin mixture will expand with a pressure drop forming the foam as discrete bubbles in continuous PVC matrix [15].

The objective of the present work was to carry out a thorough characterization of extruded expanded rigid PVC compound, using a combination of two chemical BA; azobisformamide (ABFA) and/or sodium bicarbonate (SBC), on the processability of rigid PVC compound, using a Brabender torque rheometer. The study focuses also on the effect of the addition of such a combination of chemical BA on the foaming efficiency of rigid PVC compounds using a laboratory scale extruder.

This thesis is composed of five chapters. The first presents a theoretical background on cellular PVC and the second chapter outlines the published work on cellular PVC. The third chapter presents the materials used and describes the experimental sample preparation methods as well as the different testing procedures. Chapter four and five discuss the obtained results on the processability of foamed rigid PVC, rheological (foaming efficiency), mechanical and optical properties respectively.

# **CHAPTER ONE**

## **THEORETICAL BACKGROUND**



## **I. THEORETICAL BACKGROUND**

### **I.1. Poly (vinyl chloride)**

Poly (vinyl chloride) is one of the most widely used polymer. It is available in two forms: plasticized and unplasticized. Both types are characterized by good weathering resistance, excellent electrical insulation properties, good surface properties and they are self extinguishing .

Plasticized P.V.C is flexible and finds applications in wire covering, floor tiles, toe balls, gloves and rain wear. Unplasticized P.V.C is a hard, tough and strong material which is widely used in the building industry. For example, pipes, window frames and wall cladding are often made from this material. P.V.C. is prepared starting from the vinyl chloride monomer (V.C.M.), the polymerization takes place in suspension, emulsion or bulk [16].

### **I.2. Compounding PVC ingredients.**

In the massive form PVC is a colorless rigid material with limited heat stability with a tendency to adhere to metallic surfaces when heated. For these and other reasons, it is necessary to compound the polymer with other ingredients to make useful plastic materials. By such means it is possible to produce a wide range of products.

A P.V.C compound may contain the following ingredients: PVC, stabilizers, lubricants, plasticizers, extenders, fillers, pigments, and polymeric processing aids. Other miscellaneous materials, also used occasionally, include fire retardant, optical bleaches and blowing agents [16].

#### **I.2.1. Stabilizers.**

A stabilizer can be defined as a material used to prevent the rapid deterioration or degradation of P.V.C which alters its chemical structure in a manner that leads to a decrease in its physical properties. Stabilizers are based on substances capable of neutralizing the hydrogen chloride (HCl) and improving the heat stability of P.V.C [16].

#### **I.2.2. Lubricants**

Lubricants act in several ways, their effects between resin particles prior to fusion, and between metal and polymer melt surfaces after fusion, can be considered external. Whereas their influence between resin molecules after fusion is internal with

reference to the polymer melt. The former has a higher affinity for the metal surfaces and lower compatibility in the plastic melt than the later [16].

### **I.3. Additives used in the expansion processes.**

Foaming agents used for the production of cellular plastics are normally divided into physical and chemical types according to whether the generation of gas is by a physical process (i.e. evaporation or sublimation) or by a chemical one (i.e. breakdown of the chemical structure or by other chemical reaction) [17].

#### **I.3.1. Physical blowing agents.**

Physical blowing agents undergo a phase change during foaming.

For example volatile liquids incorporated in a vinyl dry-blend are capable of producing a foam by passing from a liquid to a gaseous state. A high pressure gas expansion method using gaseous blowing agents is also concerned.

Since physical blowing agents leave no solid residues, nucleating additives are frequently needed to create sites for cell formation.

Although physical foaming agents are generally inexpensive, their use ordinarily requires specialized equipment to produce a specific cellular product [18].

#### **I.3.2. Chemical blowing agents**

Inorganic and organic compounds that liberate large volumes of gas as a result of thermal decomposition at elevated temperatures constitute a group of additives known as chemical blowing agents.

These agents are usually solid products with good thermal stability at ambient temperatures. At elevated temperatures intervals which are determined by the chemical nature of the agents and the environment in which they are being decomposed. The most commonly used foaming agents liberate, in addition to nitrogen, other gases such as carbon dioxide, carbon monoxide and hydrogen [18].

- Be easily dispersed in a vinyl compound.
- Not have an adverse effect on process properties.
- Not plate out.
- Not have a deleterious effect on the heat or light stability of the vinyl compound.
- Leave and odorless, colorless, non-staining, non-migrating, nontoxic residue.
- Not have a corrosive decomposition product.
- Release gas at a controllable rate.

- Function equally well in open or closed cellular production conditions.
- Be stable in storage.
- Leave a residue that could form nucleation sites for cells.
- Allow the formulator to develop vinyl foams for a wide range of applications.
- Not be expensive.

The major advantage using chemical blowing agents is that these additives can produce a cellular vinyl structure from a vinyl compound, which is being processed in conventional vinyl processing equipments [18].

### **I.3.2.1. Inorganic blowing agents**

Inorganic blowing agents, mostly alkali salts of weak acids, have been of limited use in the vinyl industry. The most important of these agents are: Sodium bicarbonate ( $\text{NaHCO}_3$ ), Ammonium bicarbonate ( $(\text{NH}_4)\text{HCO}_3$ ) and Sodium borohydride ( $\text{NaBH}_4$ ). They can liberate gas either by thermal dissociation or by chemical decomposition in the presence of activators.

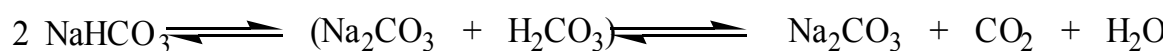
The thermal dissociation of an inorganic salt is an endothermic reversible reaction, and the reaction rate and equilibrium point depend on external pressure. For this reason, the use of inorganic blowing agents is limited to foaming at atmospheric conditions [18].

As foaming agents for vinyls, inorganic salts have the advantage of low cost, but this is counter-balanced by poor storage stability and the difficult dispersion properties of these products. Since gases generated by inorganic foaming agents are either readily condensable (e.g. water vapor) or have high diffusion rates (e.g. hydrogen), vinyl foams made with these agents are dimensionally unstable and require long annealing [18].

#### **I.3.2.2.1. Sodium bicarbonate (SBC)**

Sodium bicarbonate is well known blowing agent because of its use in baking powder. It decomposes reversibly and endothermically to give  $\text{Na}_2\text{CO}_3$ ,  $\text{CO}_2$ , and  $\text{H}_2\text{O}$  with a gas yield of 125 ml/g. Decomposition occurs over a wide temperature range, which fortunately coincides with the processing temperature window of rigid foams [18].

(1)



### I.3.2.2. Organic blowing agents

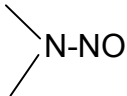
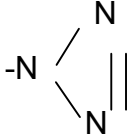
Organic compounds that release nitrogen as the main component of the liberated gas are the most important foaming agents for cellular P.V.C. The thermal decomposition of organic blowing agents is an irreversible exothermic reaction and independent on external pressure.

The decomposition rates of these products are governed by temperature or time, or both and are independent of concentration.

Interactions with other ingredients in the formulation or impurities may change the course and the rate of the blowing agent decomposition [18].

Chemically, these organic foaming agents are characterized by the functional groups shown below (table I.1):

**Table I.1:** Functional groups of organic foaming agents [18].

Characteristic functional groups of organic blowing agents	
- N= N-	Azo
	N-Nitro
-SO <sub>2</sub> -NH-NH-	Sulfohydrazo
	Azido

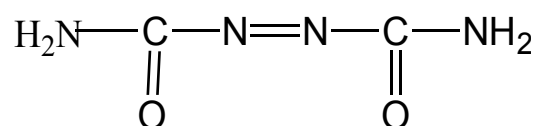
Blowing agents with the same functional groups may display widely different decomposition temperature depending on their molecular structure, but their decomposition exotherms are essentially the same. For examples, Azides generate very high exotherms, whereas sulfonylhydrazides have relatively low calorific effects. A large exotherm generated during decomposition of the blowing agent may raise the internal temperature of the foaming system beyond the degradation point of vinyl polymers. Charring of the compound will occur if heat is not dissipated quickly. Volatile solvents having a high heat of evaporation can be used as a heat sink in foamable P.V.C. composition to control the decomposition exotherm of organic

foaming agents. Table I.2 shows the properties of some commercial available blowing agents for vinyls [19].

**Table I.2:** Properties of some commercial available BA [19].

Name and structure	Decomposition point in air (°C)	Decomposition Temperature range in vinyls (°C)	Gas yield [ml/(STP)/g]
Sobi.sisobutyronitrile $\begin{array}{c} \text{CH}_3 \quad \text{CH}_3 \\   \quad   \\ \text{CN}-\text{C}-\text{N}=\text{N}-\text{C}-\text{CN} \\   \quad   \\ \text{CH}_3 \quad \text{CH}_3 \end{array}$	105	90-105	136
1 1' Azobisformamide (A.B.F.A) Azodicarbonamide $\text{H}_2\text{N}-\text{CO}-\text{N}=\text{N}-\text{CO}-\text{NH}_2$	195-200	150-200	220
P-toluenesulfonyl Semi-carbazide $\begin{array}{c} \text{CH}_3 \\   \\ \text{C}_6\text{H}_4 \\   \\ \text{SO}_2-\text{NH}-\text{NH}-\text{CONH}_2 \end{array}$	227	190-200	170

#### I.3.2.2.1. Azobisformamide (A.B.F.A)



I,I Azobisformamide, frequently called Azodicarbonamide, is the most versatile blowing agent for vinyls. It has a unique combination of valuable properties that meet the requirements of an ideal chemical foaming agent [20].

The commercially available azodicarbonamide is an orange-yellow to pale-yellow powder which decomposes in air above 195 °C (The color depends on the particle size distribution). The agent and its residue are odorless, non-staining and when

properly compounded, non-discoloring. Because A.B.F.A and its residue are nontoxic, use of the blowing agents in food applications has been sanctioned under several Food and Drug Administration (FDA) regulations [21].

Although A.B.F.A is non-soluble in common solvents and plasticizers, it disperses readily in vinyl compounds. Plasticizer dispersions of the foaming agent that can be blended directly with plastisols, dry blends and other vinyl compounds are commercially available. The storage stability of the agent, both dry and in a dispersed form, is excellent. Significantly, A.B.F.A is the only organic foaming agent that does not support combustion and is self extinguishing.

When azobisformamide is heated in an ester plasticizer above its decomposition point, it delivers gas at 220 ml (STP)/g, corresponding to one third of its molecular weight. The gas phase consists of 65% N<sub>2</sub>, 33% CO and 2% CO<sub>2</sub>. Under alkaline conditions, ammonia is also generated. The composition of the residue depends on the medium in which the blowing agent is decomposed. The residue is usually white and consists mainly of hydrazobisformamide (biurea), cyanuric acid, urazol and cyamelide.

The A.B.F.A residue may enhance the heat stability of vinyl compositions, particularly those stabilized with zinc salts. In the presence of alkalis, A.B.F.A hydrolyses rapidly at 100° C with the liberation of nitrogen, carbon dioxide and ammonia [22].

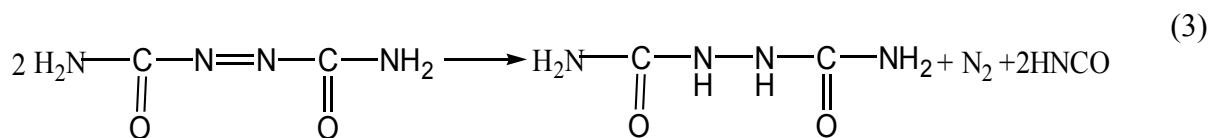
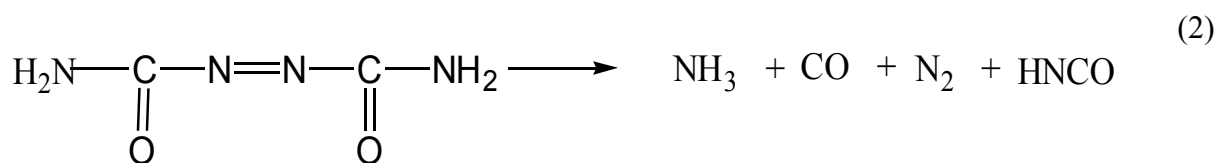
Because of its high decomposition temperature in air, A.B.F.A was originally considered unsuitable as a foaming agent for vinyls [23]. However, a later observation that many additives, including vinyl stabilizers, can lower the decomposition temperature of A.B.F.A led to successful commercial applications of the agent in the cellular industry [24].

The thermal decomposition of dry azodicarbonamide in air gives rise to the following proportions of decomposition products [25, 26]:

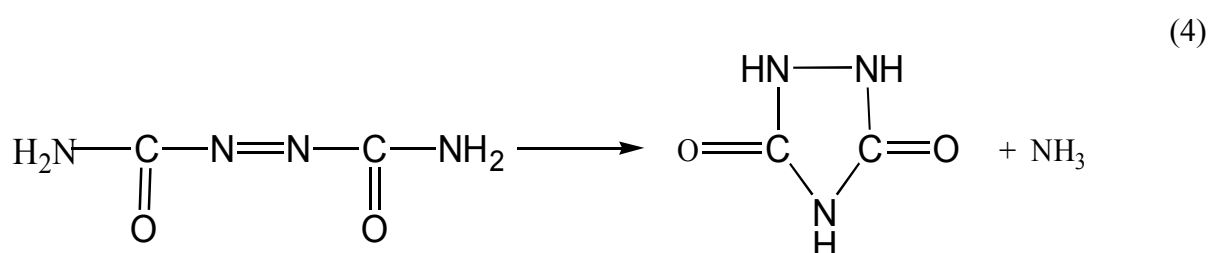
Gaseous products:	32 % by weight
Solid residues:	41 % by weight
Sublimate:	27 % by weight

The solid residue and the sublimate are composed mainly of urazole (39 %), cyanuric acid (26 %), hydrazodicarbonamide (2%), and cyamelide (1%). The percentages are calculated on the amount of azodicarbonamide used.

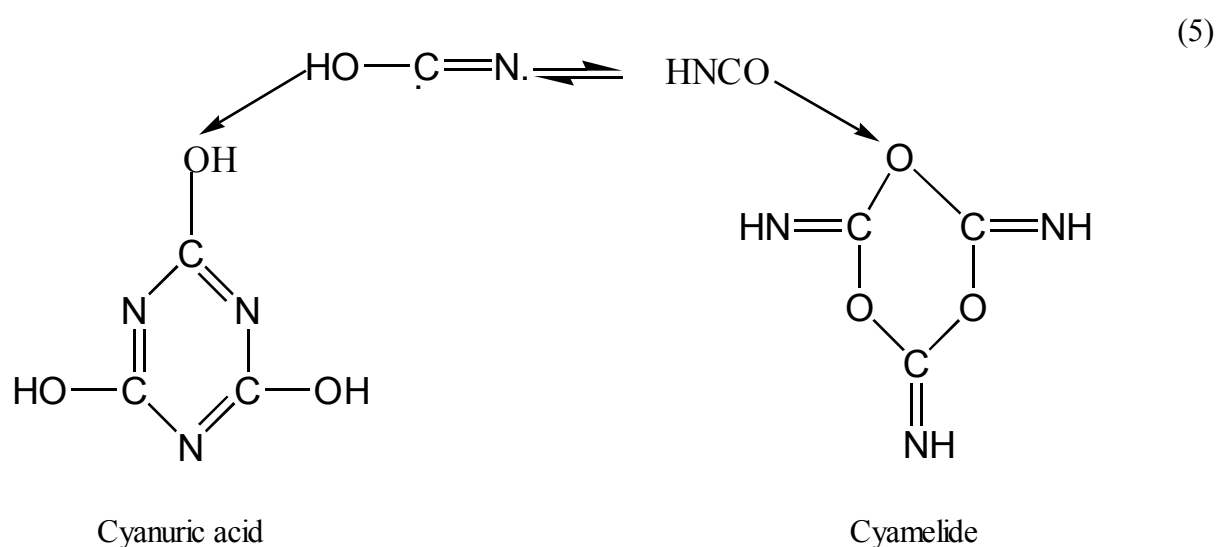
The primary decomposition of azodicarbonamide can follow two courses:



Urazole can result from the elimination of a mole of ammonia from biurea:



An equilibrium between cyanic and isocyanic acid and trimerization of each can be written:



### I.3.2.3. Chemical blowing agent activators.

Vinyl stabilizers containing lead, cadmium and zinc are the most efficient activators (kickers). These additives reduce the decomposition temperature of A.B.F.A and increase activation due to their solubility in plasticizers [27]. The activating effect of the basic metal salts is derived from the instability of the corresponding azodicarboxylates that are formed at the first step in the decomposition of A.B.F.A.

Since the dicarboxylates of lead, cadmium and zinc decompose at lower temperatures than the diamide, they initiate the thermal breakdown of A.B.F.A [28]. The activation of A.B.F.A by metal salts is concentration-dependent [29], and the rate of A.B.F.A decomposition increases as the amount of metal salt in the compound increases. Some proprietary compounds offered in the trade are said to activate the A.B.F.A catalytically [30]. Because of the high temperature stability of barium azodicarboxylate, barium salts exert no activating effect on A.B.F.A, and in their presence, the decomposition rate of the A.B.F.A is as low as it is in air. However, barium compounds show synergistic activity with lead and zinc in reducing the decomposition temperature of A.B.F.A [31]. The activation of A.B.F.A is promoted by alkaline conditions and inhibited in acidic media. For example, adding fumaric acid to lead-stabilized A.B.F.A containing plastisol increases the decomposition temperature of the blowing agent to 190°C (compared to 165 °C) in the absence of the acid. This mechanism is used in one of the chemical embossing processes [32].

A.B.F.A lends itself to being compounded with dry-blends as well as plastisols [33]. Successful processing techniques applicable to these formable compounds have not compassed the entire spectrum to vinyl technology. The chemical has been the preferred foaming agent in the manufacture of expanded vinyl fabrics [34] and floor coverings [35].

Other uses include low-density open-cell foam, extruded low-density gaskets, high density profiles, expanded jackets for electrical wires and cables [36-39].

### **I.3.3. Methods of incorporation.**

In the compounding operation, chemical blowing agents and promoters are handled like many other vinyl additives. Because of the heat sensitivity of the foaming agent, careful temperature control is essential to avoid premature generation. Blending of the blowing agent dispersion with the vinyl dry blend varies, depending on the type of vinyl compound involved in the processing. Ribbon blenders or high-intensity mixers are used in processing dry blends and calandring compounds. When only small quantities of blowing agent are to be added to an extrusion or injection molding compound, resin pellets are coated with the blowing agent by tumbling [18].

#### **I.3.3.1. Evaluation of blowing agent efficiency.**

The apparent density of a cellular product is obtained through the trial-and-error approach at tailoring the formulation to blow under optimum conditions.



Unfortunately, there is no single definition of what constitutes an optimum condition. The optimum condition will depend on the type of process, the amount of blowing agent, and the formulation. The factors of the chemical composition of the blowing agent that delineate its efficiency are its molecular weight, the number of moles of gas that can be split off, and the decomposition mechanism. The efficiency of chemical blowing agent is measured by the quantity of gas given off on decomposition. This quantity is called gas yield and is defined as the gas volume at normal temperature (0°C) and pressure (700 mm Hg) per unit of weight. The actual yield of a blowing agent in a vinyl composition may differ appreciably from the theoretical or stoichiometric gas yield because of side reactions of other additives which are present, for example, stabilizers, pigments, or resin impurities (e.g. residual emulsifiers) [18].

Determination of the actual gas yield from a chemical blowing agent heated beyond its decomposition point is the subject of A.S.T.M method D 1715, issued jointly by A.S.T.M and S.P.I. In this test, since the blowing agent undergoes decomposition in an inert environment and the heating rate is low, the test has little relevance to blowing agent effectiveness in vinyl, nor is this method applicable to measurements of the rate of decomposition. For example, the gas yield as a function of temperature or time or both [18].

Differential thermal analysis (DTA) combined with thermogravimetric analysis (TGA) can be used advantageously to follow the decomposition behavior of chemical blowing agents. For example, an organic foaming agent generates an exotherm during the decomposition, and the evolved heat as well as the volume of the liberated gas can be plotted as a function of temperature. The interval between the onset and the peak of the exotherm is considered to be decomposition temperature [40].

#### **I. 4. The foaming and expansion**

##### **I.4.1. Expansion stages**

The expansion process for the production of cellular plastics occurs in three successive stages: Initiation, growth and stabilization of cells [17].

##### **I.4.1. 1 Initiation of cell nucleation**

Cells are formed when the saturation limit for dissolved gases is reached and if the rate of gas release or expansion within the material is much greater than its rate

of diffusion to the surrounding atmosphere. The process of cell nucleation is not fully understood, but it is reasonable to assume that cells are formed at those points where solubility is least and where saturation is, therefore, reached first. This deduction can be made from a consideration of Henry's law for the solubility of gases in liquids, i.e. at given temperature (T) [17].

$$[C]_T = P [S]_T \quad (6)$$

where

C: Concentration of gas dissolved.

P: External pressure.

S: Solubility coefficient (depending on the nature of the gas and the liquid).

Hence, at a given temperature and pressure, a reduction in the solubility coefficient will bring about a simultaneous reduction in concentration of gas dissolved, and the excess gas which is expelled will form a bubble. Therefore, cell formation occurs at points of low gas solubility within the fluid mass, which may consist of finely divided solid inclusions (i.e. pigment particles, fine domains of other low solubility additives, such as lubricants, surfactants, etc.) [17].

#### **I.4.1.2. Growth or expansion of cells**

The growth rate of cells in an expansion process is determined by the rate of increase in pressure inside the cells (or by the rate of pressure decay around the cell area) and by the deformability of cell walls [17].

Its likely that nucleation of the cells does not occur simultaneously throughout the matrix and that at any given time during the expansion process, the cell size and the pressure are subjected to normal statistical variation. Due to surface tension effects, there is an excess pressure in smaller bubbles; which causes gas diffusion from one cell to another. Consequently, some of the bubbles will grow even larger, some smaller and some may disappear altogether [20].

#### **I.4.1.3. Stabilization of cells**

It is understood that if the cell growth process was not interrupted at some stage, the surviving cells would grow extremely large and the material forming the wells reaches breaking limits. Eventually, all the cells would break into on another and the whole foam structure would collapse .

In the other extreme case, it could happen that all the gas from the cells would slowly diffuse into the atmosphere, the pressure within the cells would gradually

decay and the cells become progressively smaller and disappear if the elastic strain energy in the bulk of the cell walls is the major factor controlling bubble size (e.g. thermoplastics).

Control of the growth and stabilization of cells is, therefore, essential in the production of cellular products. This is accomplished by bringing about a sudden solidification or a gradual reduction in deformability of the polymer matrix so that the pressure within the cells will not be sufficient to cause further deformation of the walls.

However, further reduction in deformability of the matrix, beyond that sufficient for foam stabilization, is necessary to impart mechanical strength to the cellular product. With thermoplastic polymeric systems, both stabilization of the cells and strengthening of the cell walls are achieved by the gradual and controlled cooling of the polymer which increases the viscosity and/or the modulus of cell walls [17].

#### **I.4.2. Cell structure**

There are two types of cellular foamed polymers: open cell and closed cell. In the closed cell type, each cell is individual, usually spherical in shape, and completely enclosed by plastic walls. This type of cell structure has good insulating properties as well as high degree of buoyancy. In the open cell type, all the cells are interconnected. This second type of cell structure is known for its absorbency and capillary action [4].

A cellular product is a solid-gas composition consisting of continuous polymer phase and a gas phase, continuous or discrete, created by a foaming agent. The cellular structure depends on the nature of the cell-foaming process, hence, additives (foaming agents) are used in expansion process [41].

##### **I.4.3.1. Die**

The focal point of the extrusion line is the die tool. It is responsible for forming the extruded strand of melt into the desired contours of the profile [42].

##### **I.4.3.2. Sizing die (calibrator)**

In the sizing die (cold shaper), the molten profile assumes its shape almost exactly. On passing through, it gives off so much heat that the average temperature drops well below its freezing point [42].

#### **I.4.4. Techniques for foam extrusion**

Two major techniques are used for extrusion of foam profiles: free foaming extrusion (F.F.E) and controlled foaming extrusion (C.F.E) [43]:

##### **II.4.4.1. Free foaming extrusion (F.F.E)**

In the free foaming, the thermoplastic material containing a BA is extruded through a conventional die. After the die, the profile is expanded almost to its final dimension then calibrated through a cold shaper in order to achieve final dimensions [43] (see figure I.1).

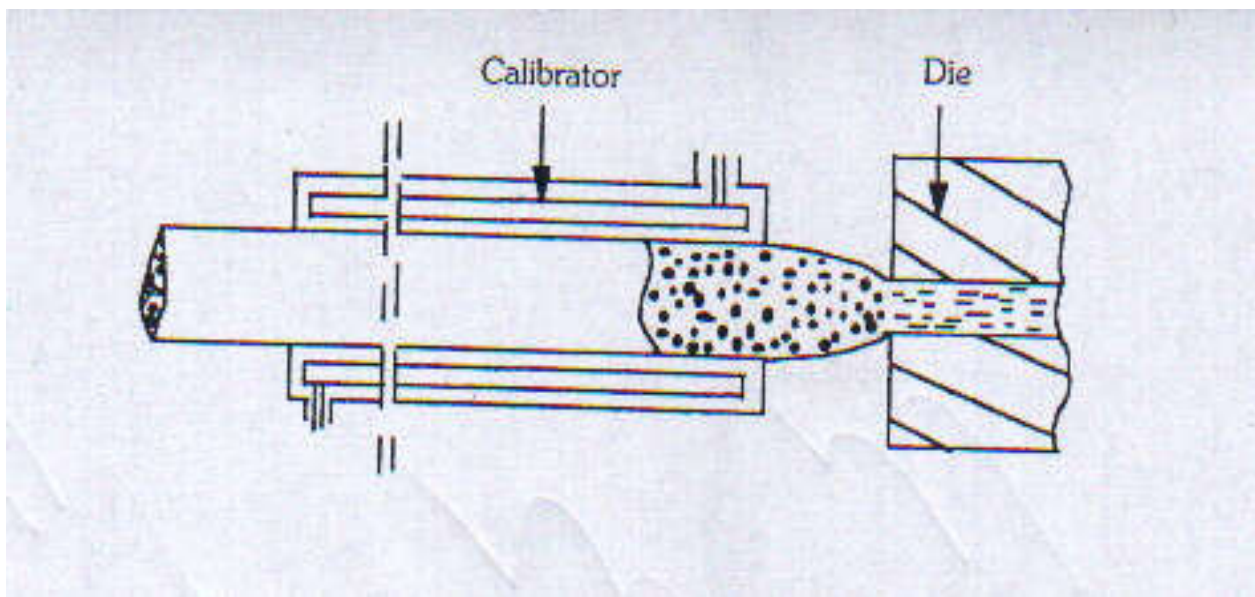


**Figure I.1:** Schematic diagram of free foaming extrusion [43].

##### **II.4.4.2. Controlled foaming extrusion (C.F.E)**

The controlled foaming, commonly called “CELLUKA” [44] is rather different from (F.F.E) because, in this case, thermoplastic material containing blowing agent is extruded through an annular die whose exterior contour is exactly the same as the internal contour of the cold shaper adjacent to the die [43].

These conditions allow very precise control of dimensions of the profile. The outer surface of the molten material is cooled by contact with the cold shaper to obtain a solid, unexpanded skin over the expanding material that foams inwardly [43] (see figure I.2).

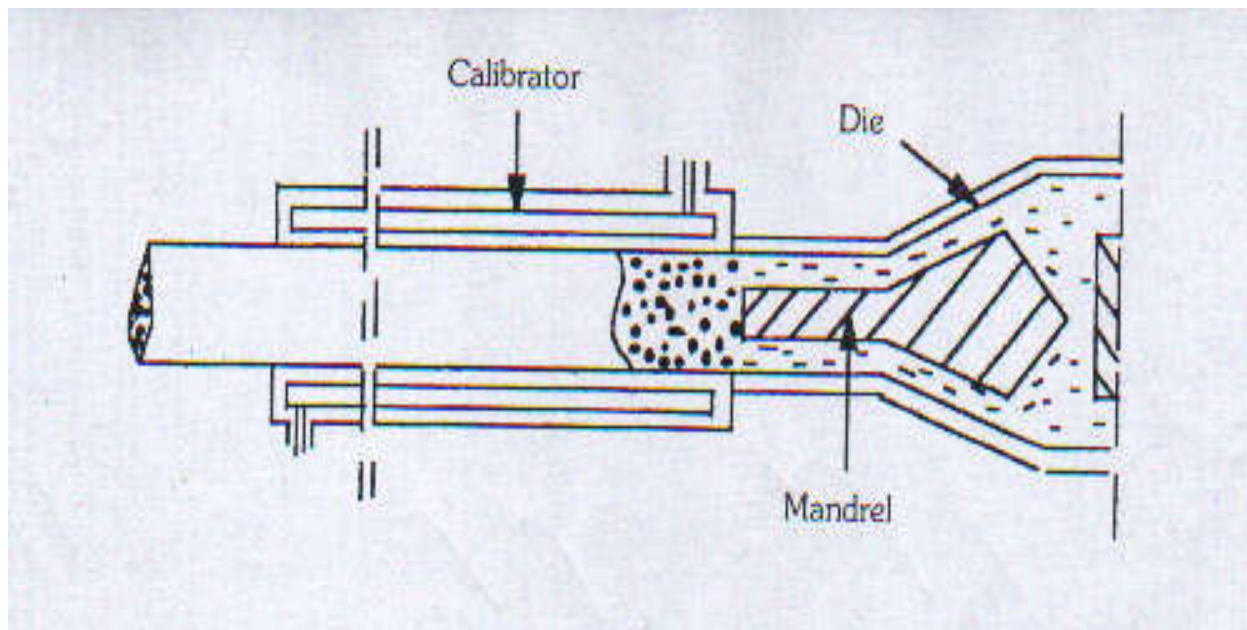


**Figure I.2:** Schematic diagram of controlled foaming extrusion [43].

## **CHAPTER TWO**

### **ADVANCES IN DEVELOPMENT OF EXTRUSION OF FOAMED RIGID PVC**

## **II. ADVANCES IN DEVELOPMENT OF EXTRUSION OF FOAMED RIGID PVC**

Research on extrusion of cellular rigid PVC is very extensive and many works have been published [12-14; 45-52]; among which those dealing with the content of this thesis. The main fields of research on this subject can be classified into three categories:

- 1- Formulation of foamed rigid PVC.
- 2- Techniques used for evaluation of chemical blowing agents.
- 3- Expansion with a combined use of chemical blowing agents.

These works will be briefly described in this chapter.

### **II.1. Formulation of foamed rigid PVC.**

- The particle size of ABFA is a factor that governs degree of activation by vinyl stabilizers. Since ABFA is non-soluble in vinyl plasticizers, activation of blowing agent takes place in a heterogeneous system and, therefore, is directly related to the active surface area. ABFA of large particle size and small surface area is more difficult than materials of fine particle size having a large area of activation. Recognition of this fact has led to the commercial acceptance of an azobisformamide series of blowing agents with particle size distribution tailored to specific applications. This was reported by H.R. LASMAN [45].

### **II.2. Techniques used for evaluation of chemical blowing agents**

- The plastograph test has been used by T. HAWKINS & Col [14] to improve its sensitivity to small changes of critical additives in the rigid PVC formulation such as thermal stabilizers and lubricants. Their technique consists of increasing rotor speed of the head mixer roller during equilibrium portion of a Brabender processing test [14].
- Dynamic heat stability of expandable semi-rigid PVC was performed using the plastograph test by C. F. TU [12]. The deterioration is partly due to the excessive heat build-up by the decomposition of ABFA.

In this study, C. F. TU reported the damaging effect ABFA on the thermal stability of the compound on the last part of the resulting curve [12]. The stability times and minimum torques of various PVC compounds, with and without ABFA were investigated. It is evident that the BA has a great

deleterious effect on the stability time of PVC compounds. Examination of the minimum torques reveals that the expandable PVC invariably has higher minimum torques than nonexpandable PVC which is probably due to the earlier formation of cross linked PVC as a result of BA decomposition. On the other hand, ABFA residues are also detrimental to the dynamic heat stability of PVC compounds but the effect is by far smaller than that of ABFA per se. However, the residues did not cause the increase in the minimum torque.

- The plastograph test method reported by C. BENNING & Col [13] allows the determination of blowing agent stability and gas evolution rate under conditions close to those of actual processing. It is not enough to make the evaluation of BA with simple bench tests and calculations. For instance, the efficiency of a BA not only includes such considerations as gas yield and cost; ease of handling processability, shelf life and its effect on the product also have significance. Several tests are now extant for measuring gas yield from a chemical BA. They include: 1) Heating a mix of agent and inert fluid and measuring products. 2) A differential thermal analysis which measures heat of reaction or decomposition exotherm. 3) Thermo-gravimetric analysis for measuring weight loss as a function of temperature. 4) ASTM D 1715-60T for total gas yield measurement. All these methods lack one essential.

Decomposition behavior is determined under conditions bearing no relation to the actual process. Use of a plastograph Brabender removes this objection.

Significant information on the thermal behavior of blowing agents in vinyl chloride polymers also can be obtained when their actual performance, that is their efficiency in lowering the apparent density of the polymer, is determined as a function of time or temperature or both [13]. From the recording strip chart, the initial sharp increase in torque (on extreme left) is due to polymer composition (see figure II.1): fluxing and equilibrating. The part of the curve following the initial fusion is an apparent equilibrium time. The length of this portion of the curve is a measure of processing stability. The increase in torque indicates cross-linking due to free radicals generated during decomposition of the BA. A decrease indicates degradation or slippage due to lubricants being present. (Mixtures of zinc stearate and ABFA do cause a decrease in torque due to lubrication).



In this technique, the BA was added when the resin was fluxed. Whereas, during processing at an industrial scale, it should be dry-blended with all the ingredients constituting the formulation before being fed to the hopper machine. C. BENNING and coworkers specified that if this was done, there will be a gas loss due to decomposition of BA on hot walls of mixer [13].

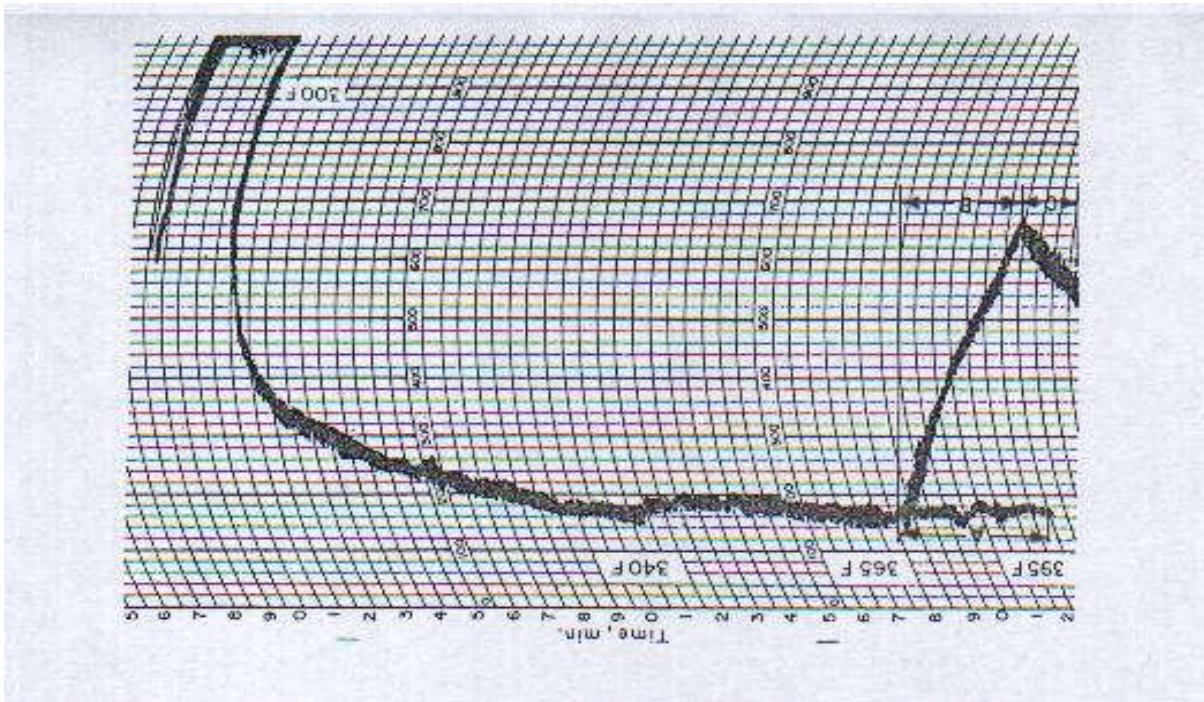


**Figure II.1:** Torque evolution as a function of time [13].

### II.3. Expansion with a combined use of chemical BA.

- In order to provide an adequate product with the highest foaming efficiency, a considerable amount of research has been done. We will list some of them; J. L. PFENNING & Col [46], F.IDE & Col [47], and K.U. KIM & Col [48]. These authors investigated foaming efficiency with BA level; but their use was restricted to only one BA [46, 47]. They reported that the density would drop with increasing BA to a minimum, and then rise with additional BA. It was also seen that the minimum of the density curve would shift to lower values and higher BA levels with increasing molecular weight of the processing aids.
- A combined use of two BA (ABFA and/or SBC), was developed by K.U KIM & Col [48], and N.L.THOMAS & Col [49]. The mixture of the BA was not based on their critical concentrations.

In their study, KIM and coworkers focused their works on ADCA / SBC ratios limited to five ratios (0/10; 1/9, 5/5, 9/1, and 10/0). The results showed no synergistic effect in term of foaming efficiency (i.e. all the values of the mixture of the BA are being restricted between those of each BA when used separately) (see figure II.2). In term of general appearance of the foamed product, ADCA favored relatively high volumetric flow rate and low melt temperature for the optimum foaming conditions, while SBC favored relatively low volumetric flow rate and high melt temperature. When the mixed BA was used, the optimum processing condition was dependent on the ratio of two BA. ADCA showed higher efficiency than SBC at the same usage level. In the case of SBC the density of foamed product was almost inversely proportional to the amount of chemical BA up to 1.25 phr ADCA and mixed ones showed a near linearity. Above 1 phr with ADCA/SBC = 9/1, however, it was very difficult to stabilize foams, in which case the cell collapse appears to be very severe about the melt temperature of 165°C.

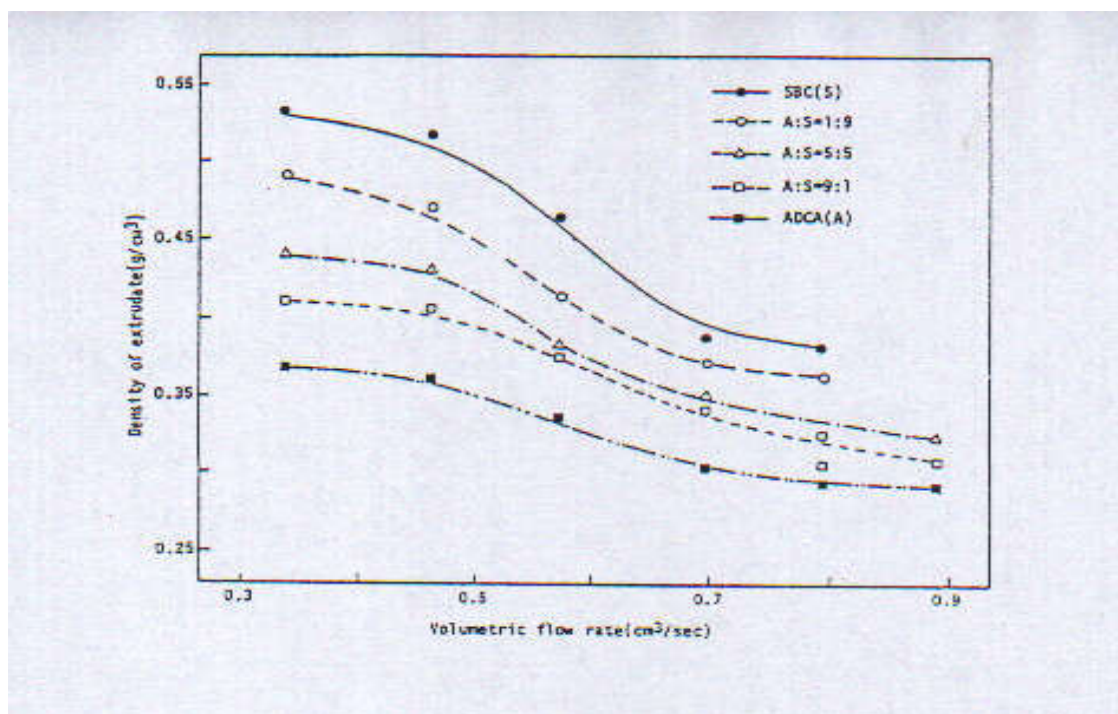


**Figure II.2:** Foam density as a function of volumetric flow rate at different ABFA /SBC ratios [48].

In their study, N.L.THOMAS and his group [49] reported that the three-dimensional plot of Fig.II.3 shows the best overall view of the response surface. Foam density is plotted on the vertical axis and decreases sharply with small additions of BA. Eventually the density reaches a minimum and the increase again as the concentration of BA continues to increase. The effects of the individual BA are seen along the adjacent sides of the three-dimensional plot. The obvious curvature in the relationship between foam density and AZO concentration contrasts significantly with the almost linear dependence of density on SBC concentration. The analysis clearly shows that the lowest foam densities are achieved using a combination of the two BA.

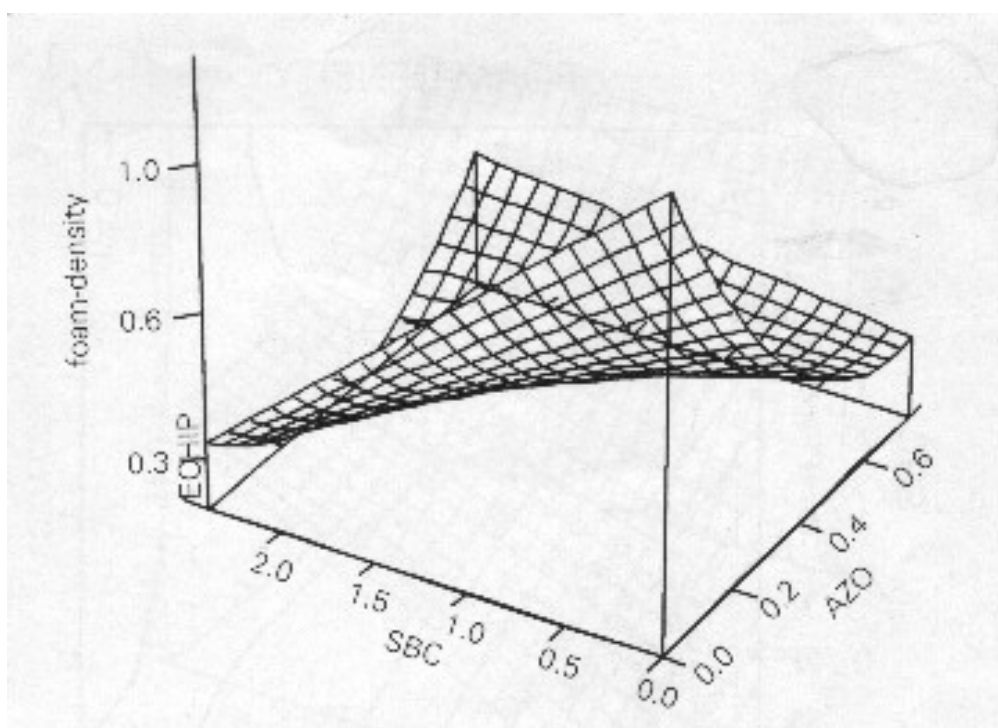


**Figure II.3:** Three dimensional plot of foam density as a function of ABFA and SBC concentration [49].

The synergism between AZO and SBC in the extrusion of rigid PVC foam (see figure II.3), as reported by these authors, is largely attributed to the complementary properties of the gaseous decomposition products  $N_2$ , and  $CO_2$ :  $N_2$  (evolved from AZO) has a relatively low solubility but high diffusivity in PVC compared with  $CO_2$  (evolved from

SBC) [49]. This results in N<sub>2</sub> bubbles readily nucleating to give a fine, even cell structure. However, because of the high diffusivity of the gas, the cell structure is prone to collapse. Conversely, CO<sub>2</sub> is more soluble in PVC and it is more difficult to nucleate bubbles of this gas. This accounts for the coarse foam morphologies observed. Once formed, however, the bubbles are more stable. They are less prone to collapse because of the lower diffusivity of CO<sub>2</sub>. A combination of AZO and SBC is clearly advantageous. The N<sub>2</sub> bubbles can provide a large number of nucleation sites and the growing cells will be stabilized by the CO<sub>2</sub>, which is slow to diffuse out. The morphologies of some the foamed samples produced in the above extrusion trial were examined. When the BA used was SBC alone, the samples had a coarse cell structure. Fine cell structures always resulted from using a combination of AZO and SBC. N.L.THOMAS and coworkers obtained a synergistic effect in term foaming efficiency even though the mixture of the BA was not based on their critical concentrations (see figure II.3). And the ranges of ABFA / SBC ratios were very significant: 21 x 21 = 441 ratios [49].

- The BA mixtures and master batches contain a mix of different exothermic and endothermic BA in a confidential ratio was developed by G. LUEBKE [50]. These master batches are combined with wood flour to give so called “wood- flour composites”. The use of the wood flour as filler in plastics to reduce the resin costs and to make a new construction material with the attributes that it has better properties, such as moisture an insect resistance. Many parameters like polymer, process temperature and application, will influence the foaming process. A certain processing temperature will require a special decomposition temperature of the BA. The different evolved gases from a BA must fit perfect with the foamed polymer, because differences of gas solubility in the polymer melt will cause a different cell structure. BA produces fine gas bubbles and solid decomposition products. The products act as a nucleating agent for foaming process.

This “self nucleating effect” of the decomposition products, combined with fine celled gas bubbles evolved by the BA, is nucleating the water coming from the wood, but not perfectly dried, lumber scrap. An improved fine cell structure in the final product is the result.

- In the foamed (cellular) PVC/wood flour composites, lower densities are achieved when the BA level is increased on a weight percentage basis to maintain a total gas evolution constant on a total weight basis. SBC appears to provide lower densities than achieved with ABFA, Both compositions processed well and surface and edge quality were better. Among other advantages, the inventions provide tough rigid PVC microcellular foam without a large amount, if any, impact modifier in the polymeric composition. Because impact modifiers are typically significantly more expensive than plastic, the microcellular foam can be produced at cost savings without sacrificing their toughness. In certain embodiments, the foams are suitable in applications that require rigidity, as well, as toughness, such as rigid profiles. This work was developed by J.R. PATTERSON [51, 52].

## **CHAPTER THREE**

### **EXPERIMENTAL**

### III. EXPERIMENTAL

#### III. Introduction

A formulation of a rigid PVC compound was prepared using a Brabender plasticorder by the optimization of the level of both internal and external lubricants to ensure a moderate fusion time. The minimum content of thermal stabilizer was leveled to reach a desired thermal stability time, the processing temperature was recorded during this step. This temperature was compared to that recorded from DSC thermal analysis. Then, the optimum blowing agent level was determined by the cell collapsing limit corresponding to the lowest density using a laboratory extruder and optical microscope.

#### III. 1 Raw material

##### III.1.1 Poly(vinylChloride)

Trade name : 4000 LL (ENIP Skikda)

Volatiles (% w/w) : 0.4

K-Value: 57

Fish eyes (Nbre/area) : 20/ 15x15 mm<sup>2</sup>

Degree of polymerization : 570- 670

Thermal stability (min) : 65

Apparent viscosity : 0.52 – 0.57

Ashes (%) : 0.03

##### III.1.2 Thermal stabilizer (Kickers)

###### III. 1.2.1 Dibasic lead phosphite

Color : white

Molecular weight : 743

PbO content (%) : 85

Specific density at 20°C : 6.9

###### III. 1.2.2 Dibasic lead stearate

Color : white

Molecular weight : 1200

PbO content (%) : 54

Specific density at 20°C : 2

##### III.1.3 Lubricants

###### III.1.3.1 Internal lubricant (Dicarbonic acid ester)

Freezing point (°C) : 43

Acid index : 0.5

Burning point ( °C) : 260

###### III.1.3.2 External lubricant (Non polar hydrocarbon wax)

Freezing point (°C) : 102 – 108

Density : 0.92 – 0.94

##### III.1.4 Chemical blowing agents

###### III.1.4.1 Azobisformamide (ABFA)

Trade name : VINSTAB AZ-3 (Hebron)

Appearance: Fine, pale yellow powder

Molecular weight: 116 g/mole

Gas volume evolved (ml/g): 200

Decomposition: 200°C

Content of active substance: min. 98 %

Density : 0.70

Average particule size (µm) : 125

### III.1.4.2 Sodiumbicarbonate (SBC)

Trade name : Normapur

Appearance: Fine, pale yellow powder

Molecular weight: 84 g/mole

Gas volume evolved (ml/g): 267

Decomposition: 100-150 °C

Content of active substance: min. 98 %

Density : 0.10

Average particule size (µm) : 280

## III.2 Formulation and mixing

### III.2.1 Formulation

We tried to keep a base formulation for all the studies, so that, at the end we assemble the results in a large experimental design data base.

The formulation suggested in our standard formulation that can be seen in table III.1 .

**Table III.1:** Formulations

PVC resin	4000 LL :K value 57 (Enip Skikda)	100 parts (per weight)
Stabilizer (Kicker)	Dibasic Lead Phosphite Dibasic Lead stearate	} 1.9 phr
Internal lubricant external lubricant	Dicarbinic cid-ester Non-polar hydrocarbon- wax	} 1 phr
Blowing agent (ABFA)	VINSTAB AZ-3 ( Hebron)	0 - 0.8 phr
Blowing agent (SBC)	NORMAPUR	0 - 1.2 phr



### **III.2.2 Mixing step**

This step consists mainly of mixing all the additives . The components were conmined in a high speed kitchen mixer for 5 mn to give a dry-free flowing white powder.

## **III.3 Tests**

### **III.3.1 Brabender Study.**

In order to determine the behavior of the PVC compounds in the extruder, several tests were performed on a torque rheometer system (Brabender), in almost the same processing conditions of temperature and roller speed, compared with extrusion conditions ( $T=180^{\circ}\text{C}$ ,  $V=30\text{ rpm}$ ). The desired amount of sample, corresponding to 65 g, was charged into heated Brabender type W 50 roller mixer.

In the Brabender torque rheometer test method for the evaluation of chemical blowing agents, the BA was added when the resin was fluxed. Whereas, during processing at an industrial scale, it should be dry-blended with all the ingredients constituting the formulation, before being fed to the hopper machine. C. Beaning & col [45] specified that if this was done, there will be a gas loss due to decomposition of BA on hot walls of mixer.

Our contribution was to overcome this problem and to get closer to real processing conditions, i.e. adding the BA with the resin at the same time. This was carried out by fluxing the compound before decomposing the BA. The former operation was adjusted by varying the concentration of external lubricant and the later was done by varying that of thermal stabilizer which is acting as ABFA kiker. In order to check if fluxing occurs really first, samples were taken from the Brabender mixer, while a run was underway and examined in term of color. At the fluxing point, the sample was still yellow (initial color). This is due to the non-decomposition of the ABFA, which is an orange powder, and when blended with PVC, it will result in yellow dry-blend. The later will turn white after decomposition of the BA

### **III.3.2 Specific gravity**

Specific gravity is one of the most important properties for rigid PVC foam.

For the determination of the specific gravity, ASTM standard D-792-91 was used.

Tests were performed at temperature :  $23^{\circ} \pm 2^{\circ}\text{C}$  and humidity:  $50 \pm 5\%$ .

Samples were cut with a band saw

Mass: 5 to 11 grams.

### III.3.3 Foaming efficiency (Extrusion)

All the formulations are extruded on the co-rotating twin screw extruder (Battenfeld) with L/D=25

A profile die is used in order to extruded 4 mm (diameter) profiles.

The parameters are :

- Screw speed: 20-50 rpm
- back pressure : 90 psi
- Feed speed : 200 (Kg/hour).
- Temperatures profile (see table III.2).

**Table III.2:** Temperature profile

Transport zone (°C)	Transition zone (°C)	Metering zone (°C)	Head (°C)	Die (°C)
150	170	180	180	180

### III.3.4 Micrography

#### III.3.4.1 Optical Microscope.

Considering that cell structure determines some of the foam physical properties of the foam, an optical microscope was used to look at the cell structure. Using this apparatus, we can observe the difference in size/appearance of the cells inside the PVC profile and close to the skin.

#### III.3.4.2 Liquid nitrogen break

Samples were prepared by cutting them with a band saw, and by cooling them in liquid nitrogen before breaking them in half.

#### III.3.4.3 Microtoming

Samples were microtomed at room temperature with a tungsten carbide blade to produce thin sections for optical microscopy.

Thin section from 5 to 10  $\mu\text{m}$  were collected.

**N.B:** All samples showed cells distortion toward the edges of the extrudates, not only due to the cell expansion, but also to the deformation during microtoming.

### III.3.5 Mechanical tests

Not having been able to obtain standardized samples, because of the unavailability of an extrusion die having rectangular cross section, and considering that the study is a comparative one, we have chosen a foamed PVC profile with circular cross section, obtained from a rod die. The obtained extrudates were then cut according to the

lengths intended for the mechanical tests: 14 cm for tensile specimens and 8 cm for impact ones.

### III.3.5.1 Method of STUDENT

Not being able to make a standardized study of the mechanical properties, we have worked out a comparative study while trying to minimize uncertainties as well as possible being able to affect the results. For that, one considered it useful to use the method of STUDENT for the calculation of the standard deviation and the standard error:

- Calculation of arithmetic nature:

$$\bar{X} = \frac{\sum_{i=1}^n X}{N} \quad (7)$$

$X_i$  : Experimental value

$n$  : A number of tests

- Calculation of the standard deviation:

$$\delta = \sqrt{\frac{\sum (X_i - \bar{X})^2}{n - 1}} \quad (8)$$

- Calculation of the standard error:

$$Er = \frac{t_{n-1} \cdot 0.95 \delta}{n} \quad (9)$$

0.95 : Confidence degree

$t$  : Critical value of the distribution of STUDENT

n	1	2	3	4	5
t	12.706	4.302	3.182	2.776	2.570

### III.3.5.2 Tensile tests

The extrudate samples, held between the two jaws of the tensile machine, were requested at a speed of 50 mm/min until the rupture.

#### III.3.5.2.1 The strain

The strain is the variation in the length with a respect to the initial length, always expressed in term of percentage:

$$\varepsilon = \Delta L / L_0 \quad (10)$$

$\Delta L$ : Defomation at a given time

$L_0$  : Initial length

#### III.3.5.2.2 The tensile stress

The tensile stress is the force referring to a given section at one given time of the test :

$$\delta = F/S \quad (11)$$

#### III.3.5.2.3 Elastic modulus

The elastic modulus or the Young's modulus is theratio of the stress to strain within the linear part of the stress-strain curve  $\delta = f(\varepsilon)$  :

$$E = \delta / \varepsilon \quad (12)$$

#### III.3.5.3 Impact tests

The impact is given to the center of the specimen, which is presented in the form of a circular rod, the resulted energy (U) is directly read on the graduated dial.

The impact strength is calculated according to:

$$a_k = U/s \quad (13)$$

U :Absorbed energy by the specimen ( j )

s: Cross sectional area of the specimen(mm<sup>2</sup>)

#### III.3.5.4 Hardness tests

It consists of the application via a calibrated spring of an effort tending to insert an indenter, of defined shape, in material to be tested, the penetration depth varies in opposite direction of hardness. The displacement of the indenter is read on a measuring graduated scale from 0 to 100.

#### III.3.5.4 Thermal tests

For the determination of decomposition temperatures of the BA, the thermal tests were elaborated on Perkin Elmer analyzer DSC, within a temperature range from 25°C to 250°C with a heating speed of 10°C/min and a sample weight of 6 mg.

## **CHAPTER FOUR**

### **PROCESSABILITY OF FOAMED RIGID PVC USING A BRABENDER PLASTOGRAPH**

## IV PROCESSABILITE OF FOAMED RIGID PVC USING BRABENDER PLASTOGRAM

### IV.1 Introduction

Many techniques have been reported as satisfactory for evaluation of solid chemical blowing agent systems [4-7], but they mainly refer to decomposition temperature and gas volume in the pure state. Works on the effect of formulated compound ingredients refer essentially to plastisol technology [8], and little information is available on decomposition under pressure [9,10]. Many researches have been reported using a Brabender torque rheometer on cellular PVC, for instance the evaluation of the hot melt properties of cellular plastisol [11], the dynamic heat stability of expanded semi rigid PVC [12], and the decomposition behavior of ABFA in rigid PVC compound [13]. Before discussing the data of the effect of BA on the processability of a rigid PVC compounds, a review of the Brabender torque rheometer process curve for an unfoamed rigid PVC compounds with critical points is necessary [14] (see Fig IV.1).

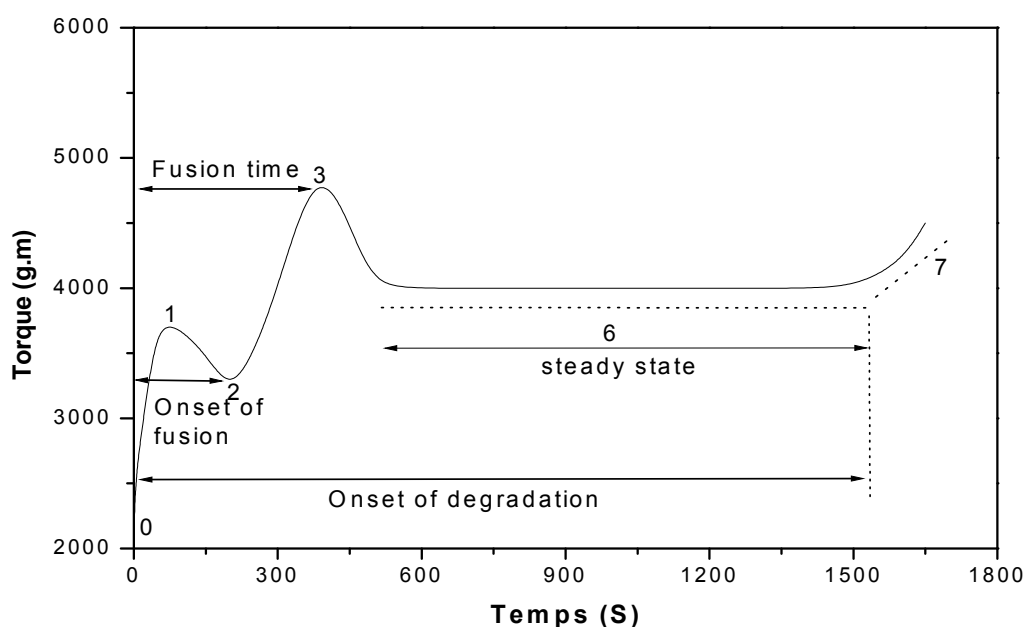


**Figure IV.1:** The brabender torque rheometer process curve for an unfoamed rigid PVC compound

Point 0 is the starting point: at this stage, the mixer was empty, i.e. a free rotation of rotors was taking place, resulting in zero torque. When a quick (sudden) loading chute was applied to compress the sample in powder state against the rotors, high torque value was temporarily recorded (point 1). Then the torque decreased rapidly due to free foaming of dry-blend particles, to reach a minimum value (point 2). Beyond this point, particles start to be fused resulting in a fused layer of the compound, limiting sample and metallic surfaces, where high shear stress were applied allowing torque to increase until (point 3). At this point, the compound is in a molten state (complete fusion) and still absorbing heat, resulting in the reduction of viscosity of the system, hence, torque decreased till point 6. This point is the position of the curve referred to as equilibrium. At this stage, the melt is homogeneous.

Point 7 is defined as the onset of cross linking or degradation. It determines the ultimate stability of the compound. This point is defined by the intersection of the slope of the difference between degradation time (point 7) and the fusion time (point 3) [14].

**N.B.** The passage from pt. 3 directly to pt. 6 is justified by the fact that expanded formulations will present two critical points (point 4 and point 5) before the equilibrium portion (point 6) which can be seen in figure IV.2.

## **IV.2 Processability on foamed rigid PVC**

### ***IV.2.1 Effect of the addition of ABFA on the plastograph of rigid PVC.***

As shown in Figure IV.2 which presents the Brabender plastograph of rigid PVC without a blowing agent and that of a formulation with 0.6 phr of ABFA, we note the appearance of a new peak right after the fusion peak. So this new peak (point 5) is attributed to the addition of ABFA [53].

For a better understanding of this new peak, the plastographs of the unfoamed formulation and that of the expanded one are presented on the same graph. Samples were taken at these critical points and examined in terms of color and density.

For the first part of the plastograph, there is almost no difference between the two curves before fusion (point 3) and the samples taken at this point are completely fused and have a similar density but different colors. The formulation containing ABFA is yellowish but the one without the blowing agent is white. The addition of ABFA results in a rapid fall in the torque after the fusion point (point 3). This is directly related to the heat released by the exothermic decomposition reaction which causes a rise of the temperature accompanied by a decrease in the viscosity resulting, therefore, in a decrease in the torque.

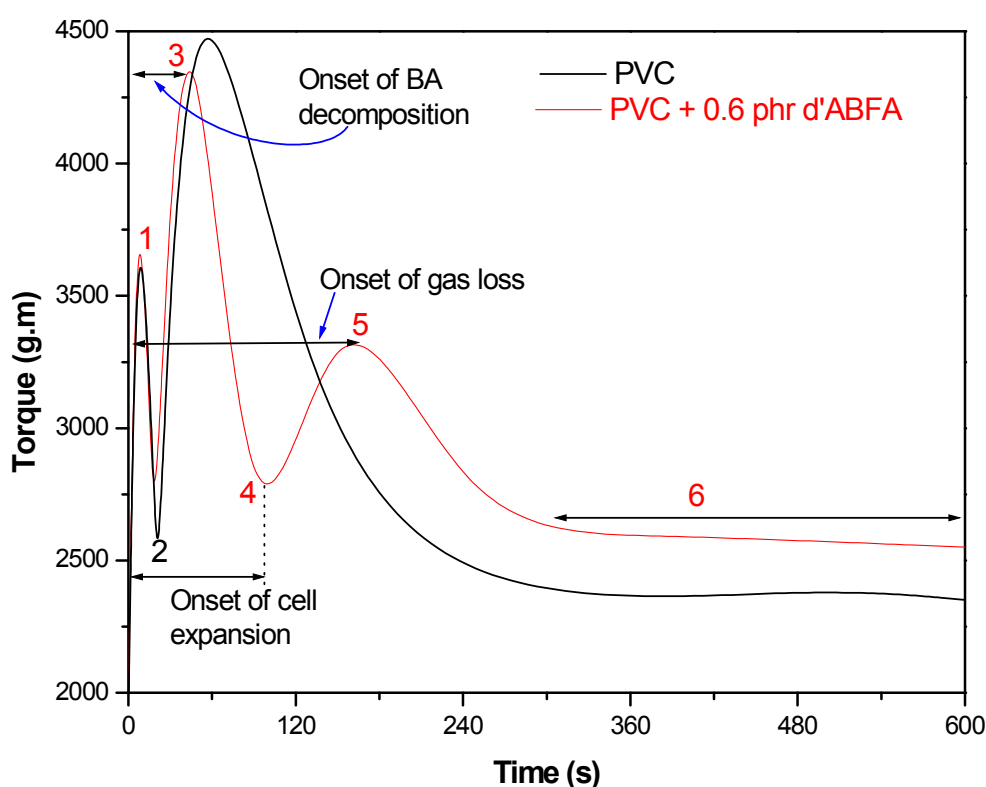


**Figure IV.2:** Torque evolution as a function of time.

This explanation is supported by the change in color from yellowish which indicates the presence of non-decomposed ABFA, to the white color indicating BA decomposition [53].

At point 4, it is deduced that the value of the minimum torque marks the end of the exothermic decomposition of ABFA and the onset of the expansion



process. This means that the cells which have been dissolved in the molten polymeric matrix start expanding. This expansion causes an increase of the pressure, leading therefore to an increase of the torque up to point 5. This assumption is supported by the important decrease of the density of the samples taken at this point (see Figure IV.3).

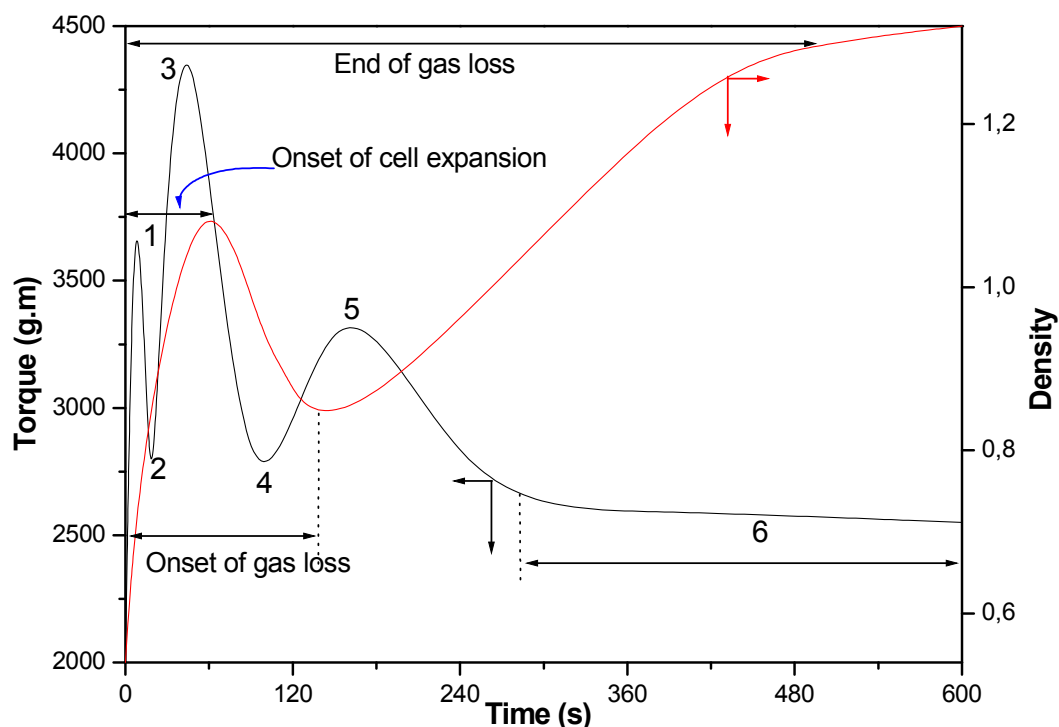


**Figure IV.3:** Torque and density evolution as a function of time (0.6 phr ABFA).

Beyond point 5, a steady decrease of the torque is noted. This is due to the fact that part of the gas escaped from the bulk to the atmosphere. The escape of the gas, which is a result of the cell interpenetration caused by a high shear deformation, leads to the decrease of the internal pressure until the major part of the gas would have escaped. This assumption was also supported by the increase in the density of the samples taken at this point [53].

At the equilibrium leveling off (point 6), the value of the torque for the formulation containing ABFA is higher than that of the one without the BA. This could be due to the presence of small cells from which gas could not escape

easily and to the partial premature cross-linking caused by the exothermic decomposition of ABFA that resulted in an increase of the pressure leading to a slight rise in the torque.

On the other hand, the increase in torque (after point 4) reported by C. BENNING & Col [13] was attributed to cross linking, which is due to free radicals generated during decomposition of ABFA; while the decrease in torque indicated degradation or slippage which is due to lubricants being present [13] (see Figure II.1).

#### **IV2.2 Effect of ABFA concentration of the rigid PVC plastograph:**

As shown in Figure IV.4, the time was not almost affected by the increase in the ABFA concentration at the point corresponding to the fusion (point 3). Whereas, the torque was reduced when increasing BA concentration from 0.6 to 1.2 phr. This could be attributed to an earlier decomposition of fraction of BA located at the fused layer of the compound, limiting sample and metallic surfaces, where particles start to be fused at an earlier stage (where high shear stresses were applied).

After the fusion point (point 3), increasing the ABFA concentration from 0.6 phr to 1.2 caused a rapid drop in the torque. This is attributed to the greater amount of heat released upon the exothermic decomposition, leading to a more rapid and higher increase in the polymeric matrix which reduced the viscosity, resulting in a rapid decrease in the torque to lower values (point 4).

It is noted that the higher the concentration of ABFA the more point 5 shifts (right hand side) with respect to time. The reason is that, at higher gas content (higher cell number) the time of gas to escape to the atmosphere became longer, hence, higher torque.

At point 6, the higher the concentration of ABFA the higher the difference between the values of the torque at the equilibrium leveling off. This could be due to the larger number of cells which are trapped inside the polymeric matrix, and to the premature partial cross-linking caused by a higher exothermicity.

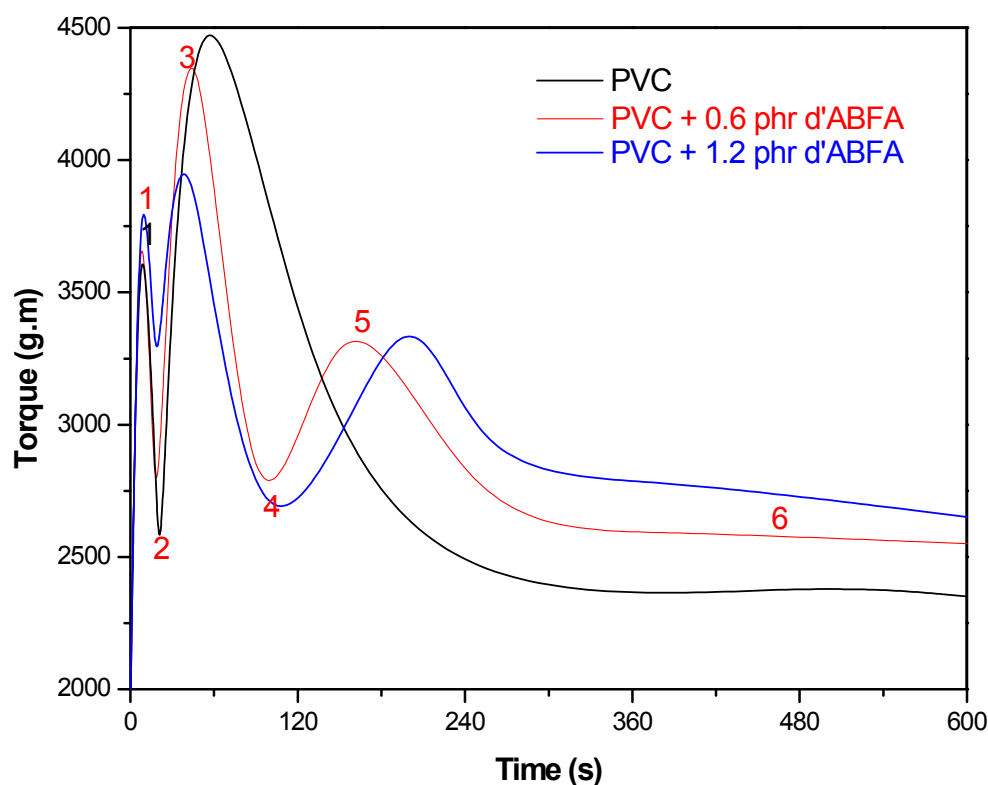


**Figure IV.4:** Torque evolution as a function of time (0.6 phr ABFA, 1.2 phr ABFA and without ABFA).

At the degradation point (point 7), the higher the BA concentration the lower the stability time causing therefore, a rapid degradation (see figure IV.5).

This is due to the amount of heat generated by the exothermic decomposition which would raise the temperature polymer matrix, and to the adverse effect of the residue which is shown in figure IV.6 where we see that the higher the amount of ABFA residue, the shorter is the stability time.

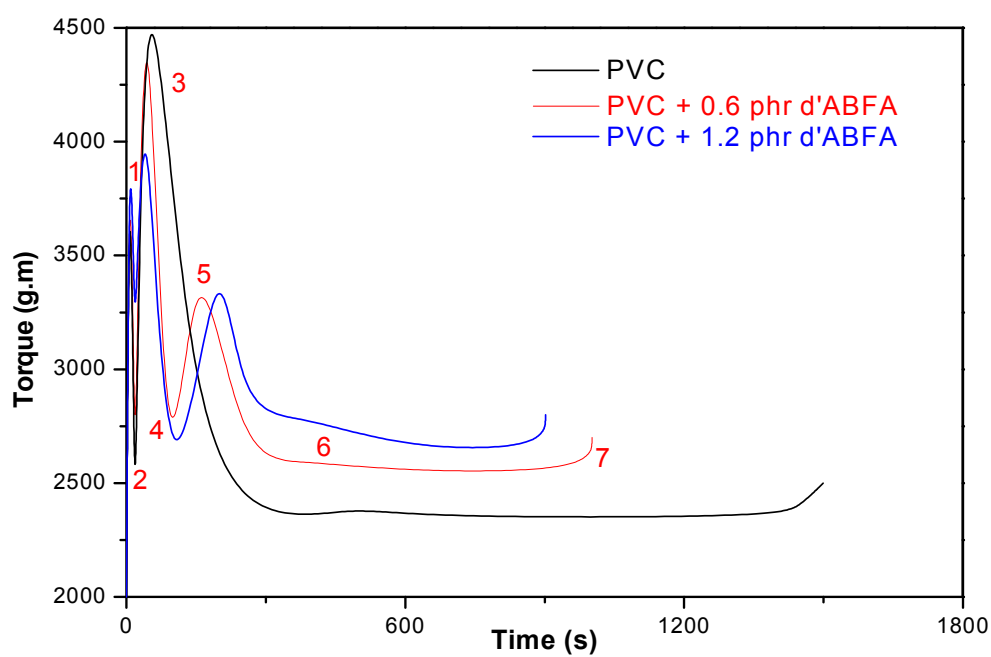


**Figure IV.5:** Torque evolution as a function of time (0.6 phr ABFA, 1.2 phr ABFA and without ABFA).

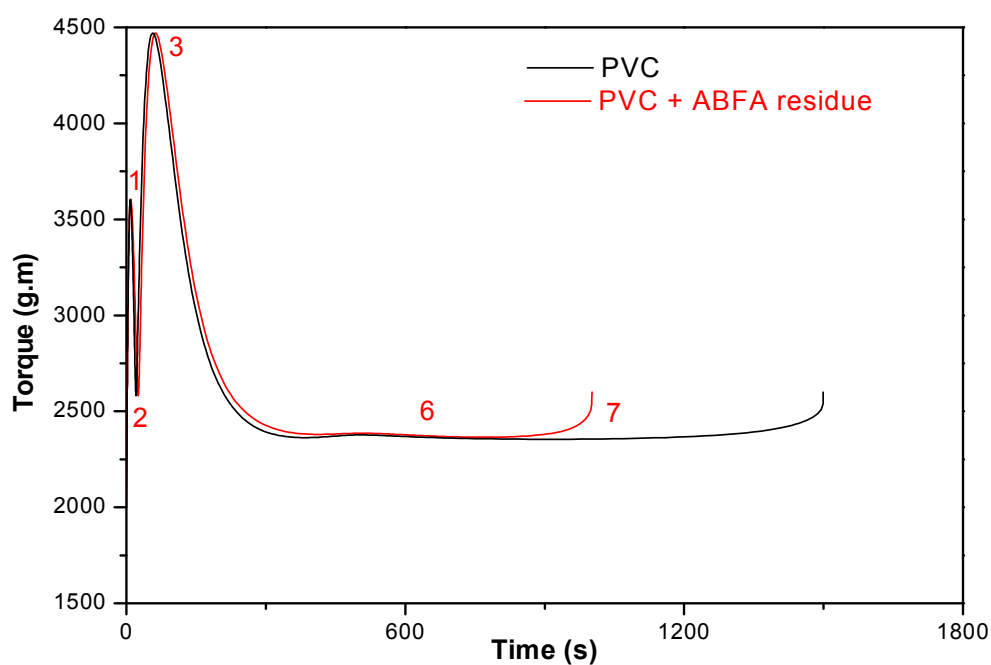


**Figure IV.6:** Torque evolution as a function of time (PVC, PVC +ABFA residue).

On the other hand, the reduction of the stability time was noticed to be more pronounced when exceeding 0.6 phr of BA concentration (see figure IV.7). This could be attributed to the fact that 0.6 phr is a critical concentration corresponding to the critical amount of heat generated by the exothermic decomposition of BA at which PVC degradation is more accelerated. This assumption is in good agreement with what was supposed before: The torque at the fusion (point 3) was reduced when increasing BA concentration from 0.6 to 1.2 phr, and was attributed to an earlier decomposition of fraction of BA located at the fused layer of the compound, limiting sample and metallic surfaces, where particles start to be fused at an earlier stage (where high shear stresses were applied).

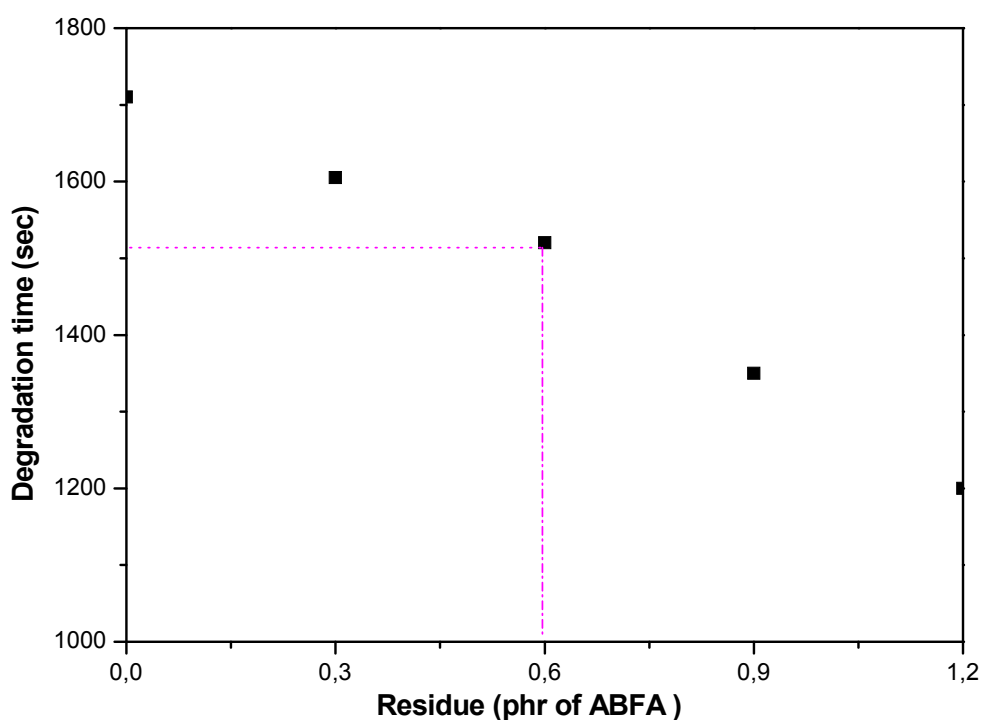


**Figure IV.7:** Thermal stability time as a function ABFA residue concentration.

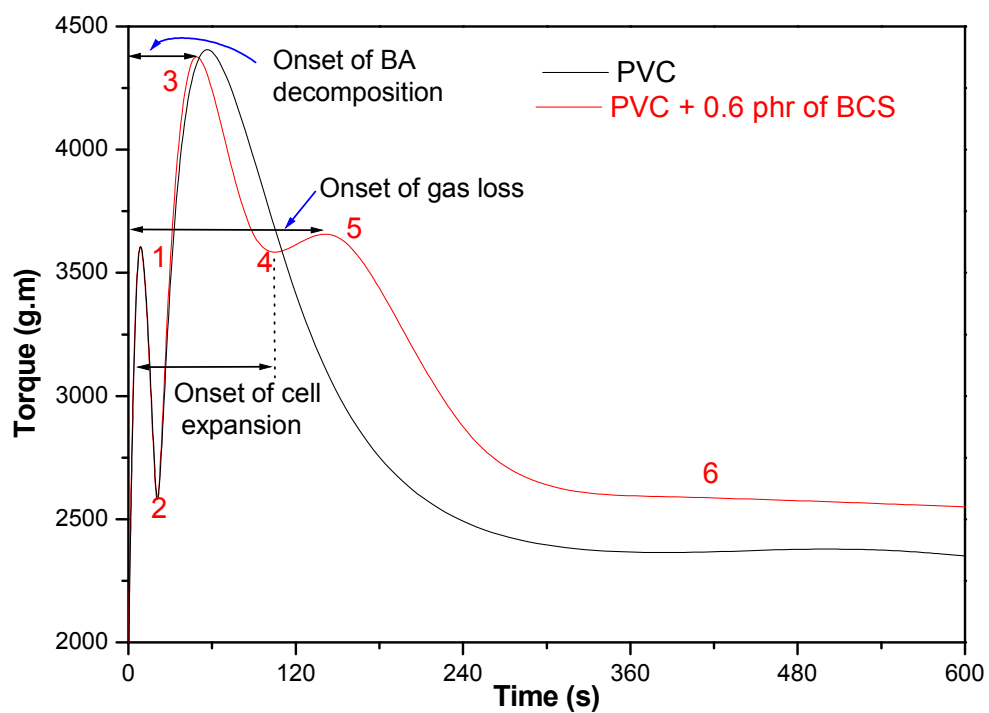
### **IV.2.3 Effect of the addition of SBC on the plastograph of rigid PVC.**

Figure IV.8 presents the plastograph of the formulation containing 0.6 phr SBC and that of the one without a blowing agent. It is seen that before the fusion point (point 3), there is almost no differences in terms of torque in time between the two curves.

After the fusion point (point 3) we were expecting a low decrease in torque for the formulation containing the BA owing to the endothermicity of the decomposition reaction of SBC. In fact, the drop in the torque was much higher. This could be due to namely the decomposition of the first SBC particles that are in contact with the overheated metallic surfaces of the mixer chamber. These particles upon decomposing created micro cells around, resulting in the decrease of the contact area between the polymeric matrix and the metallic walls of the mixer chamber, thus leading therefore to low shear stress.

Point 4 marks the end of the endothermic decomposition of SBC and the onset of the growth of the cells, and consequently the increase in the internal pressure of the polymeric matrix, leading therefore to a small increase of the torque up to point 5. This is confirmed by the low density of the sample taken at this point (see Figure IV.9). The increase in the torque does not last long because of the breaking up of swollen cells, leading hence to a decrease of the torque after point 5. This decrease leads to an increase in the sample's density. At the equilibrium leveling off (point 6) the value of the torque of the foamed formulation is higher than that of the one without the blowing agent. This could be due to the presence of some cells that remain trapped inside the melt.

On the other hand, the substitution of ABFA (which exhibits an exothermic decomposition reaction) by SBS (which decomposes endothermically) has proven that there is no cross-linking related to the increase in torque reported by C. BENNING & Col [13].



**Figure IV.8:** Torque evolution as a function of time (0.6 phr SBC and without SBC).

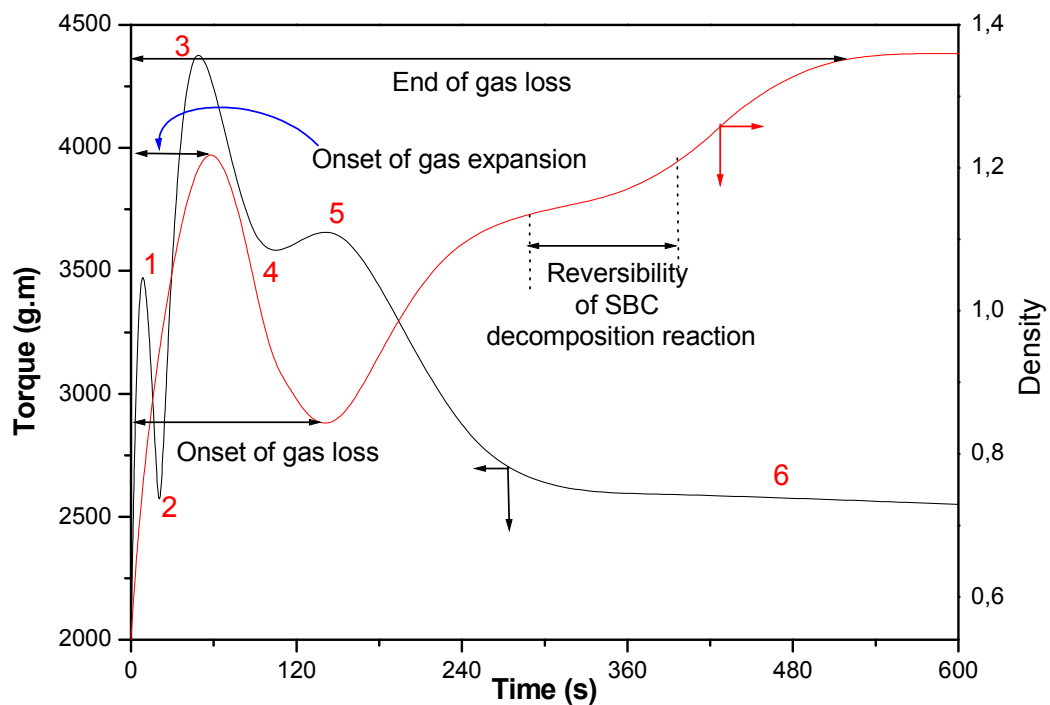


**Figure IV.9:** Torque and density evolution as a function of time (0.6 phr SBC).

#### **IV.2.4 Effect of SBC concentration on the rigid PVC plastograph.**

Before the fusion point (point 3), there is almost no differences between the two superposed curves presented in Figure IV.10 which shows the plastograph of the formulation containing 0.6 phr SBC and that of the one with 1.2 phr SBC.

After the fusion point, the drop in the torque becomes more pronounced as the concentration of SBC reaches the value of 0.4 phr. This is attributed to the formation of micro cells at the metallic surfaces of the mixer chamber and the rotors leading to a decrease in the torque. This combined with the endothermicity of SBC decomposition, would cause a further increase of the torque.

As we go from a concentration of 0.4 phr SBC to 1.2 phr, the decrease in the torque gets slower. In this case, the endothermicity of the BA decomposition starts to predominate over the formation of micro cells because of the increase of the amount of SBC. The torque decreases to point 4 which corresponds to the end of the decomposition of the BA and the onset of the growth of the cells. Then it increases at the same rate up to point 5, for both formulations even though the value of the torque for the formulation with 1.2 phr SBC is higher and shows a shift with respect to time. This is due to the high number of cells formed which will increase the pressure inside the polymeric matrix and will take more time to escape to the atmosphere.

At the equilibrium leveling off (point 6), the torque of the formulation containing 1.2 phr of SBC is slightly higher. This is attributed to the high number of the cells that remain trapped inside the polymeric matrix.

As shown in figure IV.11, at point 7 which marks the degradation of the material, we note that the higher the concentration of SBC the longer is the stability time. This is explained by the endothermicity which cools down the system during the decomposition.



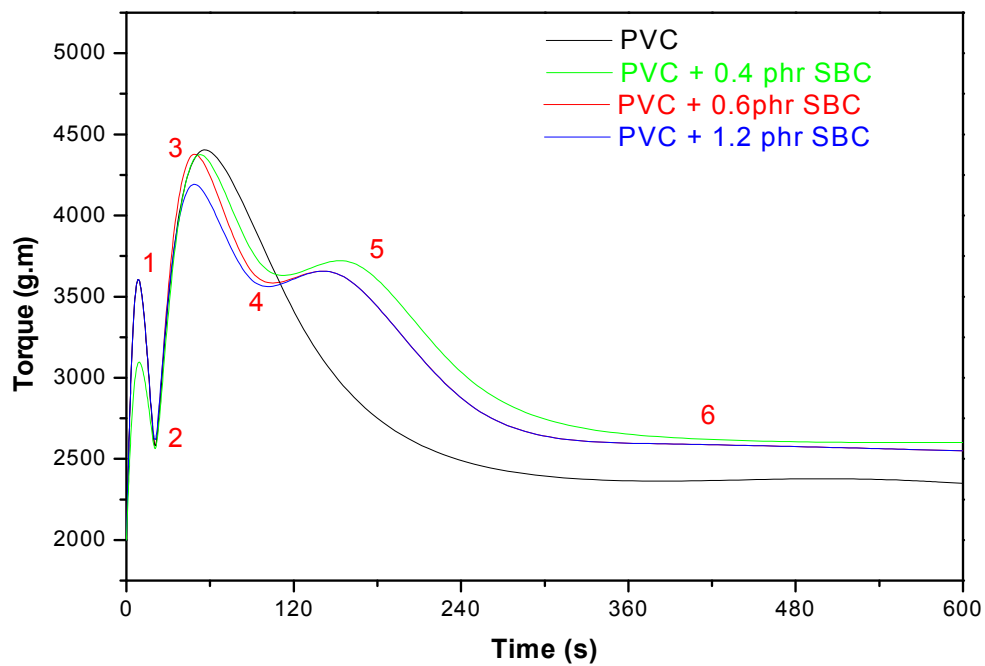


**Figure IV.10:** Torque evolution as a function of time (0.4, 0.6, 1.2 phr SBC and without SBC).

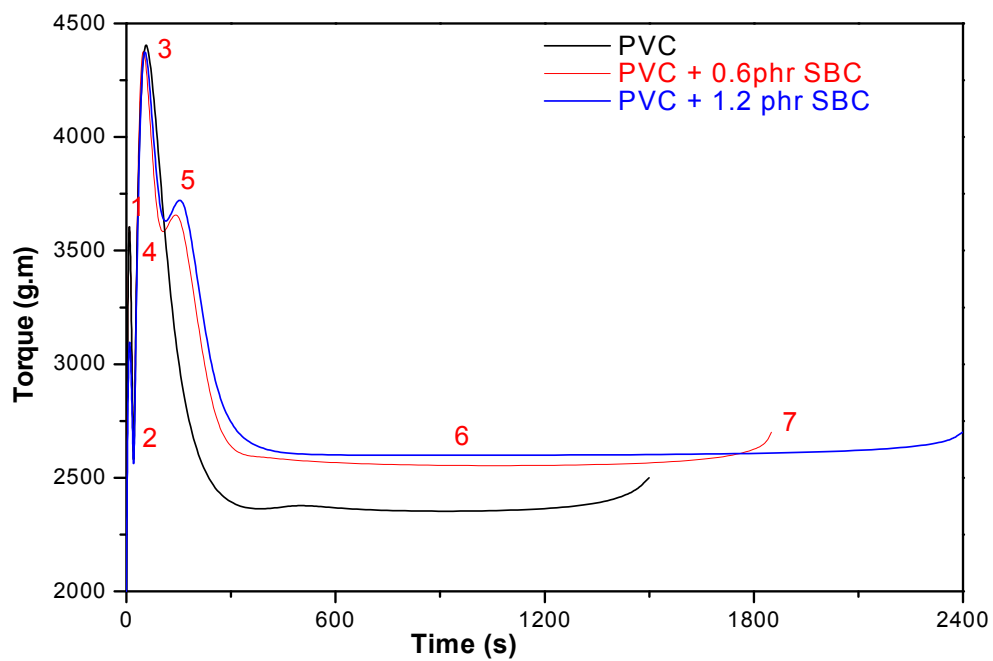


**Figure IV.11:** Torque evolution as a function of time (0.6, 1.2 phr SBC and without SBC).

### Comparison between the effects of the two types of BA:

1. As was seen in Figure IV.12, at point 3 the drop in the torque for the ABFA based formulation is higher than that for the formulation containing SBC because of the exothermicity of the decomposition reaction of ABFA which reduces the viscosity of the system.
2. The differences in the values of the torque at point 4 are directly related to the decomposition mode whether it is exothermic or endothermic.
3. At point 5 the drop in the torque for the SBC based formulation is more rapid than that of ABFA because the cells formed by SBC are random and not uniform, therefore they break up easily but those formed by ABFA are smaller and uniform.
4. The torque at point 6 for the formulation containing ABFA is higher than that of SBC. This is due to the fact that the cells formed by ABFA which are smaller and uniform remain inside the polymeric matrix; however those formed by SBC are random and not uniform and will escape easily to the atmosphere.

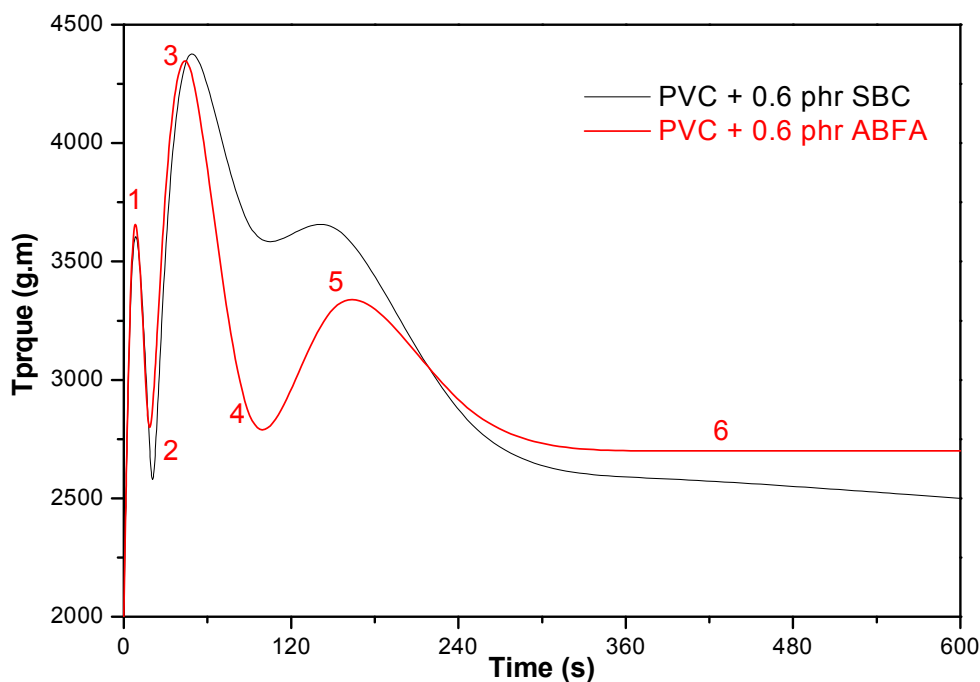


**Figure IV.12:** Torque evolution as a function of time (0.6 phr SBC and 0.6 phr ABFA).

5. The effect of the residue from SBC is shown in Figure IV.13. This residue seems to have no effect owing to the decomposition products which have rather a neutral effect on the thermal stability.

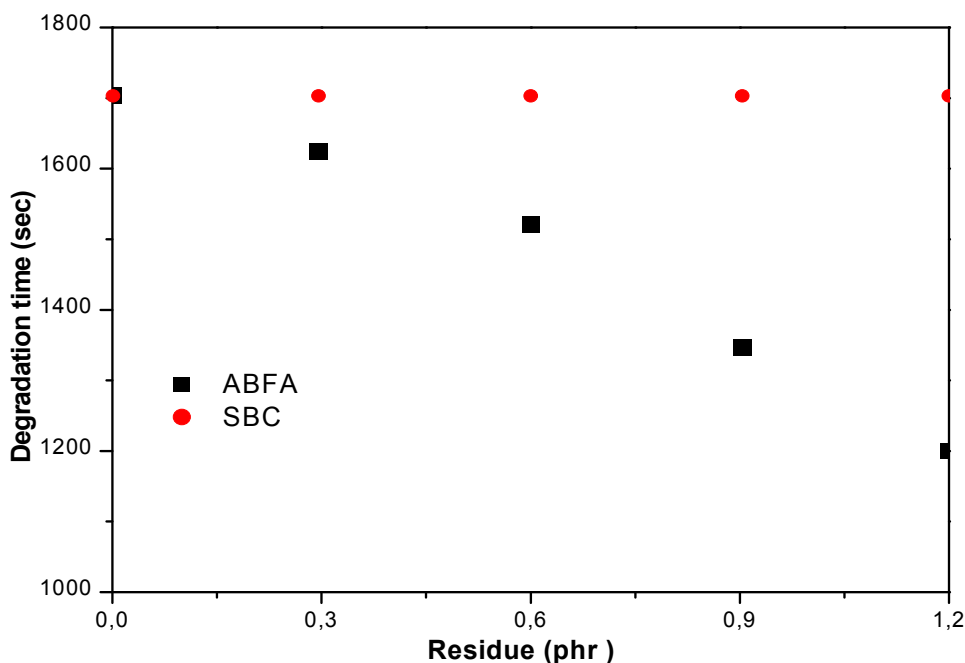


**Figure IV.13:** Thermal stability time as a function of SBC and ABFA residue concentrations

#### IV.2.5 Effect of the mixture of ABFA and SBC on the rigid PVC plastograph.

As shown in Figure IV.14, before the fusion point there is almost no differences between the curves corresponding to the formulation containing a mixture of 0.3 phr of ABFA and 0.3 phr of SBC, and the one without any BA.

After the fusion point (point 3), it is observed that the torque for the formulation containing the mixture of the two BA drops rapidly and two peaks appear (point 5 and 5') as a result of the addition of the two BA [53].

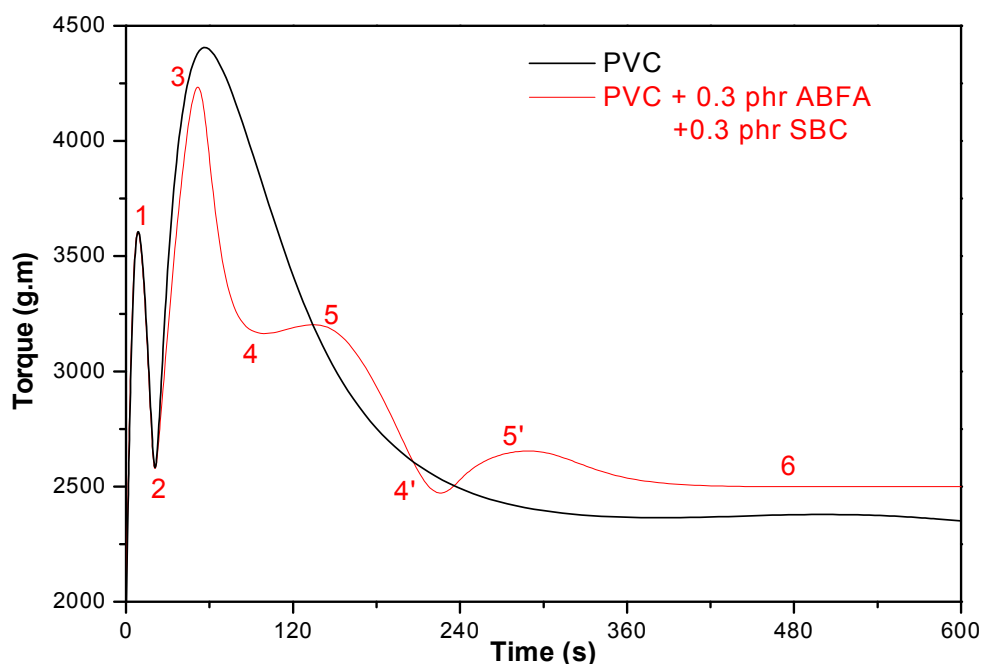


**Figure IV.14:** Torque evolution as a function of time (0.3 phr SBC + 0.3 phr ABFA).

For a better interpretation of the results, it was necessary to attribute each peak (point 5 and 5') to its BA, through an arbitrary variation of the concentration of the BA in the mixture; knowing that the higher the BA concentration the higher the peak (torque) at point 5 or 5' that represent the expansion of gas released by the BA. This was done by decreasing of ABFA concentration and keeping that of SBC constant in the first time. Then decreasing of SBC concentration and keeping that of ABFA constant in the second time. In this context, figure IV.15 shows that the first peak (point 5) is attributed to the decomposition of SBC and the second one (point 5') to that of ABFA.

The rapid fall in the torque after point 3 is due to the micro cells and the exothermicity of the decomposition reaction of ABFA which were predominant over the endothermicity of the decomposition of SBC [53].

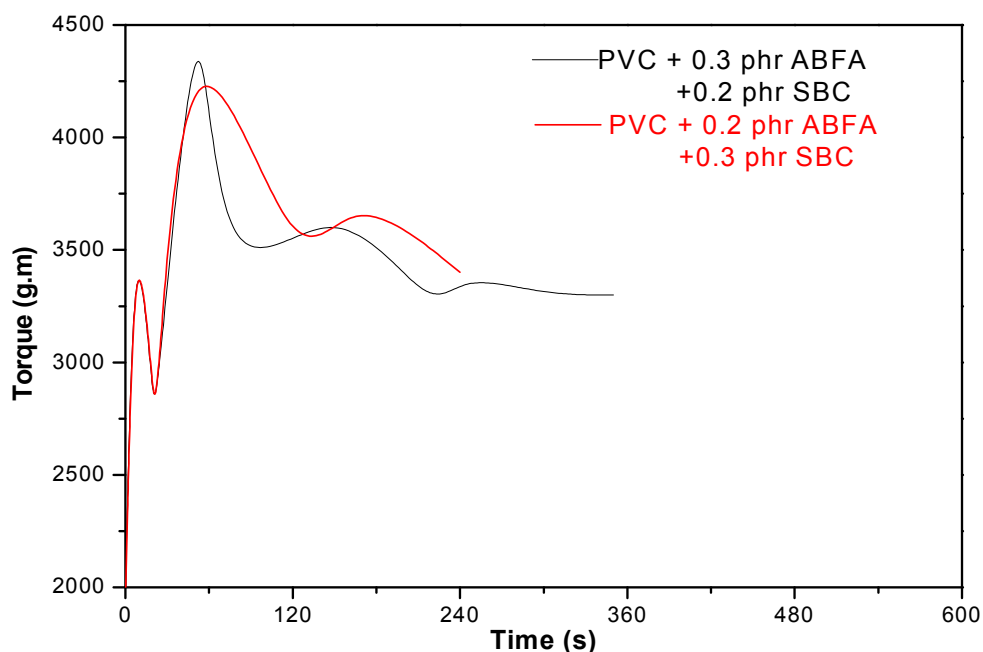


**Figure IV.15:** Torque evolution as a function of time (concentration mixture of BA ).

At point 4, the mixture of the two BA gave rise to an intermediate effect between that of ABFA and that of SBC. This is due to the combination of the exothermicity with the endothermicity of the ABFA and SBC respectively, where the first of which tends to lower the torque while the second tends to raise it.

Point 4 marks the end of the endothermic decomposition and the onset of the growth of the random and non uniform cells which will increase the torque up to point 5. This increase in the torque was confirmed by the decrease in the density of the samples taken at this point (see Figure IV.16). These cells would allow the escaping of the gas owing to their form and distribution resulting in the decrease in the torque after this point. This decrease of the torque is also supported by the slight increase in the density of the samples taken at this point. At this point the exothermic decomposition of ABFA initiates the decrease in the torque down to a minimal point (point 4'), which marks the end of the exothermic decomposition and the onset of the growth of the uniform cells. The torque increased up to point 5' above which it started to decline because of the breaking up of the cells leading to an increase of the

density of the samples. The shift of the time of point 4' and point 5' with respect to point 4 and point 5 for the formulation containing ABFA is due to the endothermicity which precedes these two points and which cooled the system down causing the delay of the decomposition of ABFA (ABFA decomposition is temperature dependent). At the stability leveling off (point 6), the torque of the formulation containing the BA is higher than that of the formulation without a BA because of the remaining cells inside the polymeric matrix.

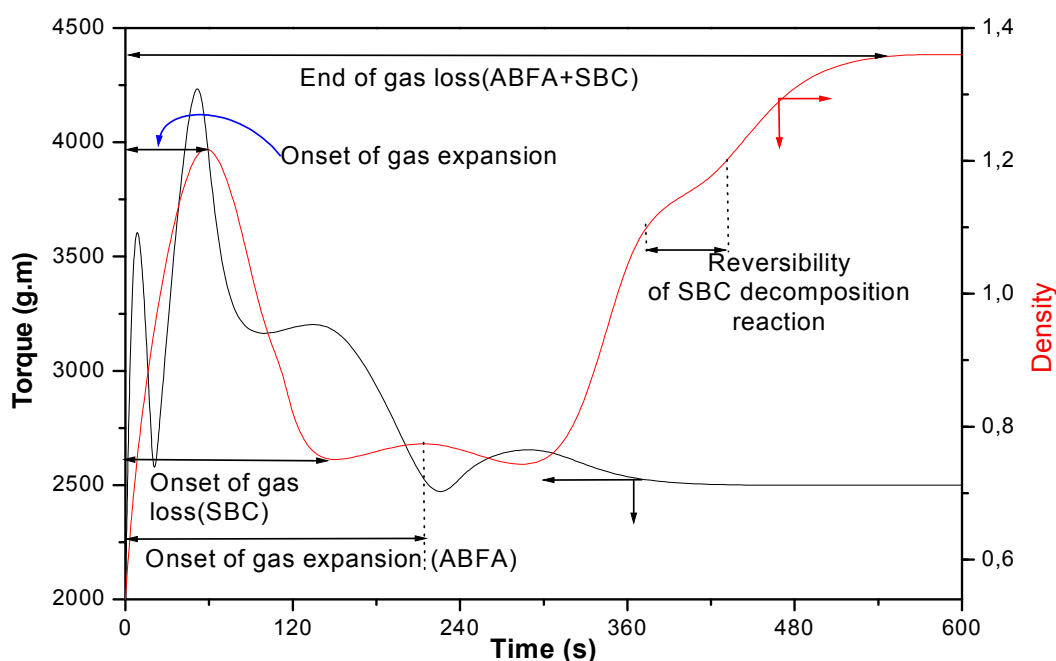


**Figure IV.16:** Torque and density evolution as a function of time (concentration mixture of BA ).

#### IV.2.6 Effect of the concentration of ABFA and SBC mixture on the rigid PVC plastograph

Figure IV.17 presents the superposition of the three plastographs namely that of the formulation containing 0.3 phr of ABFA and 0.3 phr of SBC, that of formulation containing 0.6 phr ABFA and 0.6 phr SBC, and that of formulation without any BA.

At point 3 the torque decreases rapidly as the concentration is increased. This is attributed to the exothermicity of the decomposition reaction of ABFA which over dominates the endothermicity. Then, as the amount of ABFA diminishes the torque falls down to point 4 which marks the end of the endothermic decomposition of SBC

allowing a slight decomposition of ABFA and the onset of the growth of the cells. This process will cause an increase of the torque up to a value lower than that of the formulation containing 0.3 phr of ABFA and 0.3 phr of SBC (point 5). This increase is due to the exothermicity that gets more pronounced causing an increase in the temperature and consequently a decrease in the viscosity. Starting from point 5 the cells start to break up allowing the escape of the gas resulting therefore in a decrease of the torque down to point 4', where the exothermic decomposition ends and the growth of the cells restarts. This growth will cause an increase in the torque up to point 5' after which it will decrease steadily, owing to the uniformity of the cells, down to the stability leveling off (point 6).

At point 6 the value of the torque for the higher concentration is higher, this is attributed to the great number of cells that remain trapped inside the polymeric matrix and to the partial premature PVC cross-linking resulted from exothermic decomposition of ABFA.

As shown in Figure IV.18, it is noted that at point 7 (the degradation point) the higher the concentration of the mixture the lower the stability time. This is due to the exothermicity which caused a rise in the temperature and also to the adverse effect of the ABFA residue on the thermal stability (See Figure IV.19).

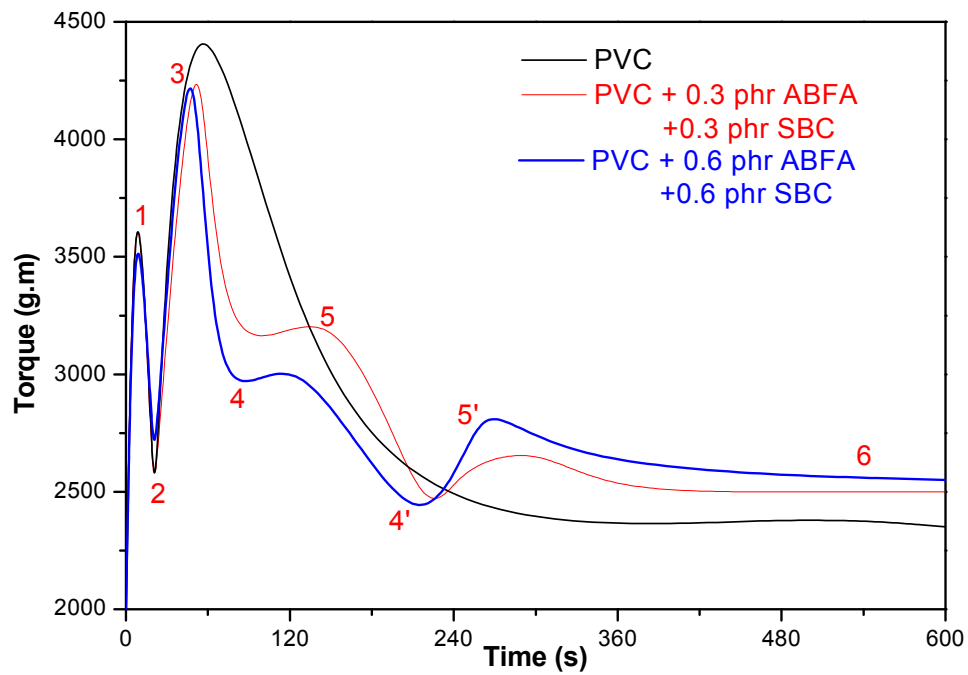


**Figure IV.17:** Torque evolution as a function of time (concentration mixture of BA ).

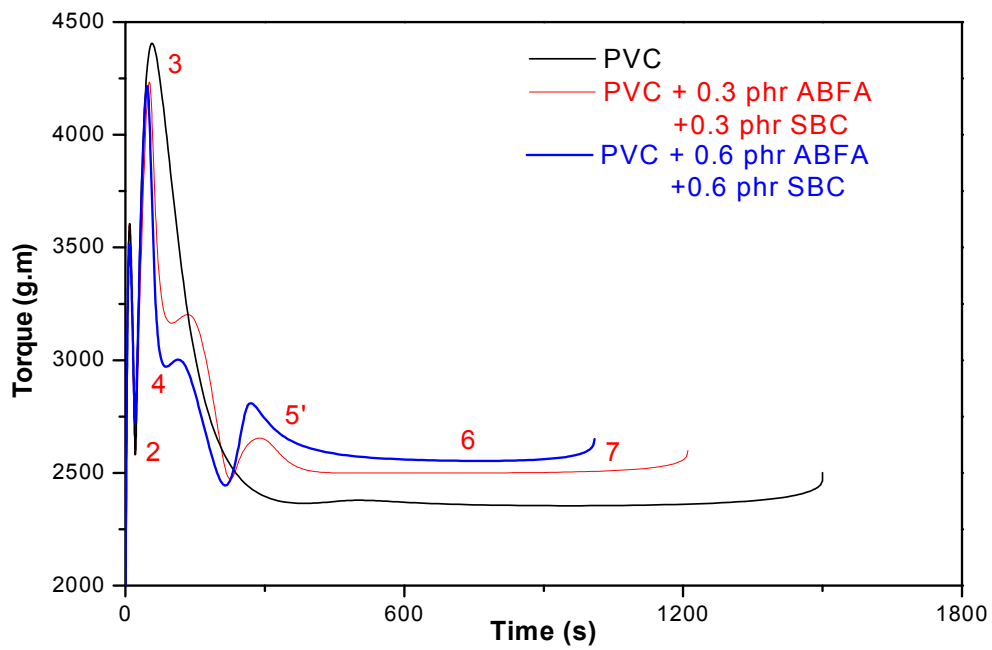


**Figure IV.18:** Torque evolution as a function of time (0.6 and 1.2 phr BA mixture)



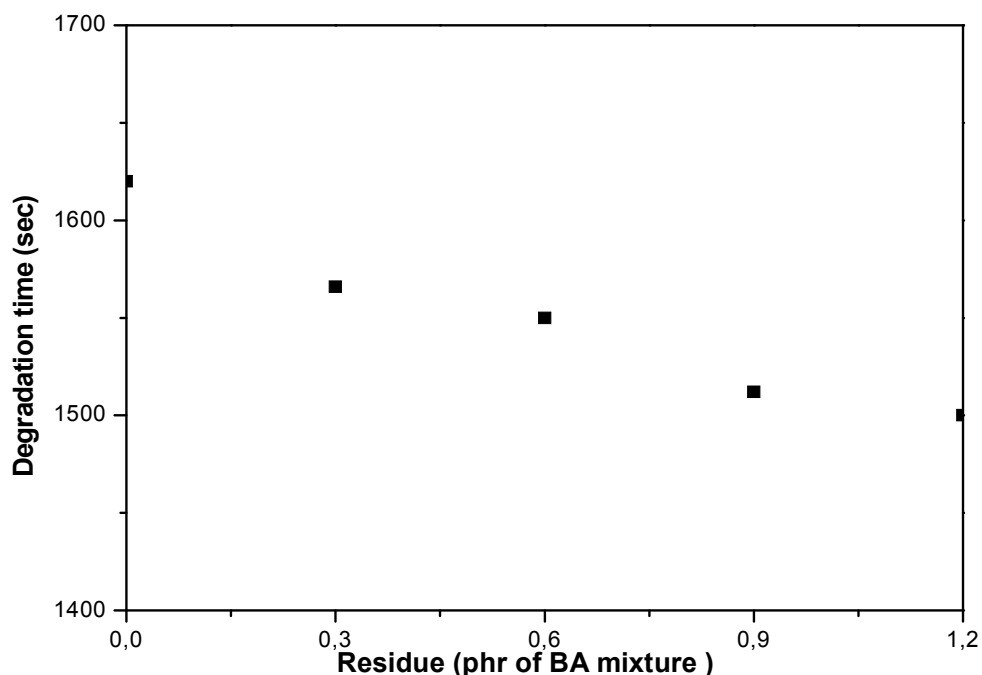


**Figure IV.19:** Thermal stability time as a function BA mixture residue Concentration

### IV-3. Differential Scanning Calorimetry (DSC)

#### V-3-1. DSC thermogram of ABFA.

The thermograph which is presented in figure IV.20 shows that ABFA decomposes at 220° C, a temperature higher than the processing temperature that was used in the BRABENDER plastograph (180° C). Such a processing temperature would not be high enough for the decomposition temperature with the addition of kickers (thermal stabilizers). As shown in figure IV.21, these kickers have in fact lowered the decomposition temperature down to 165° C.

#### V-3-2. DSC thermogram of SBC.

Contrarily to ABFA, the SBC thermogram showed that it decomposes at lower temperature without being activated. This decomposition temperature, measured from the endothermic peak which is shown in figures IV.22 and IV.23 was found to be 150°C. This would make the decomposition possible at the processing temperature (180° C) using the BRABENDER plastograph.

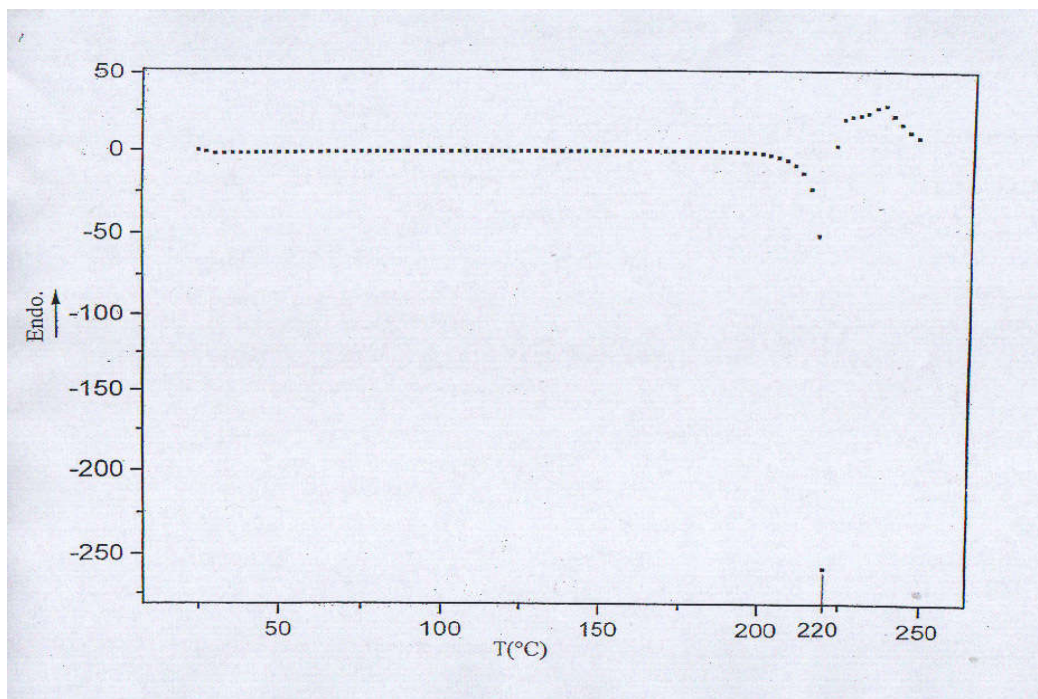


**Figure IV.20:** DSC thermogram of ABFA

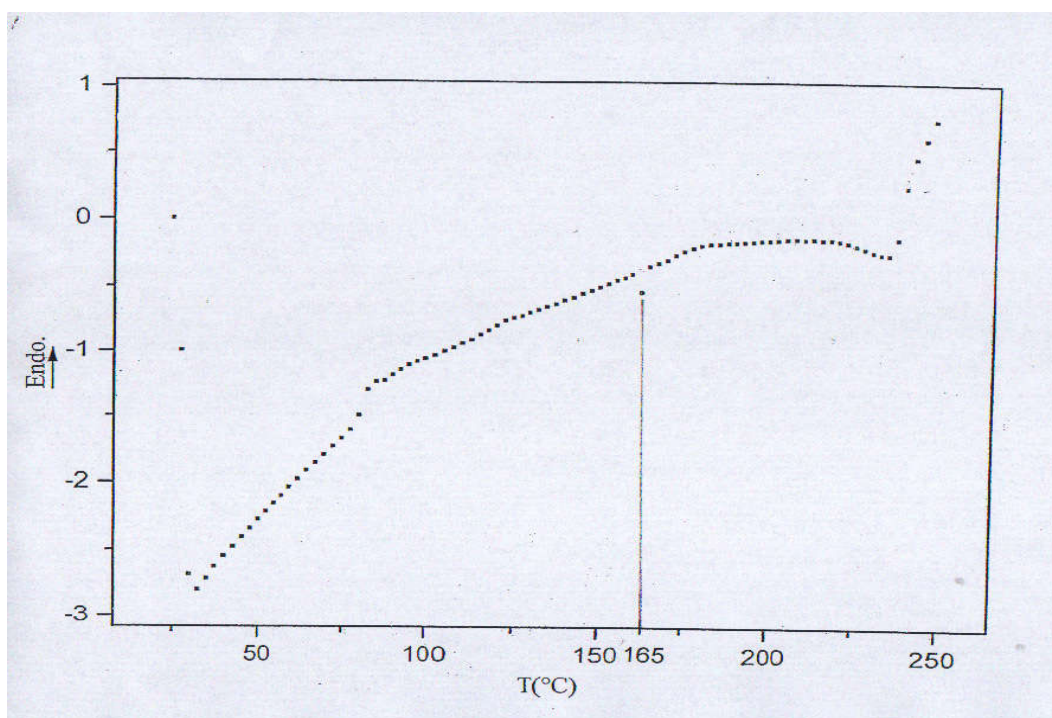


**Figure IV.21:** DSC thermogram of ABFA within formulated PVC

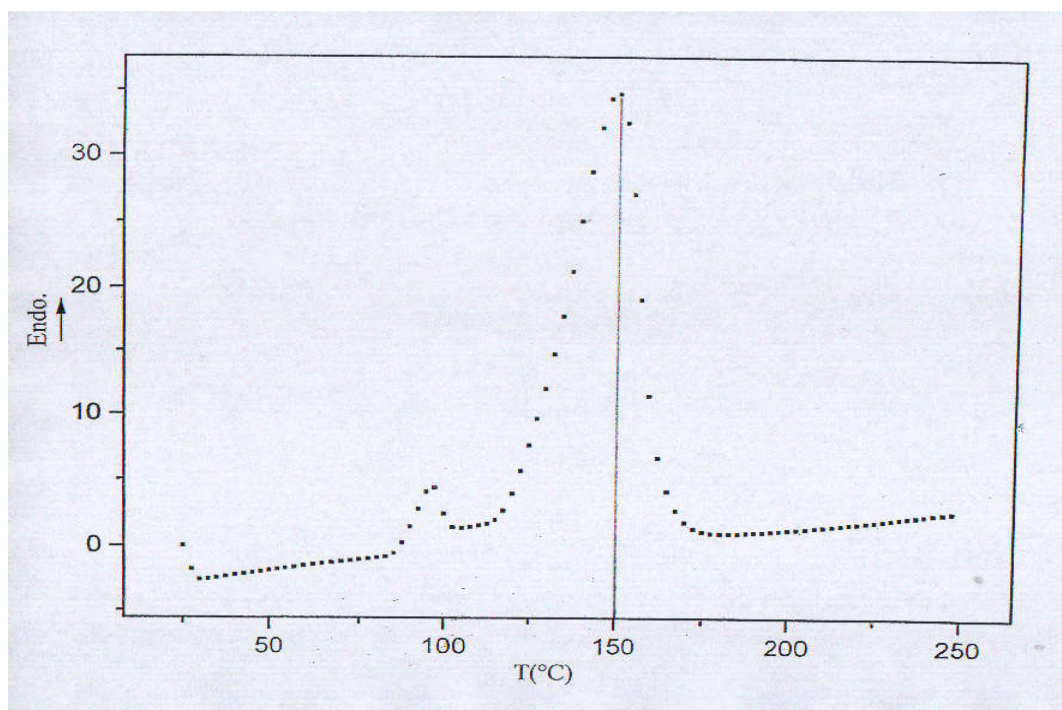


**Figure IV.22:** DSC thermogram of SBC.

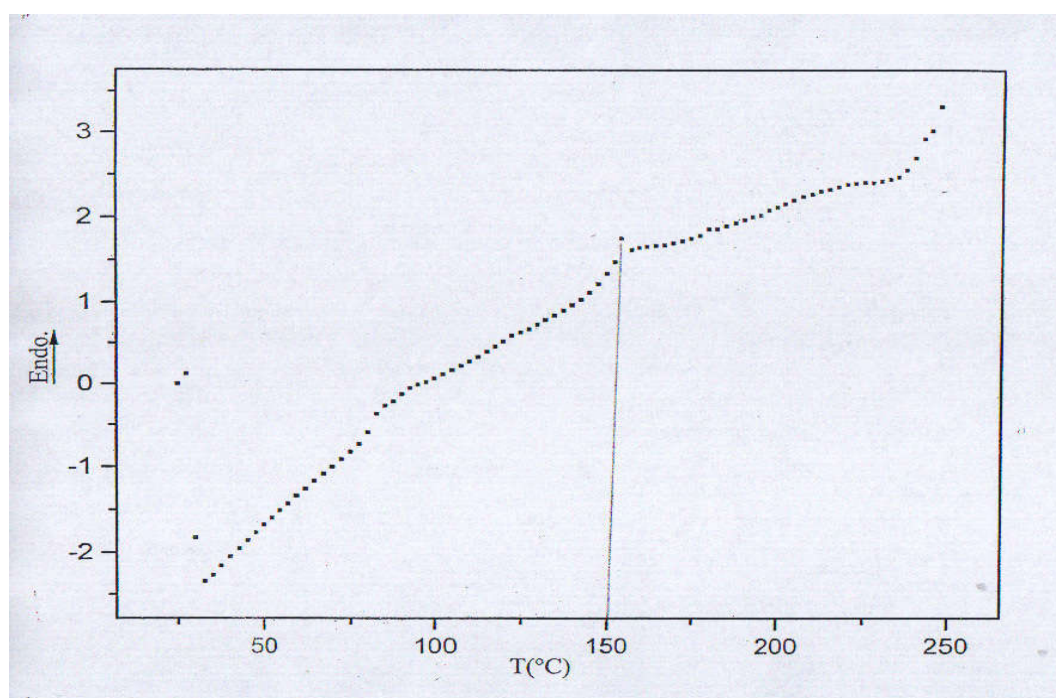


**Figure IV.23:** DSC thermogram of SBC within formulated PVC



### V-3-3. DSC thermogram of the mixture (ABFA+SBC).

The thermogram represented in figure IV.24, showed that the decomposition of the two BA when mixed together within a rigid PVC formulation containing kickers, takes place at different temperatures. It was noticed that the decomposition temperature of SBC exhibited almost no change ( $148^{\circ}\text{C}$ ) compared when used alone ( $150^{\circ}\text{C}$ ). Whereas, that of ABFA was found to increase from  $165^{\circ}\text{C}$  (when used alone) to  $172^{\circ}\text{C}$ . This is attributed to the endothermic reaction of SBC ( $T=148^{\circ}\text{C}$ ) which precedes that of ABFA which cooled the system down causing the delay of the decomposition of ABFA to higher temperature (ABFA decomposition is temperature and time dependent).

These results are in good agreement with those obtained with the BRABENDER plastograph (figure IV.14); The shift with respect to time of point 4' and point 5' with respect to point 4 and point 5 for the formulation containing ABFA is due to the endothermic reaction of SBC which precedes these two points (4' and 5') and which cooled the system down causing the delay of the decomposition of ABFA (ABFA decomposition is temperature and time dependent).

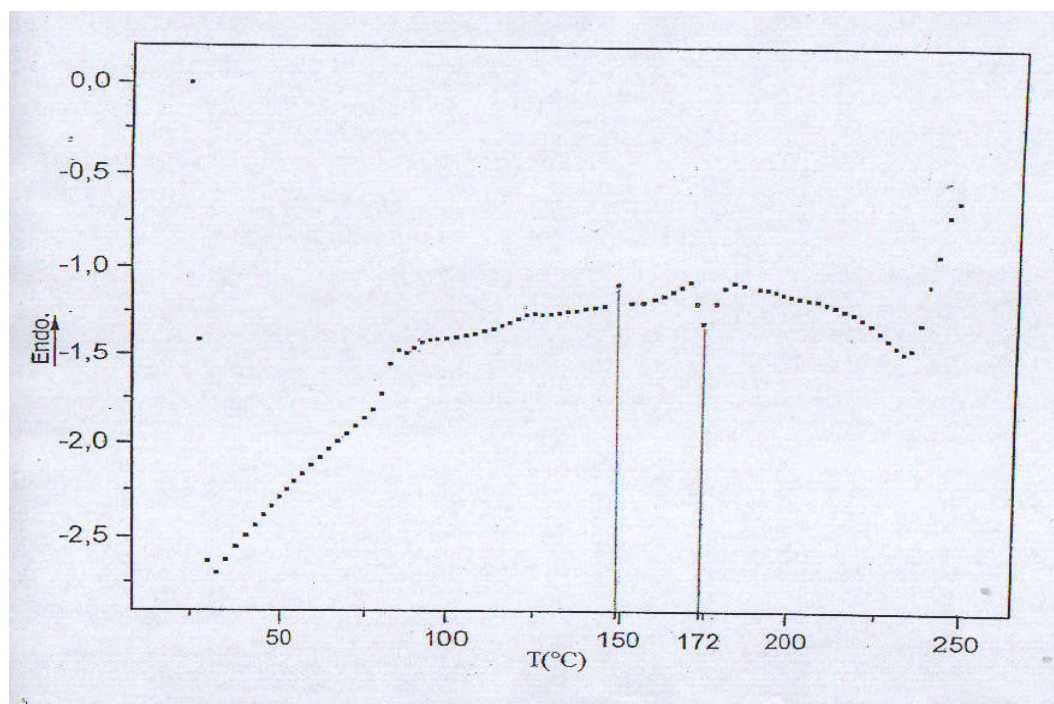


**Figure IV.24:** DSC thermogram of the mixture (ABFA+SBC) and PVC

## CONCLUSIONS

- The BRABENDER has proven to be a universal instrument in the vinyl polymers industry. Its use in our study proved that it is a valid tool to help understand the behavior of rigid PVC formulations containing BA through the follow up of the decomposition and the expansion mechanisms.
- The addition of ABFA and SBC separately gives rise to one new peak after that of fusion, but the addition of their mixture results in the apparition of two different peaks.
- The value of the minimum torque (after the gas expansion) for ABFA is lower than that of SBC. Its value for the mixture of BA, is intermediate between those of the individual ones.
- The higher the concentration of BA the higher the torque at the stability leveling off.
- The thermal stability time decreases with the increase of the ABFA concentration. However, it increases with the increase of SBC concentration. With the mixture of the two blowing agents the thermal stability time exhibits the same trend as that of ABFA alone.

## **CHAPTER FIVE**

### **RHEOLOGICAL (FOAMING EFFICIENCY), MECHANICAL AND MORPHOLOGICAL PROPERTIES**

## V. RHEOLOGICAL (FOAMING EFFICIENCY), MECHANICAL AND MORPHOLOGICAL PROPERTIES

### V.1. Rheological and morphological properties (using BA separately).

#### V.1.1. Extent of expansion

##### V.1.1.1. Variation of the extrudate diameter with the ABFA concentration

As shown in figure V.1, as the concentration of the BA increases the extrudate diameter increases up to an optimum value that corresponds to an ABFA concentration of 0.4 phr, above which it decreases regardless of the extrusion rate. This can be attributed to the fact that if BA concentration is too high (i.e. high cell number), the pressure exerted on the melt by the expanding cells can only be relieved by gas diffusion toward and subsequently through the walls of the extrudate. This will prevent an attainment of an expansion higher than that of optimum level (0.4 phr).

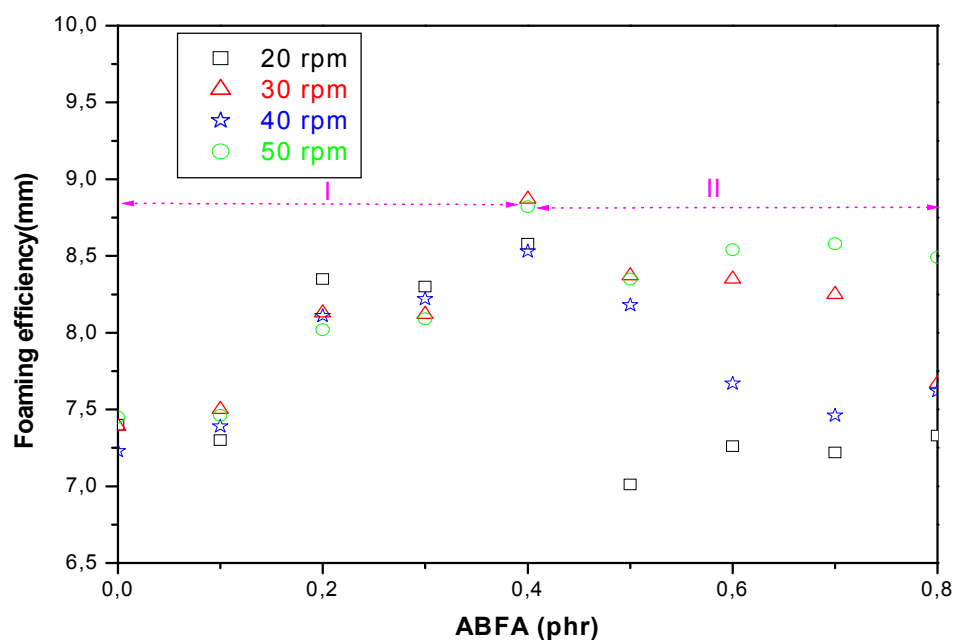


**Figure V.1:** Extrudate diameter as a function of ABFA concentration

On the other hand, at low concentration of ABFA (See figures V.2 and V.3), the expansion is low since the number of the formed cells is reduced and having smaller size (average cell size is about 20  $\mu\text{m}$ ).

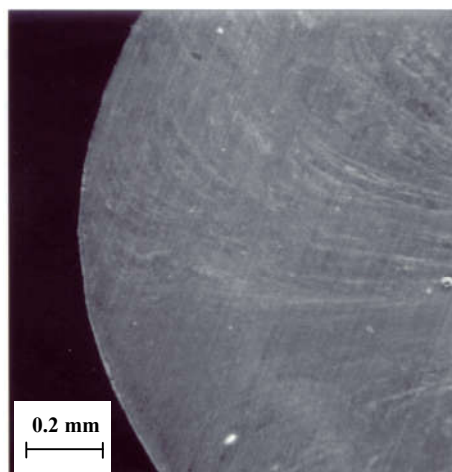
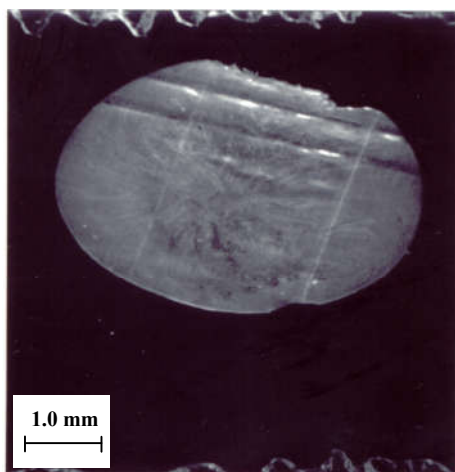


**Figure V.2:** **a**- Optical micrograph (x 9) of unfoamed rigid PVC extrudate.  
**b**- Optical micrograph (x 45) of extrudate sample boarder of unfoamed rigid PVC

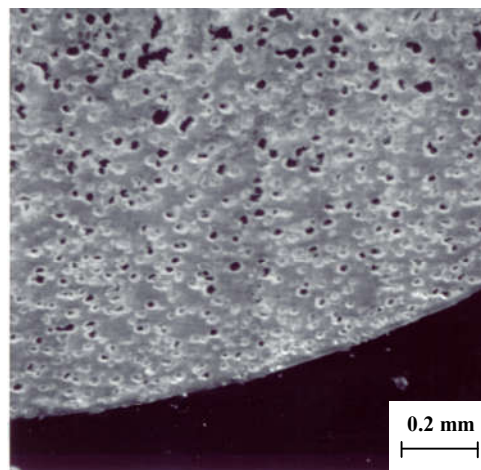
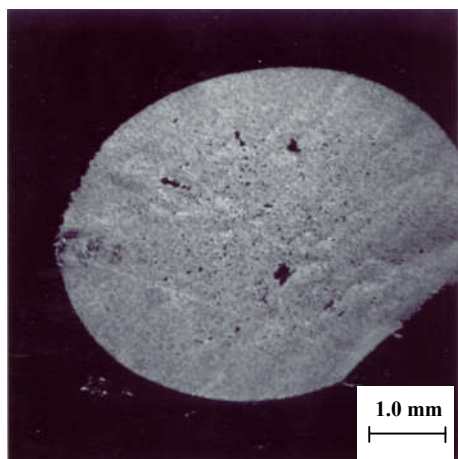
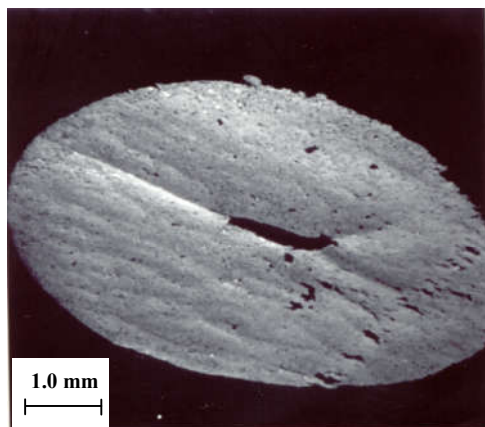


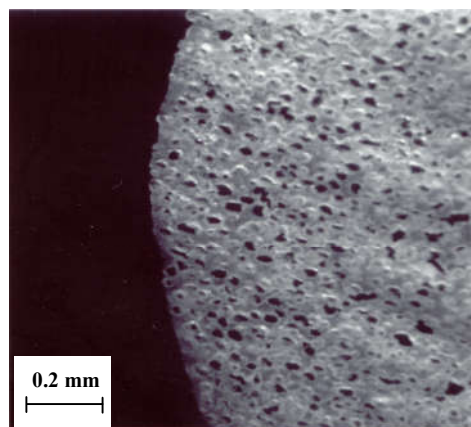
**Figure V.3:** **a**- Optical micrograph (x 9) of foamed rigid PVC extrudate (0.2 phr ABFA).  
**b**- Optical micrograph (x 45) of extrudate sample boarder of foamed rigid PVC (0.2 phr ABFA)

At the optimum concentration (0.4 phr) the number of the cells formed favors the state of equilibrium between the pressure inside the cells and the pressure developed by the polymeric matrix (See figures V.4).





**a**

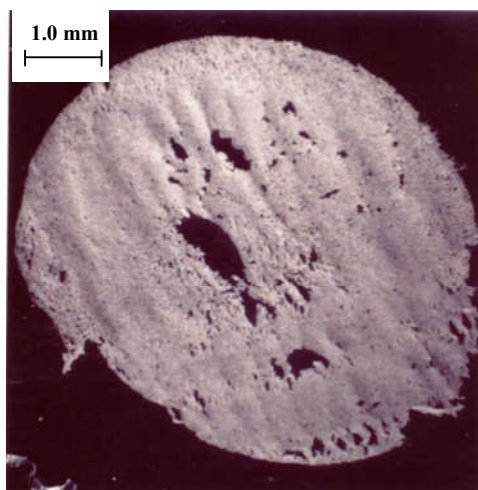


**b**

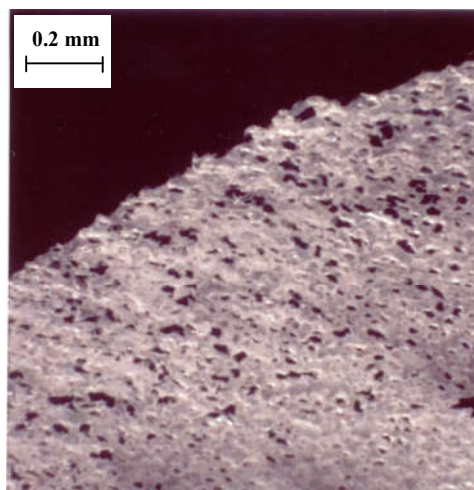
**Figure V.4: a-** Optical micrograph (x 9) of foamed rigid PVC extrudate (0.4 phr ABFA) at 40 rpm.

**b-** Optical micrograph (x 45) of extrudate sample boarder of foamed rigid PVC (0.4 phr ABFA) at 40 rpm.

However, above a concentration of 0.4 phr the number of the cells formed increases proportionally with the concentration of the BA leading to the break up of the cellular structure (at the extrudate center) and the escape of the gas through the extrudate wall, with an average cell size of about 45  $\mu\text{m}$  (See figure V.5).



**a**



**b**

**Figure V.5: a-** Optical micrograph (x 9) of foamed rigid PVC extrudate (0.5 phr ABFA) at 40 rpm.

**b-** Optical micrograph (x 45) of extrudate sample boarder of foamed rigid PVC (0.5 phr ABFA) at 40 rpm.

It was also found that the optimum expansion occurs at extrusion speeds of 40 and 50 rpm. At these speeds, the pressure developed by the screw prevents the premature expansion of the gas that is soluble in the polymeric matrix before exiting from the die. Once the polymer emerges from the die, the initiation and the growth of the cells start to take place. The growth of the cells will be hindered by the progressive cooling by the air at the outer (superficial) layer of the extrudate. In addition to that, the fraction of the BA which has not decomposed acts as a nucleating site, thus favoring the formation of small and closed cells (average cell size is about 30  $\mu\text{m}$ ) with a good surface of outer layer of the extrudate (See Figures V.4 and V.6).

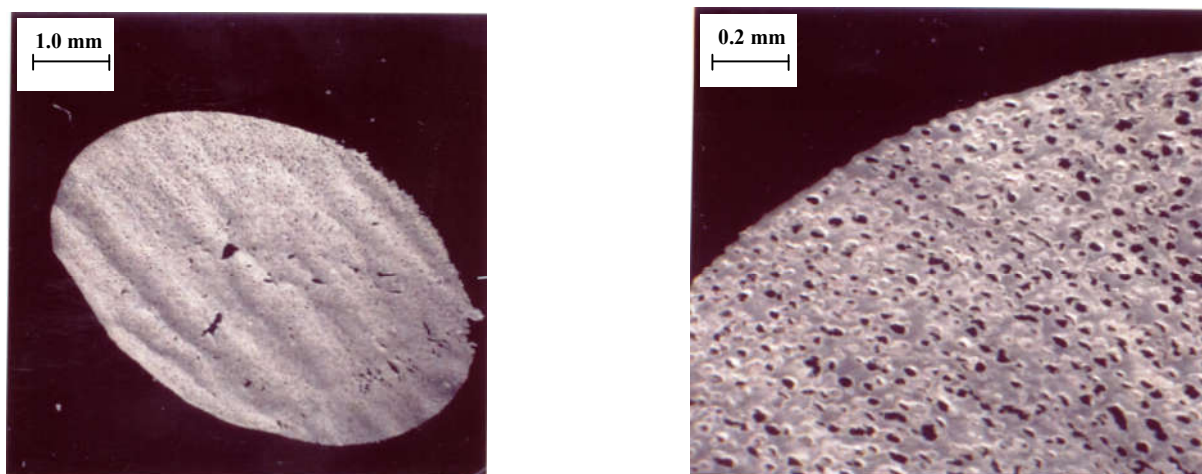


**Figure V.6:** **a-** Optical micrograph (x 9) of foamed rigid PVC extrudate (0.4 phr ABFA) at 50 rpm  
**b-** Optical micrograph (x 45) of extrudate sample boarder of foamed rigid PVC (0.4 phr ABFA) at 50 rpm

At low extrusion speed, the residence time is so long that brought about a serious flow instability (very bad extrudate outer surface) with low expansion. This is attributed to the fact that at low extrusion rates the pressure exerted by the fluid matrix along the extruder screw is so low that the gas resulting from the premature decomposition, caused by a long residence time, expands easily, giving rise to larger cells (average cell size is about 70  $\mu\text{m}$ ). On emerging from the die, the cells would have reached large interconnected dimensions leading to an open structure (See Figures V.7).

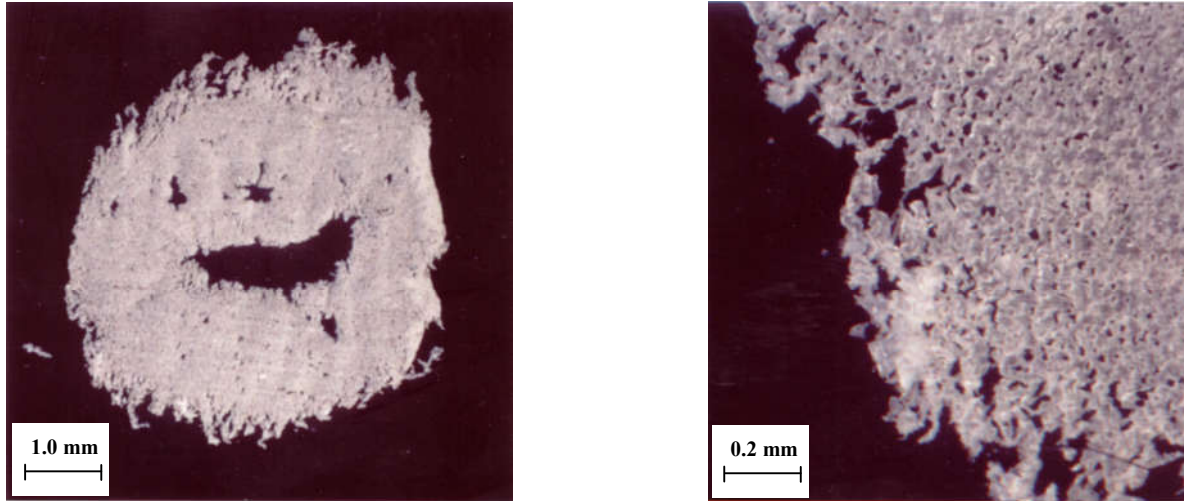


**Figure V.7:** **a-** Optical micrograph (X 9) of foamed rigid PVC extrudate (0.4 phr ABFA) at 10 rpm.  
**b-** Optical micrograph (X 45) of extrudate sample boarder of foamed rigid PVC (0.4 phr ABFA) at 10 rpm

#### V.1.1.2 Variation of expansion with ABFA concentration.

The extrudate diameters measured are in fact the combination of two contributions: extrudate swelling due the polymeric nature of the material, and swelling caused by the expansion of the gas resulting from the decomposition of the BA. For a better interpretation of the results, it is preferable to separate these two contributions by eliminating die swell knowing that it can be quantified at zero concentration of the blowing agent. Die swell can be eliminated by calculating the percentage expansion (% Exp.) as:

$$\% \text{ Exp} = \frac{S_i - S_o}{S_o} \times 100 \quad (14)$$

Where,  $S_i$  is the cross-sectional area at a given concentration of the BA.

$S_o$  is the cross-sectional area at a zero concentration of the BA.

Therefore: (15)

$$\% \text{ Exp} = \frac{D_i^2 - D_o^2}{D_o^2} \times 100$$

Where,  $D_i$  is the extrudate diameter at a given concentration of the BA.

$D_o$  is the extrudate diameter at zero concentration of the BA

In this way, one obtains the percentage expansion due only to the BA decomposition; considering at the same time that the variation of die swell with the concentration of the BA is negligible.

It is to be noted that the works published by B. C. KIM and co-workers [47], those of D. DEANNIN and al [54], those of H. J. BARTH [55], and those of J.L. PFENNIG and M. ROSS [15] treated the results in term of extrudate diameter meaning that die swell was neglected.

As shown in Figure V.8, it was found that the variation of the percentage of expansion showed the same trend as that of the variation of the extrudate diameter with the ABFA concentration. It is also possible to consider the extent of expansion by measuring the cross-sectional area at 0 phr and at 0.4 phr (at 40 rpm). This was found to be 697 mm<sup>2</sup> and 1091 mm<sup>2</sup> respectively. It is to be noted that the percentage expansion and the increase in the cross-sectional area (60% increase in this case) are entirely due to the BA since die swell effect is excluded.

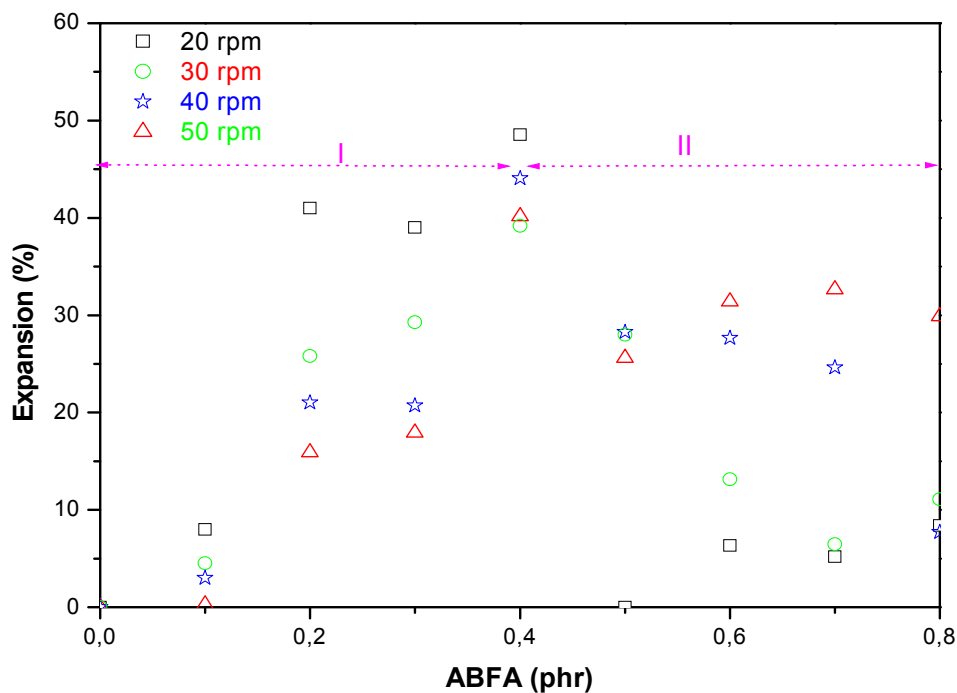


**Figure V.8:** Percentage of expansion as function of ABFA concentration

### V.1.1.3 Variation of the extrudate diameter with the SBC concentration.

As for ABFA, it was found that as the concentration of SBC increases the extrudate diameter increases up to an optimum value corresponds to a critical concentration of 0.6 phr above which it decreases regardless of the extrusion rate. This can be attributed to the fact that if BA concentration is too high (i.e. high cell number), the pressure exerted on the melt by the expanding cells can only be relieved by gas diffusion toward and subsequently through the walls of the extrudate (Figure V.9). This will prevent an attainment of an expansion higher than that of optimum level (0.6 phr).

The microscopic examination of the extrudates showed that the average cell sizes for 0.2 and 0.6 phr are respectively 400 and 650  $\mu\text{m}$  (See figures V.10 and V.11).

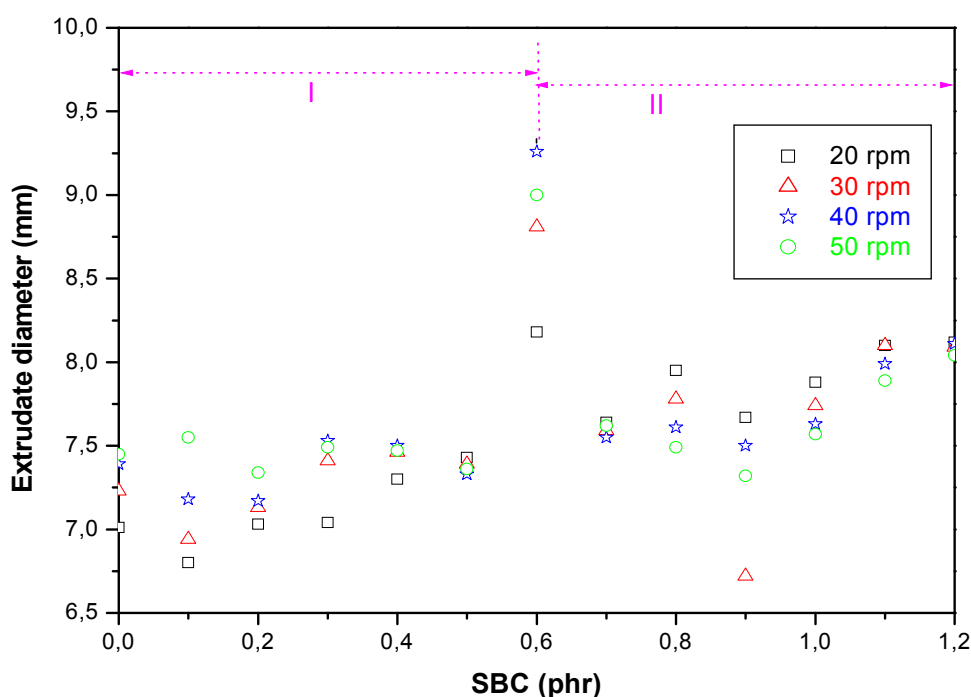
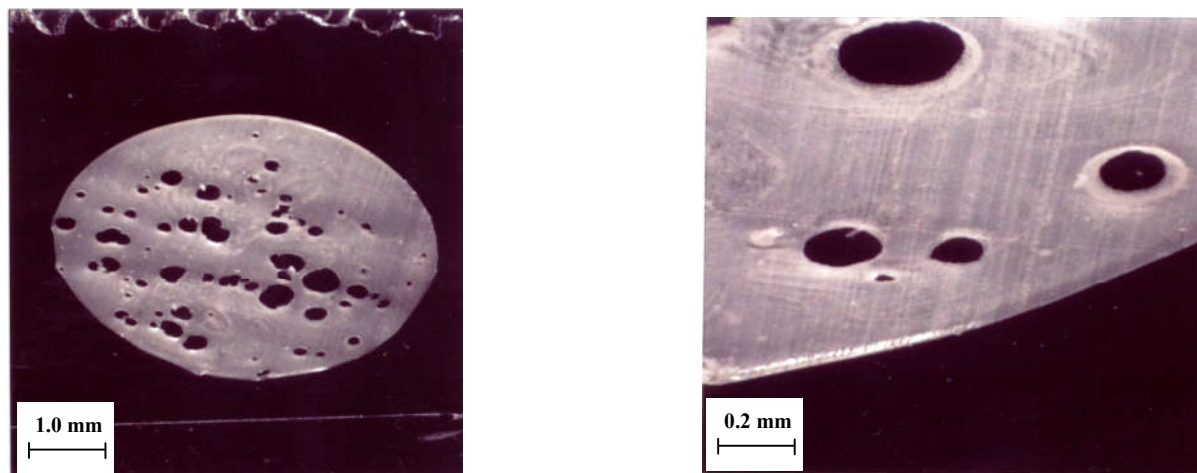


**Figure V.9:** Foaming efficiency as function of SBC concentration at 20 and 40 rpm

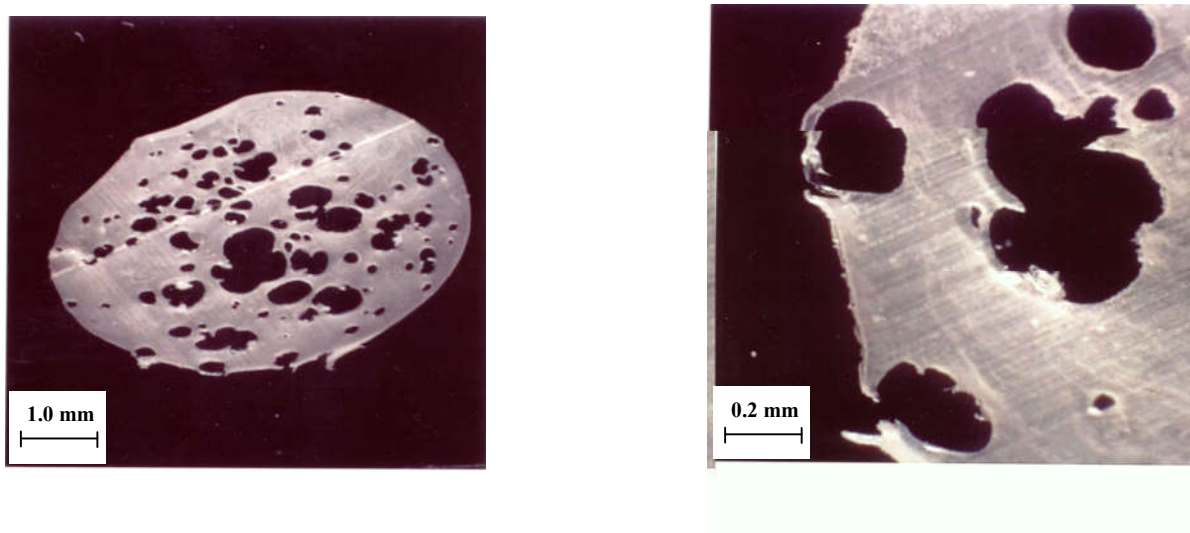
Above the optimum concentration of 0.6 phr, the number of cells increases considerably leading to their interconnection and, therefore, a broken up structure will result. As shown in figure V.12, the microscopic examination has shown that upon decomposing the SBC agent forms a structure where the cells have different sizes (average cell size is about 800  $\mu\text{m}$ ) and partially communicate. This is in accordance with data reported in the literature [11]. The resulting open cellular structure could be



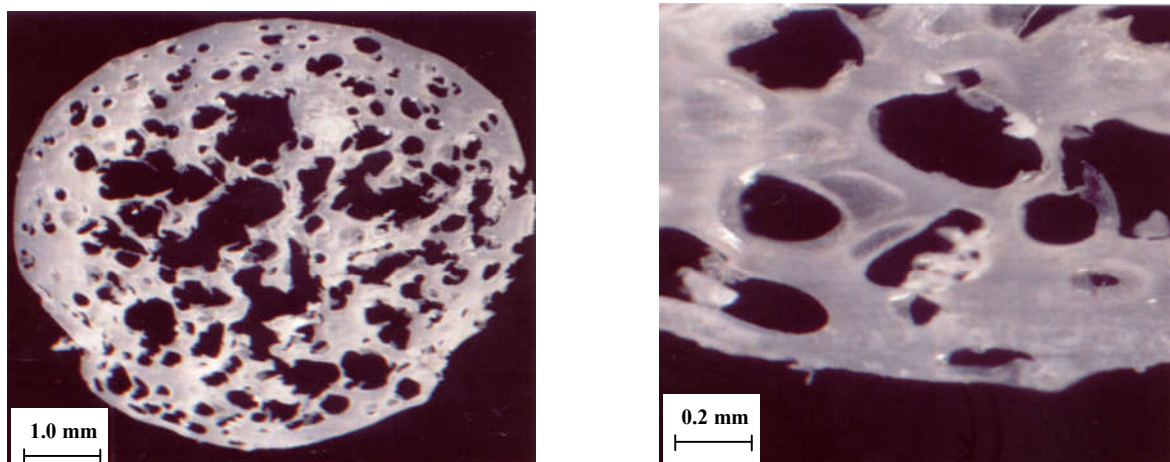
attributed to diffusion phenomenon; the major product that results from SBC decomposition is  $\text{CO}_2$  which is characterized by a higher diffusion rate compared to  $\text{N}_2$  released by the ABFA agent [49].



**a**  
**Figure V.10: a-** Optical micrograph (x 9) of foamed rigid PVC extrudate (0.2 phr SBC) at 40 rpm.  
**b-** Optical micrograph (x 45) of extrudate sample boarder of foamed rigid PVC (0.2 phr SBC) at 40 rpm.



**a**  
**Figure V.11: a-** Optical micrograph (x 9) of foamed rigid PVC extrudate (0.6 phr SBC) at 40 rpm.  
**b-** Optical micrograph (x 45) of extrudate sample boarder of foamed rigid PVC (0.6 phr SBC) at 40 rpm.



**a** **b**

**Figure V.12:** **a-** Optical micrograph (x 9) of foamed rigid PVC extrudate (0.8 phr SBC) at 40 rpm.  
**b-** Optical micrograph (x 45) of extrudate sample boarder of foamed rigid PVC (0.8 phr SBC) at 40 rpm.

#### **V.1.1.4 Variation of expansion with the SBC concentration.**

As shown in figure V.13, it was found that the variation of the percentage of expansion showed the same trend as that of the variation of the extrudate diameter with the SBC concentration.

#### **V.1.1.5 Comparison between ABFA and SBC**

##### **The cellular structure.**

It is noted, owing to the microscopic examination of the extrudates with the SBC (figure V.11) that present a random cellular structure where the cells partially communicate. This could be explained by the particle size distribution of the SBC which is characterized by a major fraction of particles with a diameter larger than 280  $\mu\text{m}$  (broad distribution) that gave rise to large cells partially communicating (average cell size is about 650  $\mu\text{m}$ ). Concerning the ABFA, the microscopic examination of the extrudates (figure V.4) showed that they present a structure characterized by small and uniform cells (average cell size is about 30  $\mu\text{m}$ ). This is also explained by the particle size distribution which showed that the entire particles of ABFA have a diameter Of 125  $\mu\text{m}$ .

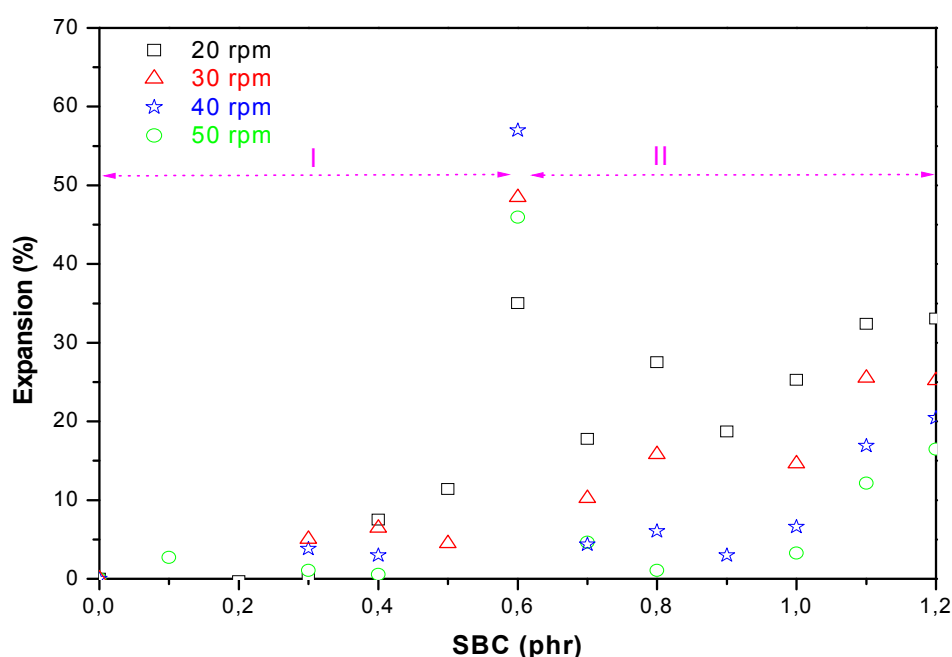


**Figure V.13:** Percentage of expansion as a function of SBC concentration

#### The corresponding concentration to the optimum:

It was found that the optimum expansion occurs at a concentration higher in the case of SBC agent than that with ABFA; that is 0.6 phr for SBC and 0.4 phr for ABFA. This is attributed to the followings:

- The endothermicity of the decomposition reaction of SBC results in a higher viscosity of the polymeric matrix. This combined, with the reversibility of this decomposition reaction, does not allow the low amount of the gas released to act. But the decomposition reaction of ABFA is exothermic and, therefore, favors a lower polymeric matrix viscosity.
- Water, being one of the SBC decomposition products in a form of vapor, contributes to the expansion process at the processing temperature. However, contraction of the large proportion of the cells takes place during cooling when this water vapor condenses while the polymeric matrix is still deformable (in molten state).



## V.2. Mechanical properties (using BA separately)

### V.2.1 Tensile properties

#### V.2.1.1- Variation of elastic modulus

##### - Azobisformamide (ABFA)

As shown in Figure V.14, it was found that the elastic modulus decreased with increasing the BA concentration for all extrusion rates. This is explained by the fact that since the number of the cells formed is proportional to the concentration of ABFA, the number of weak points will increase resulting in a decrease of the rigidity compared to that of compact structure. On the other hand, the extent of elastic modulus reduction was found to reduce beyond 0.4 phr (corresponding to the optimum of expansion) since increasing the BA concentration in this range, will act in the same way as going back to the initial compact structure (due to the great extent of escaped gas to the atmosphere when emerging from the die).

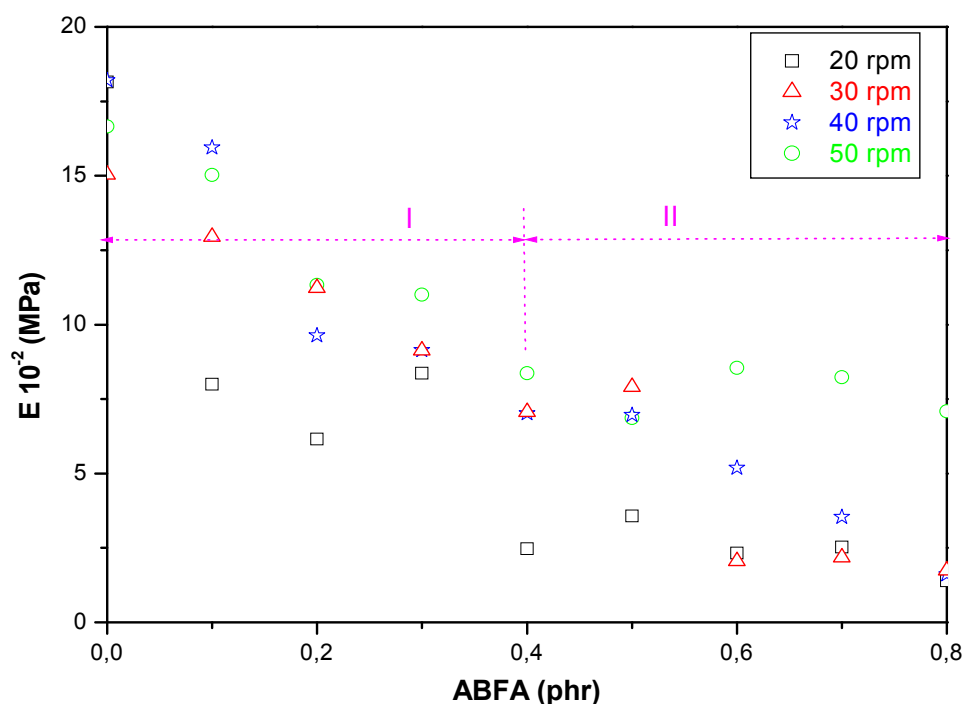


**Figure V.14:** Elastic modulus as a function of ABFA concentration

##### - Sodium Bicarbonate (SBC).

As for ABFA, it was also found that the elastic modulus decreases with increasing SBC concentration till 0.6 phr (Figure V.15). On the other hand, the elastic modulus was found almost to increase beyond 0.6 phr (corresponding to the optimum of

expansion). This is probably due to the fact that more compact structure is reached compared to that obtained with ABFA.

The fluctuations showed by the curve is related to the random structure developed with SBC.

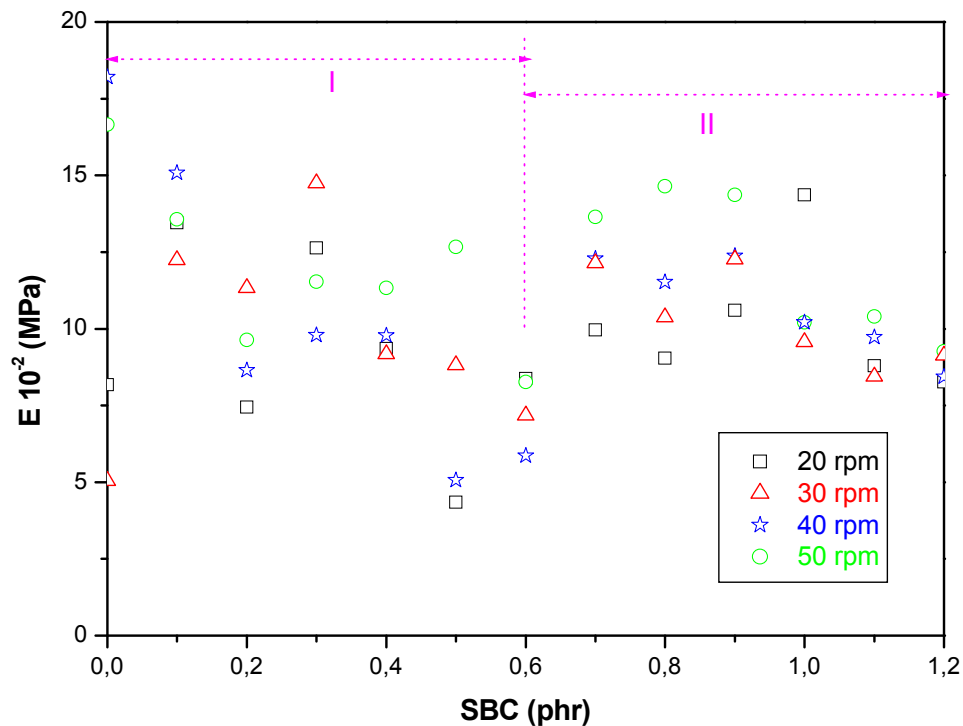


**Figure V.15:** Elastic modulus as a function of SBC concentration

#### - Comparison.

The first thing to be pointed out for ABFA, is the fact that the modulus decreased almost linearly with the increase of BA concentration, and the extent of elastic modulus reduction was found to reduce beyond its critical concentration. However, in the case of SBC, the elastic modulus was found to increase beyond its critical concentration (see figure V.16). This can be explained by the following reasons:

- Higher critical concentration (0.6 phr compared to 0.4)
- Higher average cell size (650  $\mu$ m compared to 30)
- Reversibility of the decomposition reaction of SBC
- Condensation of the vapor during the cooling

These factors tend to increase the extent of escaped gas to the atmosphere when emerging from the die, resulting in more compact structure.

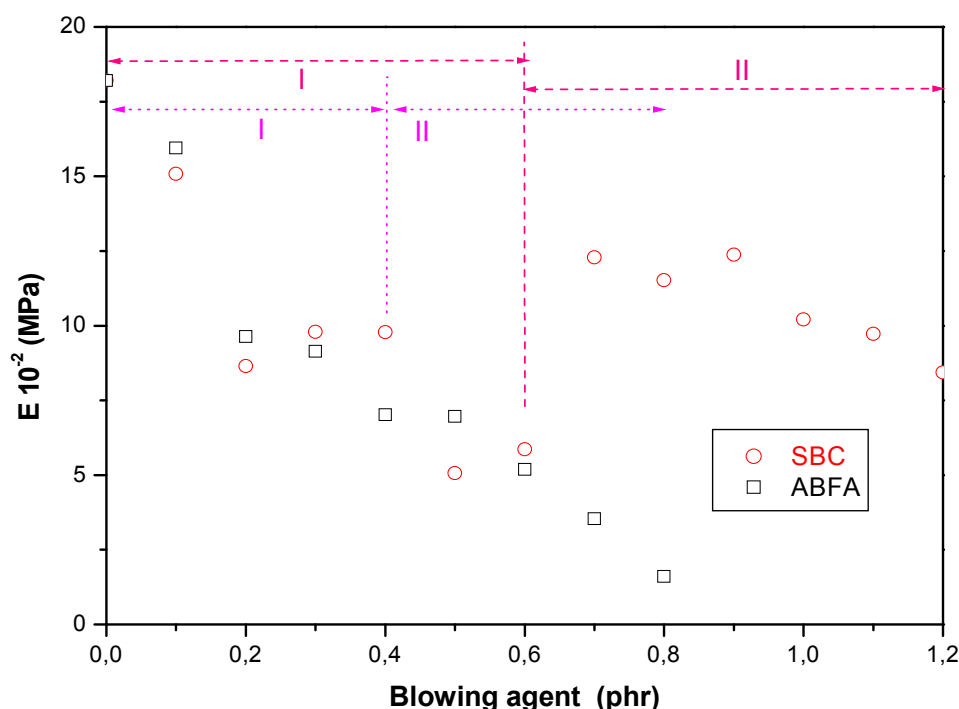


**Figure V.16:** Elastic modulus as a function of BA concentration at 40 rpm

## V.2.1 2 Variation of tensile stress at break

### Azobisformamide (ABFA)

It was found that as concentration of ABFA increases the tensile stress at break decreases sharply (figure V.17). This is due to the number of cells; meaning that the increase in the number of cells causes a decrease of the strength of the material.

### Sodium bicarbonate (SBC)

The same trend was found with the SBC agent; that is a decrease in the tensile stress at break with increasing SBC concentration (figure V.18). It is to be noted that the presence of a lowest value corresponding to a concentration of 0.6 phr. This could be attributed to the fact that rupture is more pronounced in a range where there was a high extent of expansion as a result of the reasons mentioned above.

### Comparison:

The decrease in the tensile stress at break is almost uniform for both BA (figure V.19), except that for the ABFA based formulation, the decrease is more pronounced

and reaches lower values than those obtained with the SBC. This is could be attributed to the endothermicity of the decomposition reaction of SBC permitting hence the extrudates not to degrade even at high concentrations. Contrarily, those of ABFA will prematurely degrade due to its exothermic decomposition and therefore became weak.

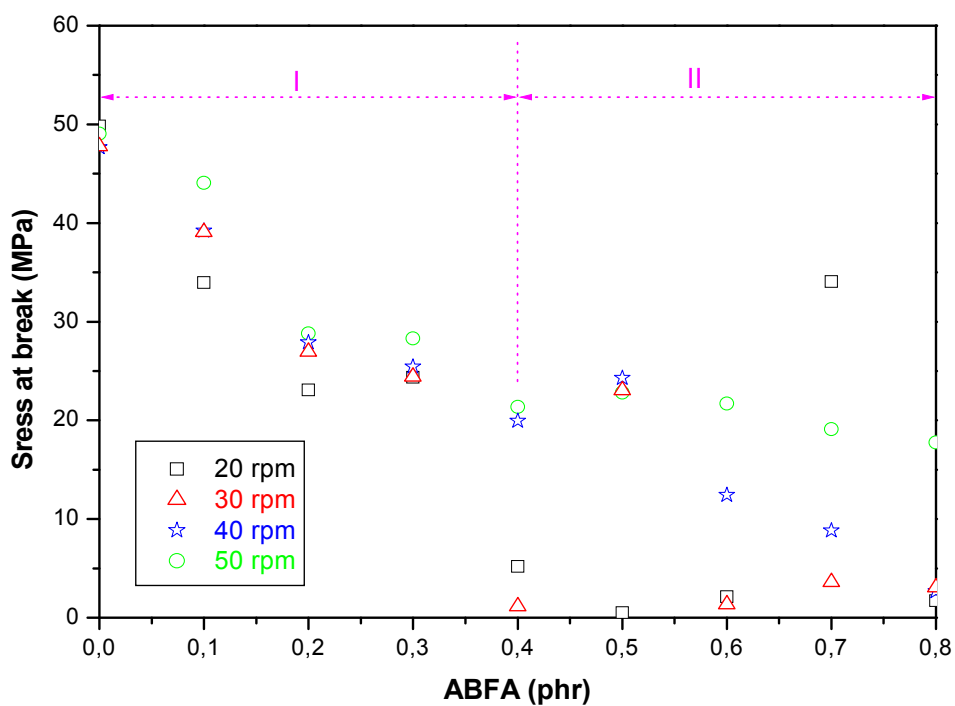


**Figure V.17:** Stress at break as a function of ABFA concentration

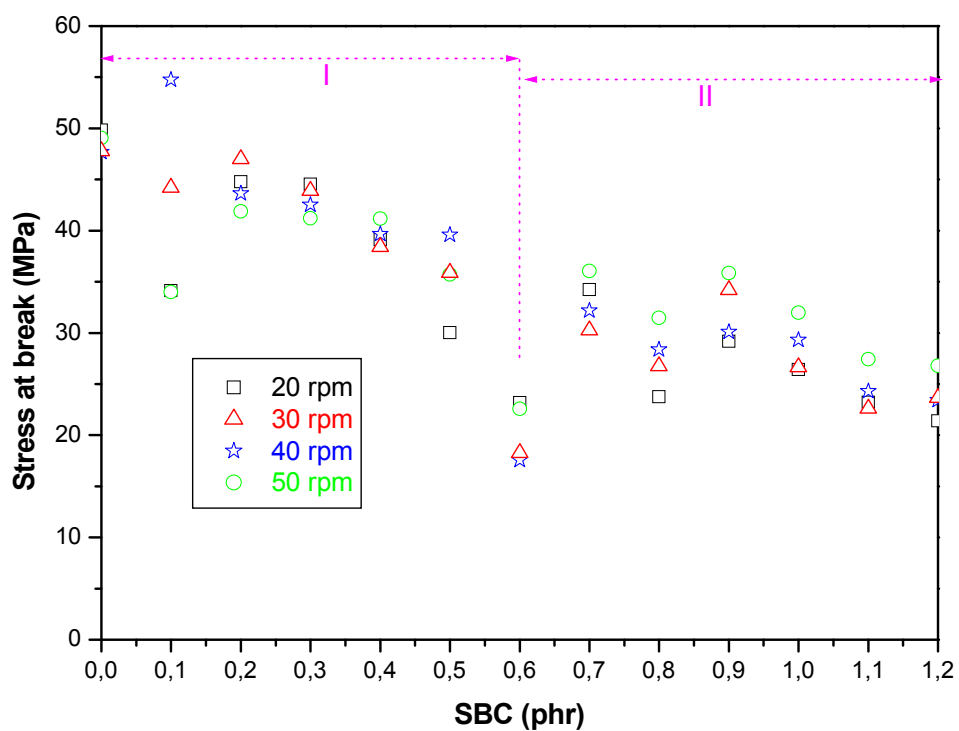


**Figure V.18:** Stress at break as a function of SBC concentration.

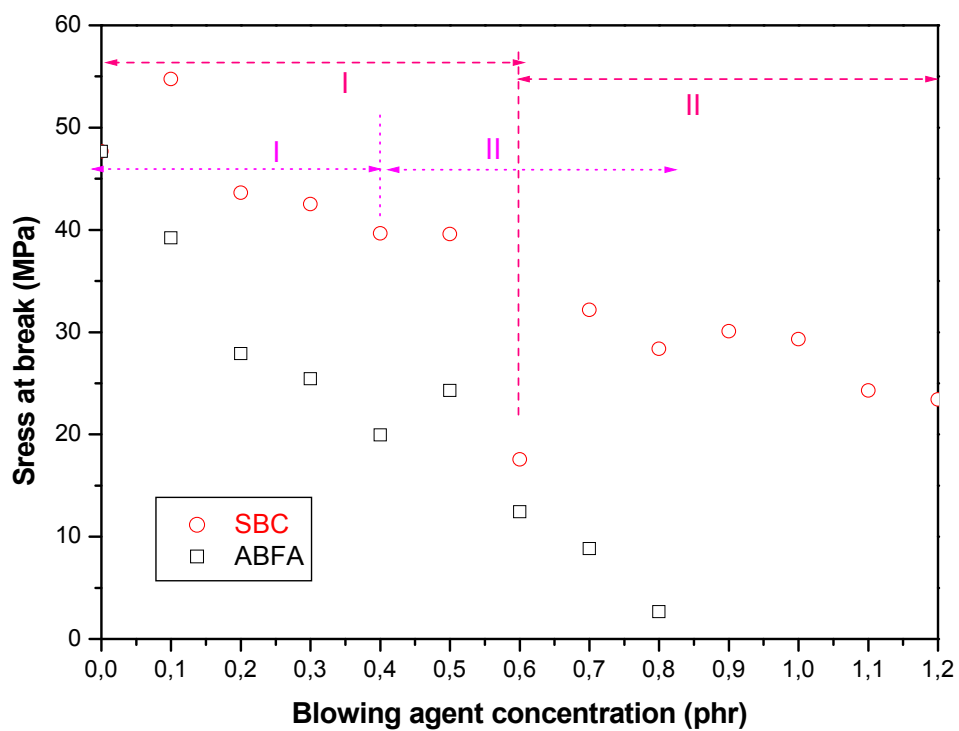


**Figure V.19:** Stress at break as a function of BA concentration at 40 rpm

### **V.2.1 3 Variation of strain at break**

#### **a) Azobisformamide (ABFA).**

As shown in figure V.20, it was found that for ABFA concentrations between 0 and 0.3 phr, the strain at break remains almost constant and it falls to low values beyond 0.4 phr. Since the material is rigid the values of the strain at break remains more or less constant for the first part of the curve. But, concerning the decrease noted above 0.4 phr, the reason is mainly due to the higher amount of the gas released which collapsed the cells, and also due to the exothermicity of the decomposition reaction of ABFA that caused the premature degradation and the weakening of the extrudates.

#### **b) Sodium bicarbonate (SBC)**

Since the cellular structure was random as a result of SBC decomposition reaction, rupture was also random and was reflected through the strain at break results which presented many fluctuations as shown in figure V.21.

#### **c) Comparison.**

As shown if figure V.22, it is noted that for BA concentration less than 0.5 phr the strain is almost the same for both types of BA, but above 0.5 phr in the case of SBC, the strain at break values are higher than those of ABFA. This is due to the interconnection of the cells and the communicating cellular structure which were developed.

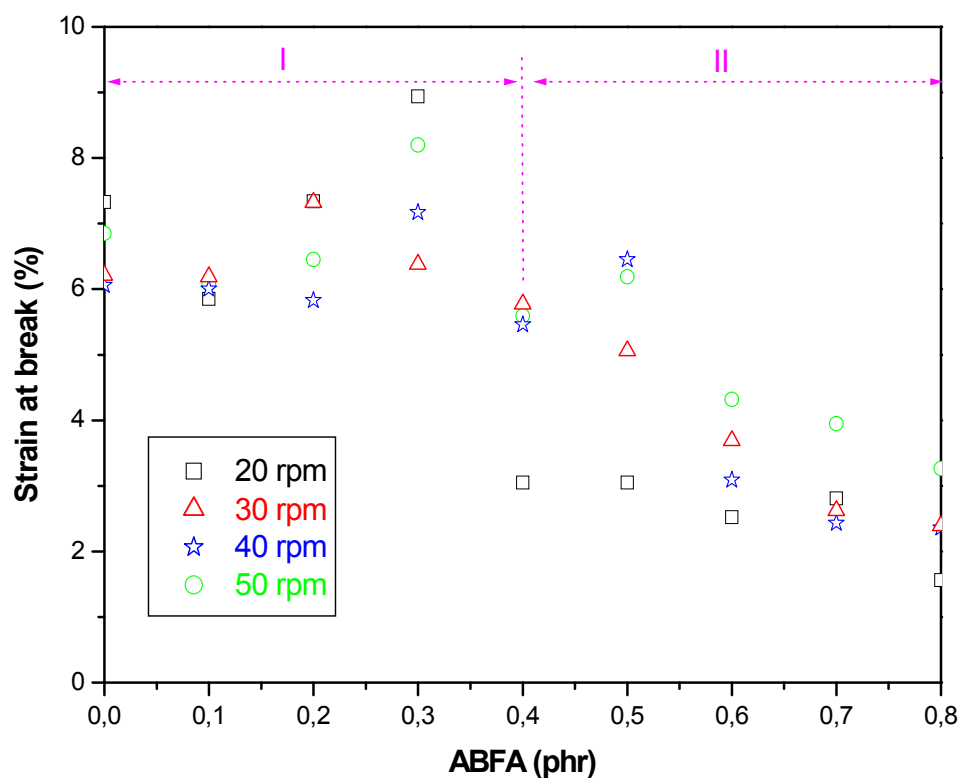


**Figure V.20:** Strain at break as a function of ABFA concentration

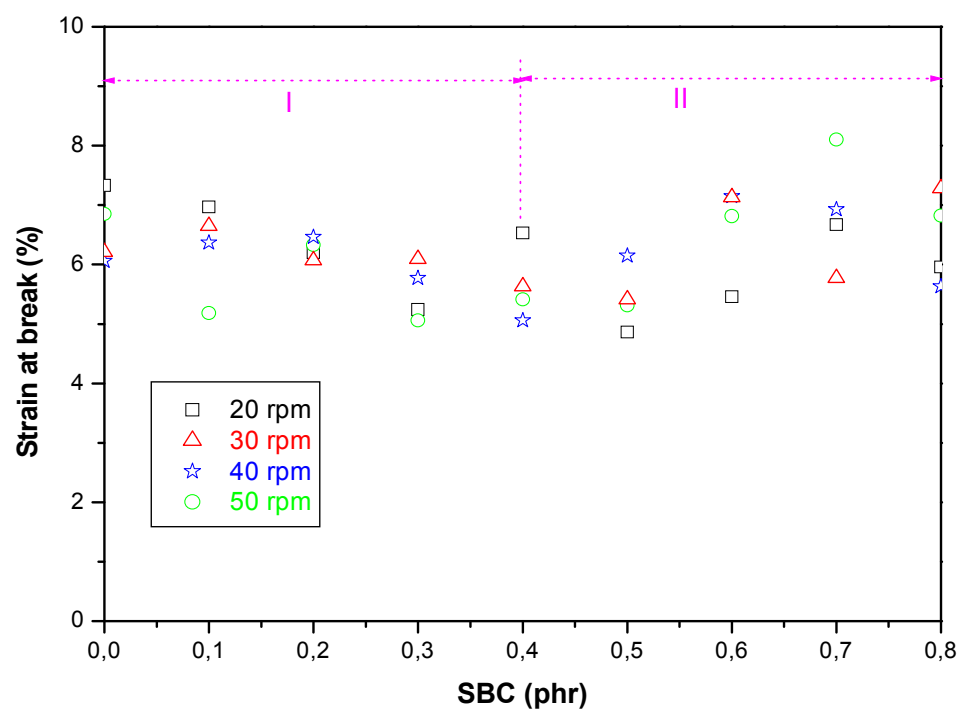


**Figure V.21:** Strain at break as a function of SBC concentration

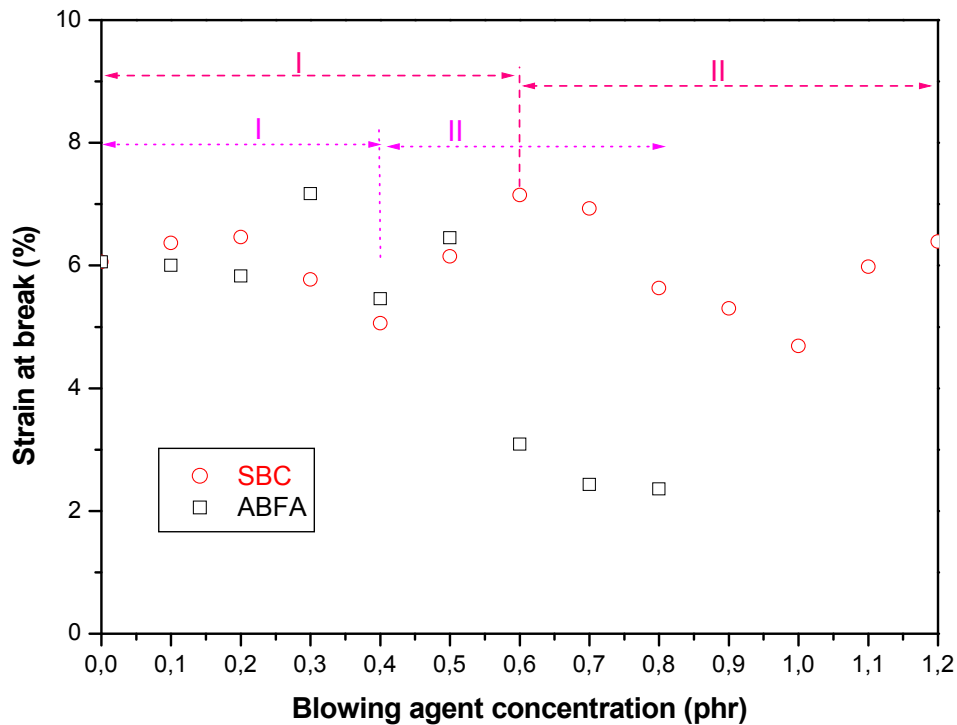


**Figure V.22:** Strain at break as a function of BA concentration at 40 rpm

#### V.2.1 4 Variation of energy at rupture.

##### a) Azobisformamide (ABFA)

It is observed that the energy at rupture generally decreases with the increasing of ABFA concentration, and at high concentrations it falls owing to the open up structure that developed especially at low extrusion rates (figure V.23).

##### b) Sodium bicarbonate (SBC)

Owing to the random cellular structure developed by the SBC, it is not easy to interpret the results because of their great scattering (figure V.24).

##### c) Comparison.

As shown in figure V.25, it is noted that below 0.5 phr the trend is the same for both types of BA; but above this concentration and for the ABFA, the energy at rupture falls reflecting the communicating open cellular structure that was developed.



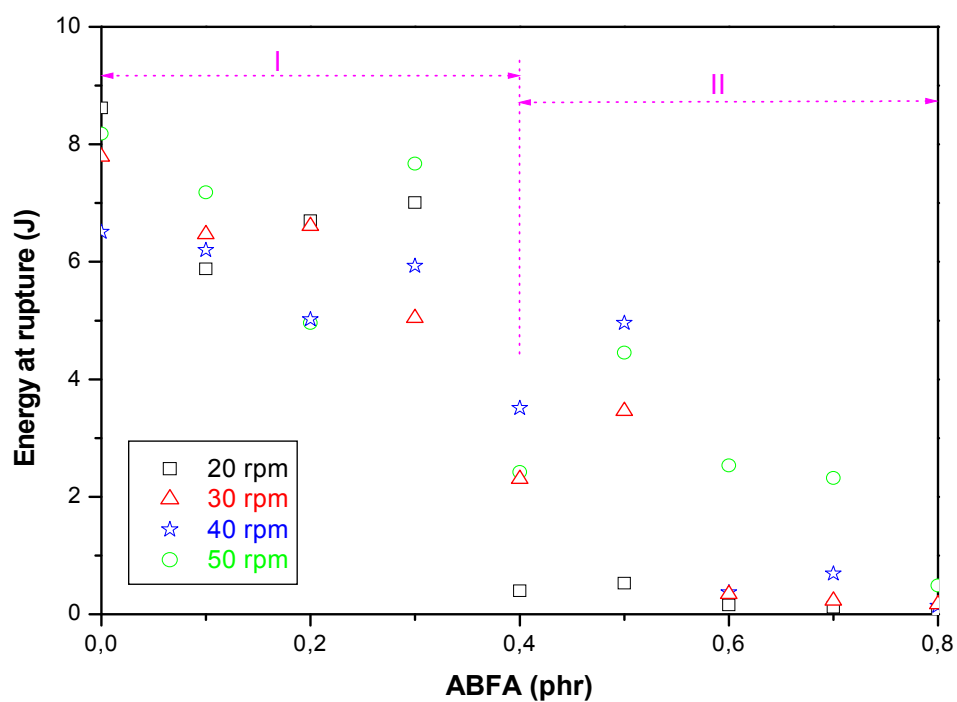


**Figure V.23:** Energy at break as a function of ABFA concentration

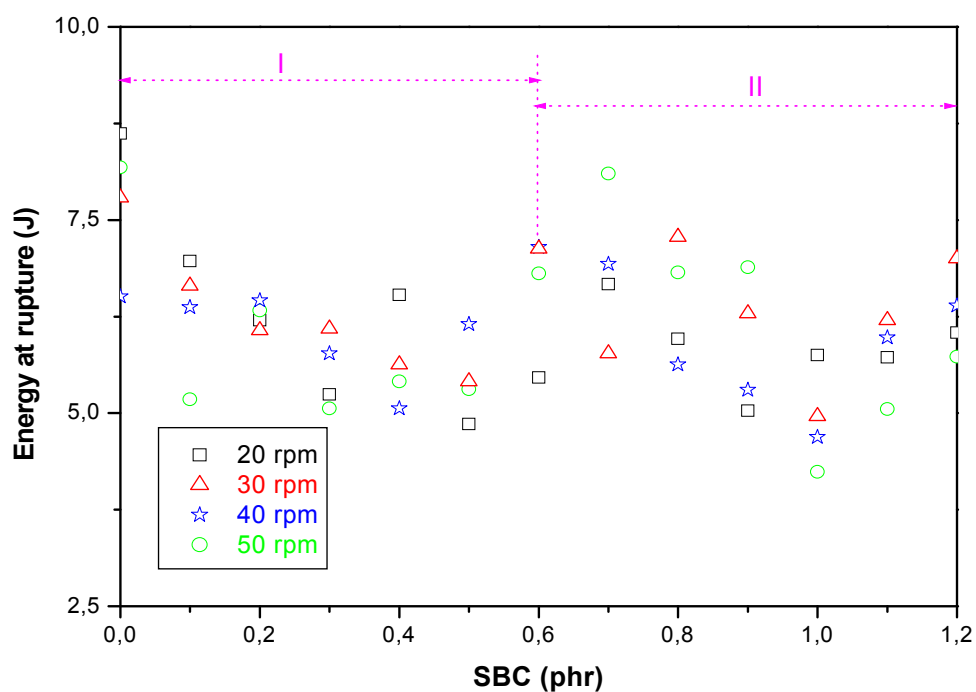


**Figure V.24:** Energy at rupture as a function of SBC concentration

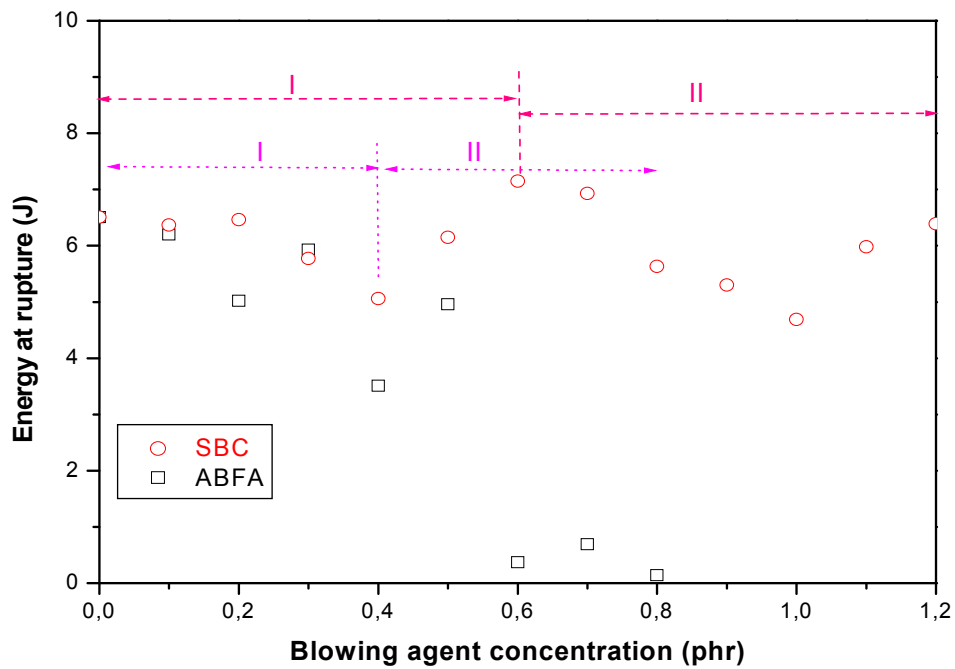


**Figure V.25:** Energy at rupture as a function of BA concentration at 40 rpm.

## V.2.2 Variation of unnotched Izod impact

### a) Azobisformamide (ABFA).

As shown in figure V.26 for all extrusion rates, the resilience decreases with the increase of ABFA concentration. This is due to the cellular structure that forms weak points resulting in the initiation of rupture and consequently the samples break up easily upon the impact. However, at zero phr the material is compact and, therefore, exhibits a higher resistance to impact.

### b) Sodium bicarbonate (SBC).

The same trend was found with the SBC based samples (figure V.27).

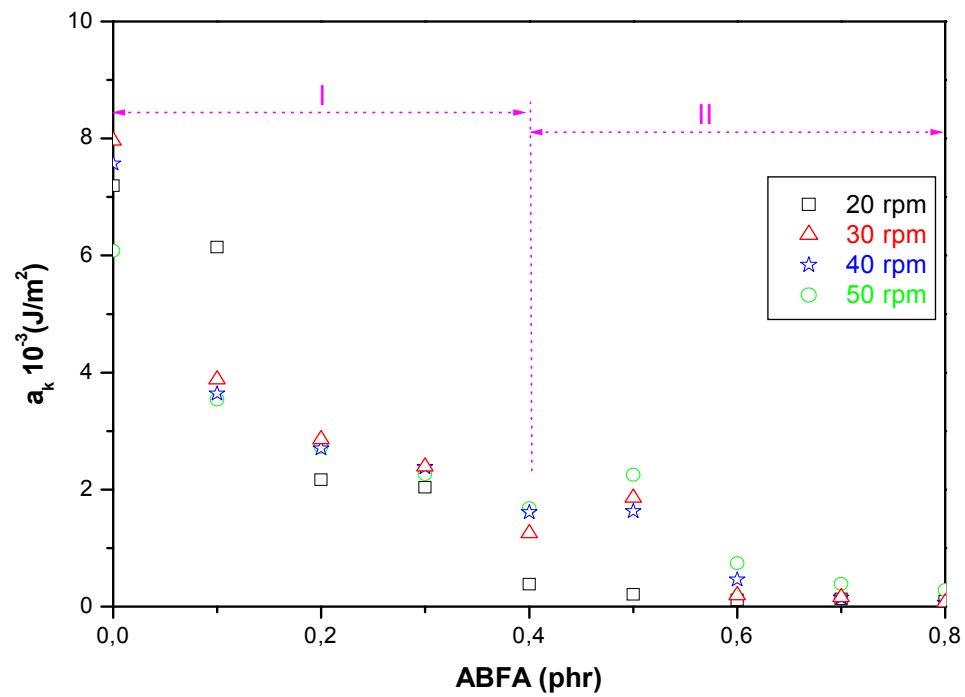


**Figure V.26:** Resilience as a function of ABFA concentration

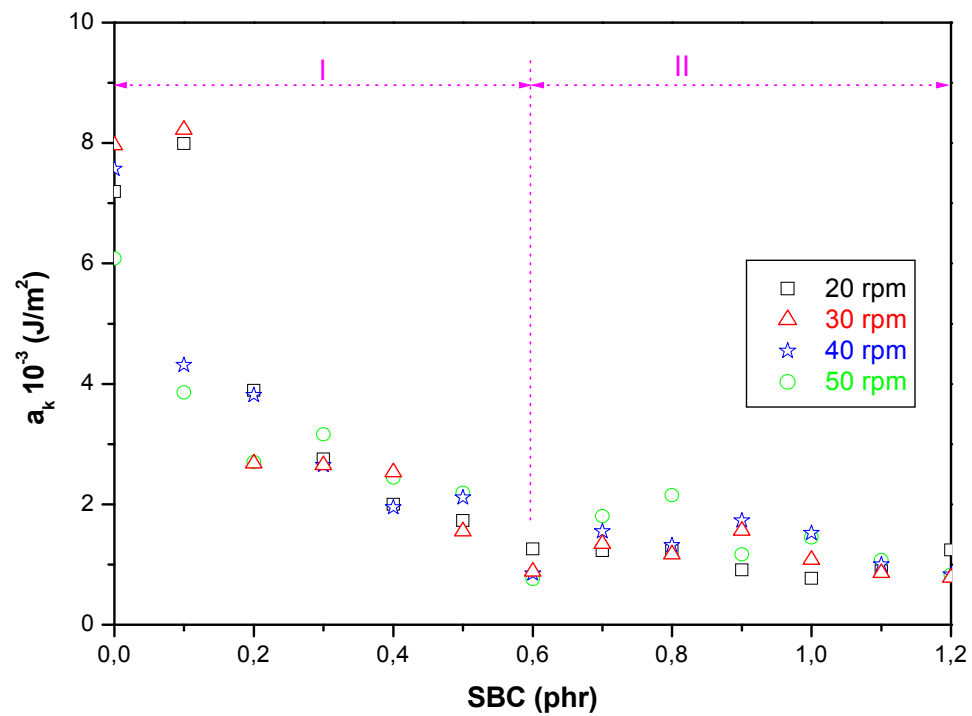


**Figure V.27:** Resilience as a function of SBC concentration

### **V.2.3 Variation of hardness**

#### **a) Azobisformamide (ABFA)**

It is noted that whatever the extrusion speed, the hardness decreases with the increase of ABFA concentration (See figures V.28 and V.29). This is due to the developed cellular structure during the extrusion in an expansion-free mode (air cooling) leading to formation of a thinner wall of the extrudate (A hardness is surface properties). On the other hand, it is easier for the hardness indenter to penetrate into a cellular material than into a compact one.

#### **b) Sodium bicarbonate (SBC).**

The same trend was observed as the concentration of SBC increased (figure V.30 and V.31) except that at 0.6 phr, there was a drastic decrease in hardness was observed; since at this concentration the maximum expansion took place, leading to formation of a thinner wall of the extrudate with high average cell size. Beyond it, a great extent of gas has escaped from the extrudate surface to the atmosphere.

#### **c) Comparison.**

It is observed that the hardness values obtained with SBC are higher than those of ABFA because it is more probable for the indenter to meet the cells at the extrudate surface in the case of ABFA than it is for SBC-based material.

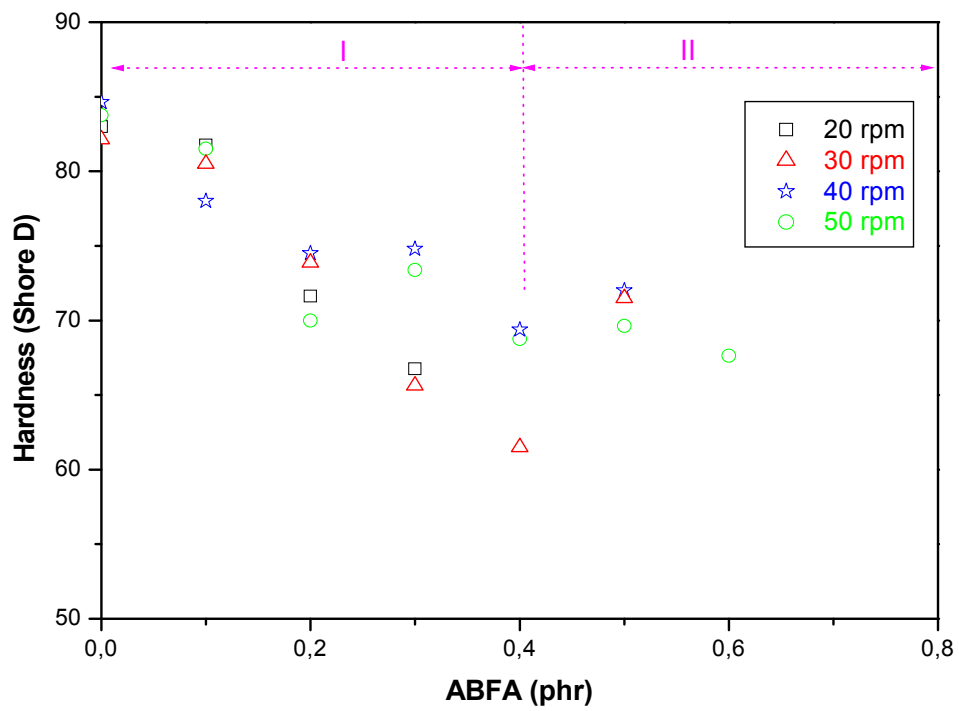


**Figure V.28:** Hardness (Shore D) as a function of ABFA concentration (First lecture)

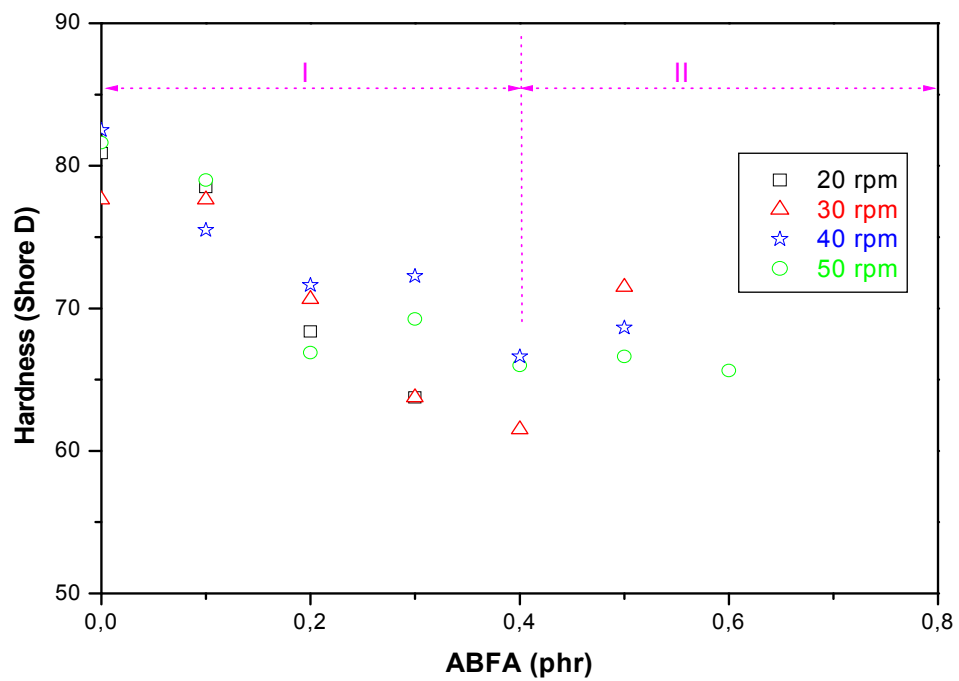


**Figure V.29:** Hardness (Shore D) as a function of ABFA concentration (Second lecture)

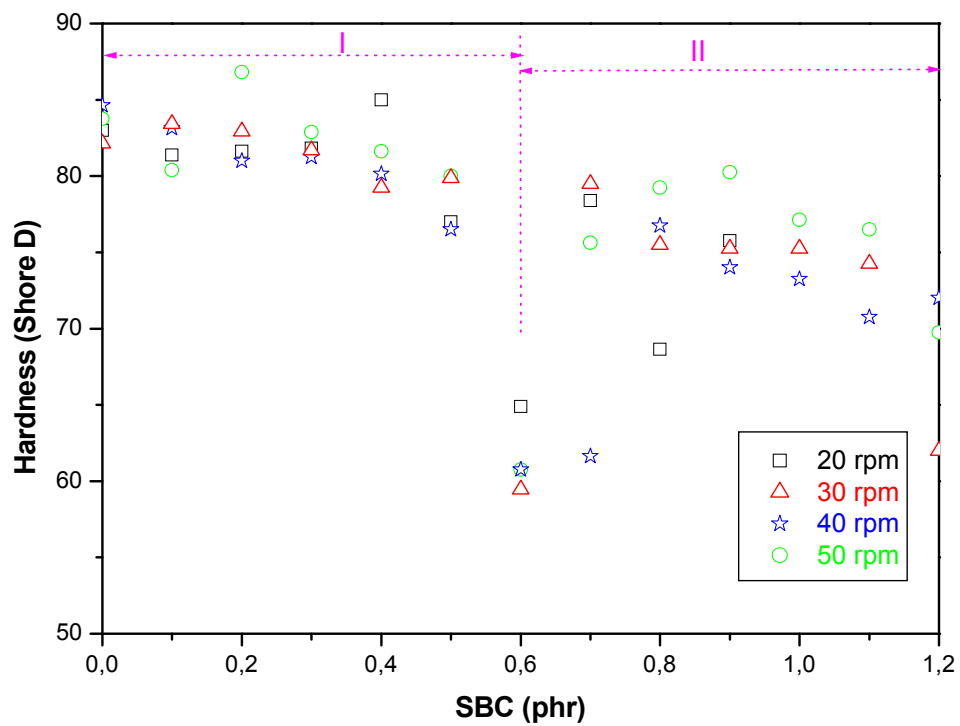


**Figure V.30:** Hardness (Shore D) as a function of SBC concentration (First lecture)

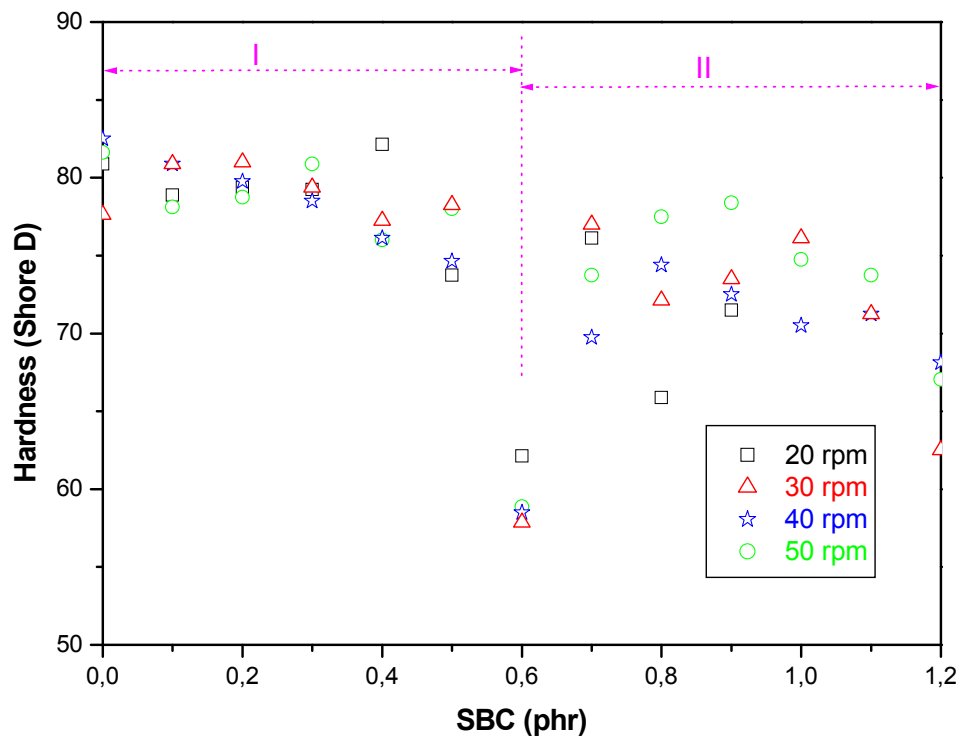


**Figure V.31:** Hardness (Shore D) as a function of SBC concentration (Second lecture)

### V.3. Rheological and optical properties (using a mixture of BA)

The mixture of the two BA was prepared by taking into consideration two parameters; namely:

- The optimum concentration for optimum expansion for each BA alone.
- The state of the surface of the extrudate.

According to the previous results, it was found that the optimum concentration (at 40 and 50 rpm) was 0.4 phr for the ABFA and 0.6 for the SBC. At these concentrations the extrudates presented a smooth surface. Illustration of these compositions is given in the following demonstration:

$\left\{ \begin{array}{l} 100\% \text{ ABFA} \\ 0\% \text{ SBC} \end{array} \right.$	$\longrightarrow$	$C_{\text{Tot}} = 0.40 \text{ phr}$
$\left\{ \begin{array}{l} 70\% \text{ ABFA} \\ 30\% \text{ SBC} \end{array} \right.$	$\longrightarrow$	$\left\{ \begin{array}{l} 0.4 \times 70/100 = 0.28 \\ 0.6 \times 30/100 = 0.18 \end{array} \right. \quad C_{\text{Tot}} = 0.46 \text{ phr}$
$\left\{ \begin{array}{l} 50\% \text{ ABFA} \\ 50\% \text{ SBC} \end{array} \right.$	$\longrightarrow$	$\left\{ \begin{array}{l} 0.4 \times 50/100 = 0.20 \\ 0.6 \times 50/100 = 0.30 \end{array} \right. \quad C_{\text{Tot}} = 0.50 \text{ phr}$
$\left\{ \begin{array}{l} 30\% \text{ ABFA} \\ 70\% \text{ SBC} \end{array} \right.$	$\longrightarrow$	$\left\{ \begin{array}{l} 0.4 \times 30/100 = 0.12 \\ 0.6 \times 70/100 = 0.42 \end{array} \right. \quad C_{\text{Tot}} = 0.54 \text{ phr}$
$\left\{ \begin{array}{l} 0\% \text{ ABFA} \\ 100\% \text{ SBC} \end{array} \right.$	$\longrightarrow$	$C_{\text{Tot}} = 0.60 \text{ phr}$

**NB:** It is to be noted that the total concentration ( $C_{\text{Tot}}$ ) varies depending on the individual proportions of the two BA; contrarily to the works of K. U. KIM and al who maintained the total concentration constant [48]. And do not take into account the critical concentration of each BA when they are added separately.

### V.3.1 Extent of expansion

#### V.3.1.1 Variation of the extrudate diameter with ABFA percentage

It is noted that the extrudate diameter as a function of the mixture (ABFA/SBC) concentration, exhibits values higher than those of each BA used separately, i.e. synergetic effect (See figures V.32, V.33 and V.34).

- Synergism is obtained at a speed of 40 and 50 rpm.
- The optimum expansion (synergism) is obtained at 70% ABFA within the mixture of BA.
- The presence of two points of antagonism; the first of which is at 30% ABFA, and the second at 90% ABFA at a speed of 40 and 50 rpm.

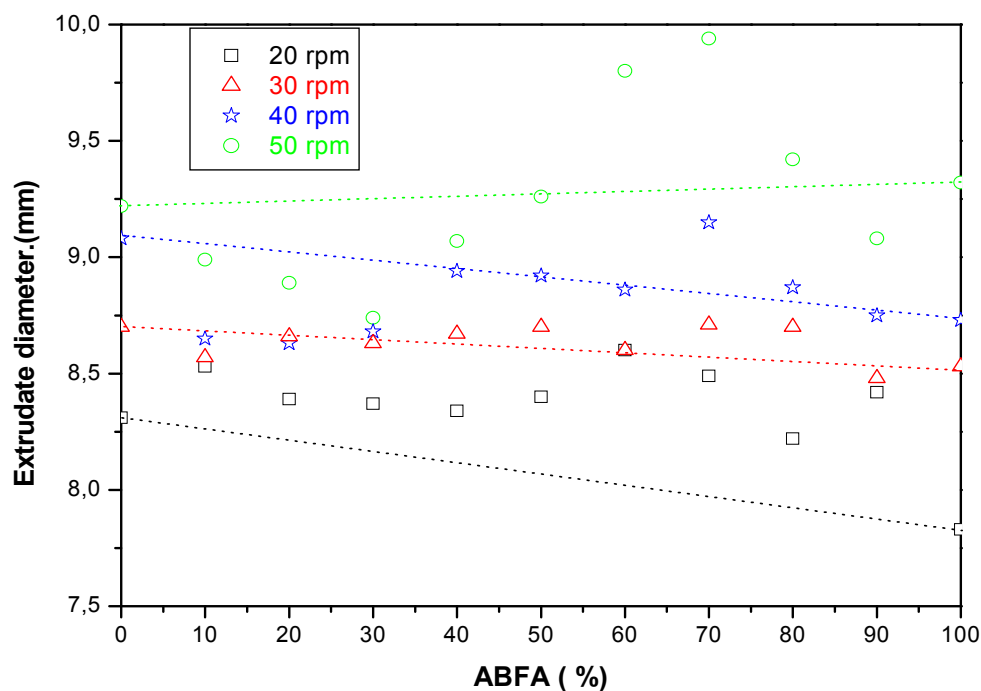


**Figure V.32:** Extrudate diameter as a function of ABFA percentage (%)

The microscope examination of the extrudates obtained using the mixture of the two BA showed that their cellular structure is:

- Open, large and random cells (average cell size is about 70  $\mu\text{m}$ ) for 30% ABFA within the BA mixture (See figures V.35).
- Closed, fine and almost uniform cells (average cell size is about 25  $\mu\text{m}$ ) for 70% ABFA within the BA mixture (See figures V.36 and V.37).



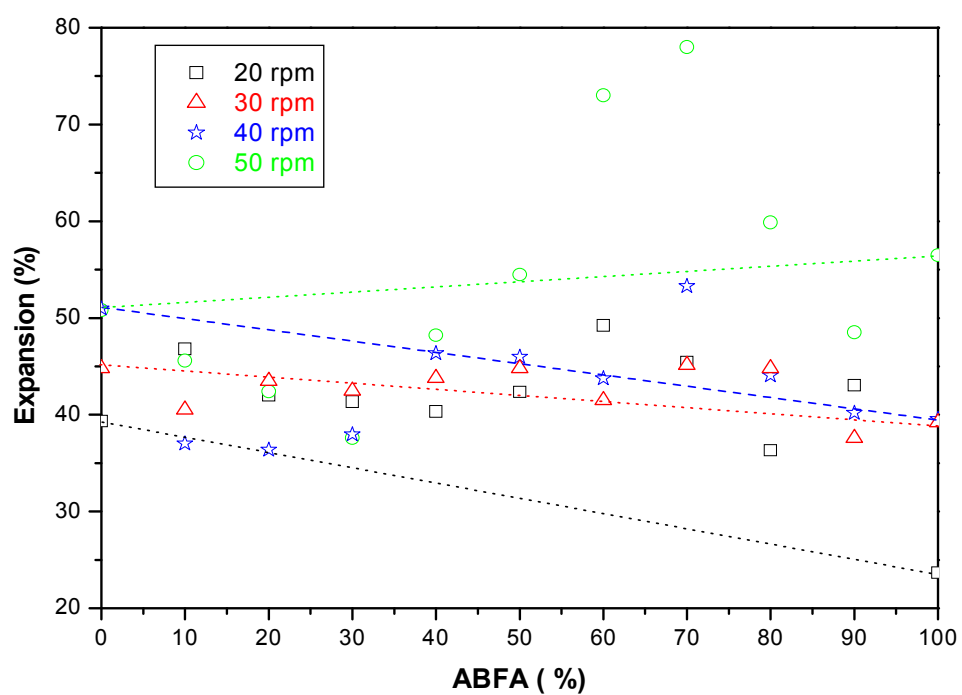


**Figure V.33:** Percentage expansion as a function of ABFA percentage (%)

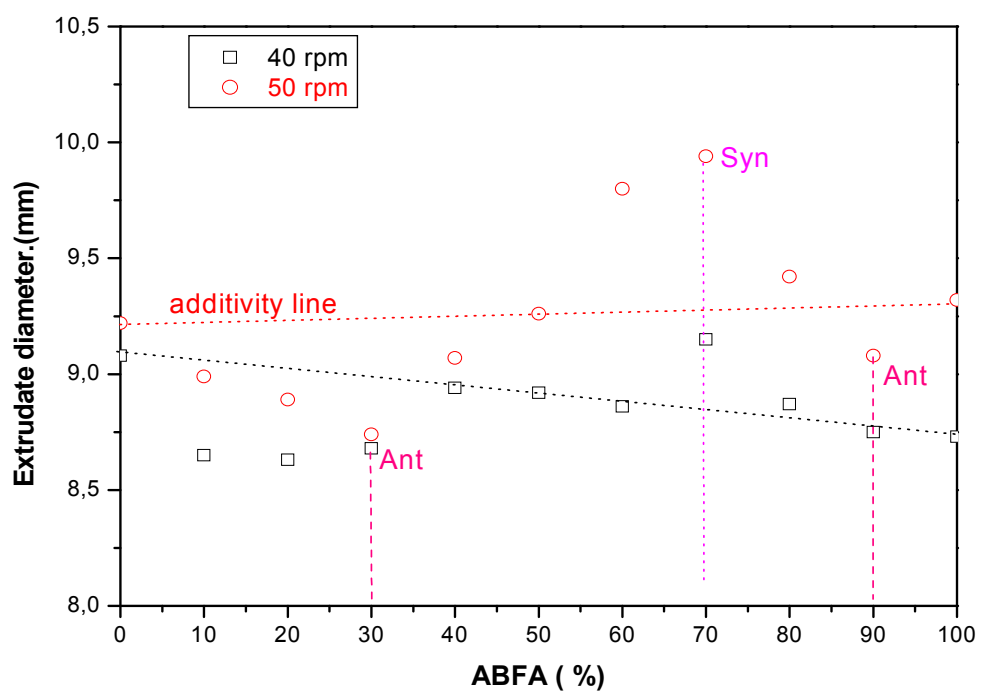
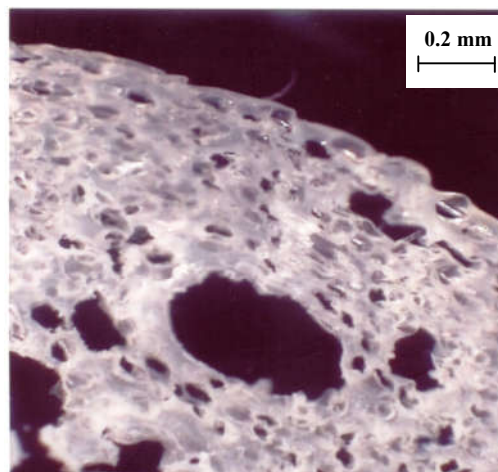
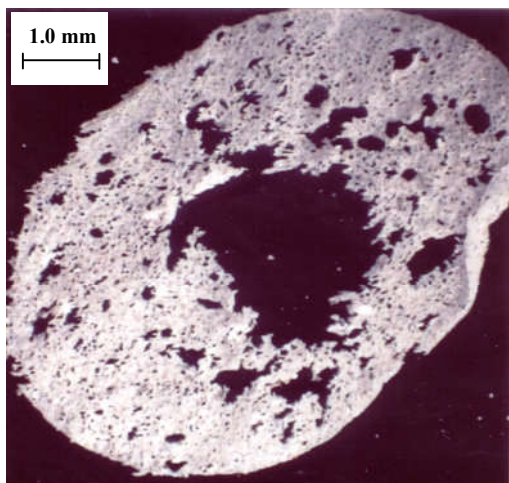


**Figure V.34:** Percentage expansion as a function of ABFA percentage at 40 and 50 rpm



**a** **b**

**Figure V.35: a-** Optical micrograph (x 9) of foamed rigid PVC extrudate (30% ABFA of BA mixture based on their optimum concentrations) at 50rpm

**b-** Optical micrograph (x 45) of extrudate sample boarder of foamed rigid PVC (30% ABFA of BA mixture based on their optimum concentrations) at 50rpm.

The antagonism can be explained by the following interrelated factors:

- Below 40% ABFA, the ratio of kicker/ABFA is high in the way of decreasing the extent of ABFA proportion within the BA mixture (at a constant kicker concentration within formulated PVC); we are in the situation as we are increasing the extent of kicker concentration within formulated PVC (at a constant ABFA concentration within the BA mixture). This will contribute to decrease the ABFA decomposition temperature below the processing temperature (premature decomposition of ABFA) which will result in some of the evolved gas will escape from the hopper of the extrudate before total fusion of PVC takes place; therefore a lower expansion is obtained.

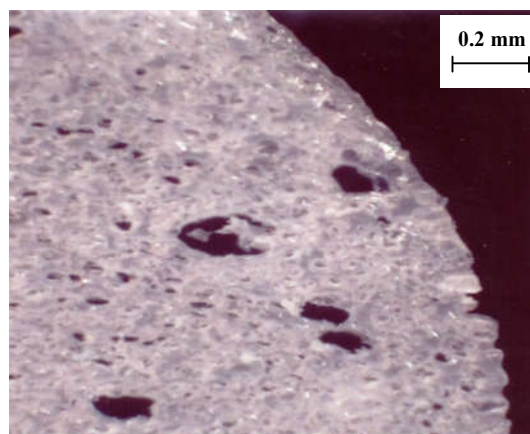


**Figure V.36:** **a** Optical micrograph (X 9) of foamed rigid PVC extrudate (70% ABFA of BA mixture based on their optimum concentrations) at 50rpm  
**b** Optical micrograph (X 45) of extrudate sample boarder of foamed rigid PVC (70% ABFA of BA mixture based on their optimum concentrations) at 50rpm

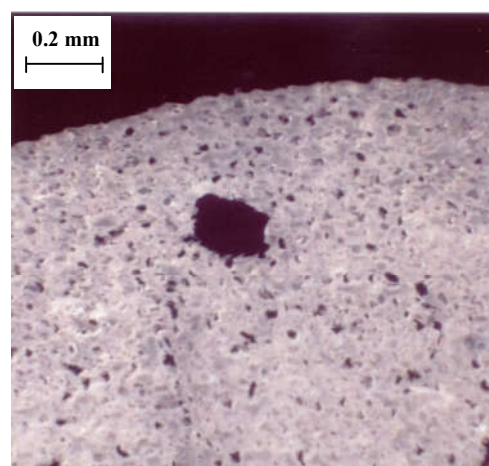
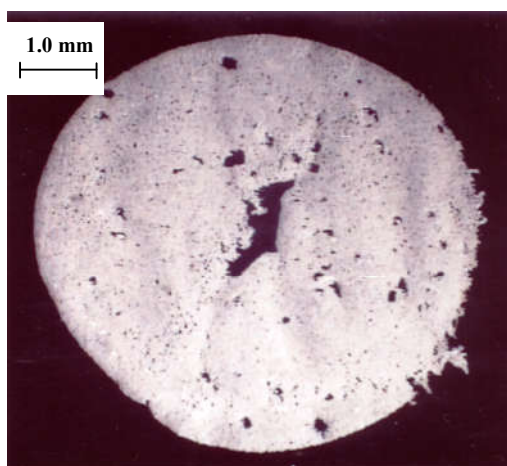


**Figure V.37:** **a** Optical micrograph (X 9) of foamed rigid PVC extrudate (70% ABFA of BA mixture based on their optimum concentrations) at 40rpm  
**b** Optical micrograph (X 45) of extrudate sample boarder of foamed rigid PVC (70% ABFA of BA mixture based on their optimum concentrations) at 40rpm

- In addition to that, in the same range (below 40% ABFA), the higher the proportion of SBS in the mixture the greater the amount of heat absorbed (-227 Kcal/mole at 170°C) when decomposing. This will lead to an increase in polymeric matrix viscosity; hence the released bubbles have a difficulty to expand resulting in a lower expansion.

On the other hand, the synergism can be explained by the following interrelated factors:

- At 70% ABFA, the higher the proportion of ABFA in the mixture the greater the amount of heat released (10 Kcal/mole at 230°C) when decomposing. This will lead to a decrease in polymeric matrix viscosity and, therefore, to a better expansion resulting from a better efficiency of the gases released.

- In addition to that, in the same range (at 70% ABFA), the ratio of kicker/ABFA is low in the way of increasing the extent of ABFA proportion within the BA mixture (at a constant kicker concentration within formulated PVC). This will contribute to increase the ABFA decomposition temperature above the processing temperature which will result in a fraction of ABFA to decompose after leaving the die (that is looked for); therefore a higher expansion is obtained.

This synergism will change to an antagonism (at 90% ABFA) when the ratio of kicker/ABFA is too low in the way of increasing the extent of ABFA proportion within the BA mixture (at a constant kicker concentration within formulated PVC); therefore a great extent of ABFA will not decompose at all even leaving the die: we are in the situation as the SBC is acting alone with a lower concentration; hence a lower expansion is obtained.

A combined use of two BA was developed by N.L. Thomas & col [49]; even though the mixture of the BA was not based on their critical concentrations, the results showed a synergistic effect in term foaming efficiency (i.e. some of the values of the mixture of the BA are not being restricted between those of each BA when used separately) (see figure II.3). The synergism between ABFA and SBC, as reported by the author, is largely attributed to the complementary properties of the gaseous decomposition products  $N_2$ , and  $CO_2$ :  $N_2$  (evolved from ABFA) has a relatively low solubility but high diffusivity in PVC compared with  $CO_2$  (evolved from SBC) [49].

In order to quantify the extent of expansion, it has been calculated in terms of percentage. It is noted that, the general trend of the variation of the percentage expansion with ABFA concentration within the BA mixture, presented in figure V.33 and V.34, is the same as that of the variation of the extrudate diameter.

The following table (table V.1) illustrates these variations in terms of extrudate diameter and surface area.

**Table V.1:** Extent of expansion (diameter versus surface area)

Concentration (phr)	Extrudate Diameter $D_i$ (mm)	Extrudate Diameter ( $D_i^2$ (%) $\times 10^{-2}$	Surface (mm <sup>2</sup> )	Surface (%)
0	7.45	0	697	0
0.6 SBC	9.20	0.23	1067	53
0.4 ABFA	9.32	0.25	1091	56
0.46 (70% ABFA)	9.94	0.33	1241	78

**N.B:** It is worth noting here that the increase in the extrudate diameter obtained with the mixture represents an important economical benefit since the product resulting from the mixture would cost less with a better expansion compared to that when ABFA is used alone. Knowing that the cost of ABFA is largely higher (five times) than that of SBC, the saved cost from the BA at 70% ABFA within the BA mixture is about 24% lower with a lower density. At the same density, the cost saved, at 70% ABFA within the BA mixture, can reach 40% lower.

#### **V.4. Mechanical properties (using a mixture of BA)**

##### **V.4.1 Tensile properties**

##### **V.4.1.1 Variation of elastic modulus**

As shown in figure V.38, it was found that the modulus as a function of the variation of the mixture concentration (i.e.; ABFA/SBC: 0.4/0.6) exhibits values higher than those obtained with each blowing agent used separately. This synergism is due to the fact that the mixtures exhibit an antagonism in terms of expansion.

Concerning the optimum expansion (70%), it is observed that it obeys to the additivity law. The same observation holds true for the concentration of 90% ABFA. The opposite is true for points situated below the additivity line.

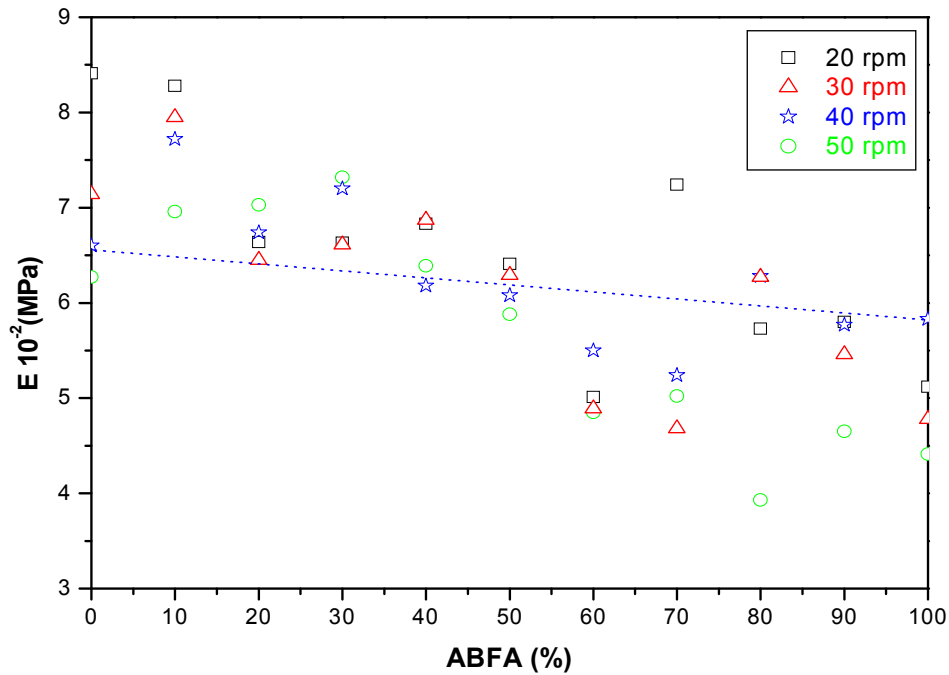


**Figure V.38:** Elastic modulus as a function of ABFA percentage (%)

#### V.4.1. 2 Variation of tensile stress at break

It was found that the stress at break as a function of the variation of the mixture concentration (i.e. ABFA/SBC: 0.4/0.6) exhibits sometimes synergism but sometimes it shows antagonism. Concerning the optimum expansion, as shown in figure V.39, the antagonism is due to the fact that the mixtures exhibits, in terms of extrudate diameter, synergism that reflects a better expansion offering hence flaw sites which are superior in number and/or in dimensions. This trend resulted, therefore, in the decrease of the stress at break.

#### V.4.1 3 Variation of strain at break.

As shown in figure V.40, the strain at break as a function of the variation of the mixture concentration (i.e. ABFA/SBC:0.4/0.6) does not exceed the value of 8% indicating the rigid character of the extrudates obtained from those mixtures.

#### V.4.1. 4 Variation of energy at rupture

The general trend of the energy at break (figure V.41) shows an increase followed by a decrease. This is due to the fact that the material passes from a rigid compact state

to a rigid cellular state; therefore the stress at break decreases resulting in a decrease of the energy at break.

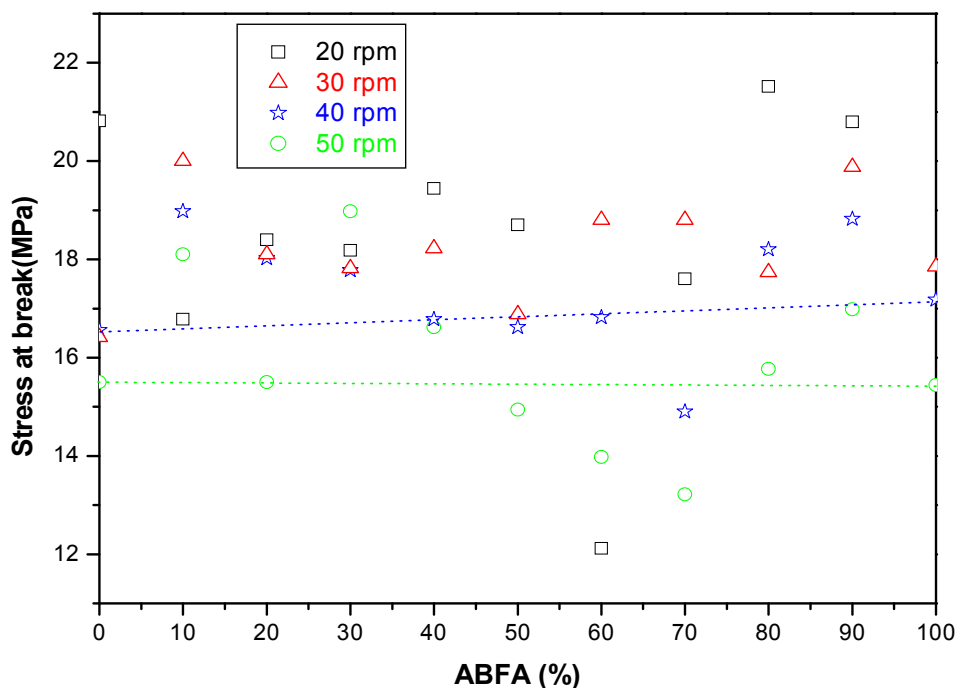


**Figure V.39 :** Stress at break as a function of ABFA percentage (%)

#### V.4.2 Variation of unnotched Izod impact

As shown in figure V.42, it was found that the resilience increases slightly when increasing ABFA content. This is due to the fact that the ABFA blowing agent favors the formation of small and uniform cells.

#### V.4.3 Variation of Hardness

As shown in figures V.43 and V.44, it is noted that the hardness, for the concentrations less than or equal to 50% ABFA, exhibits values higher than those obtained for concentrations exceeding 50% ABFA.

This is attributed to the fact that for concentrations smaller than 50% the cells are irregular in form owing to the dominance of SBC and, therefore, the hardness as a function of SBC content is higher than it is as a function of ABFA.

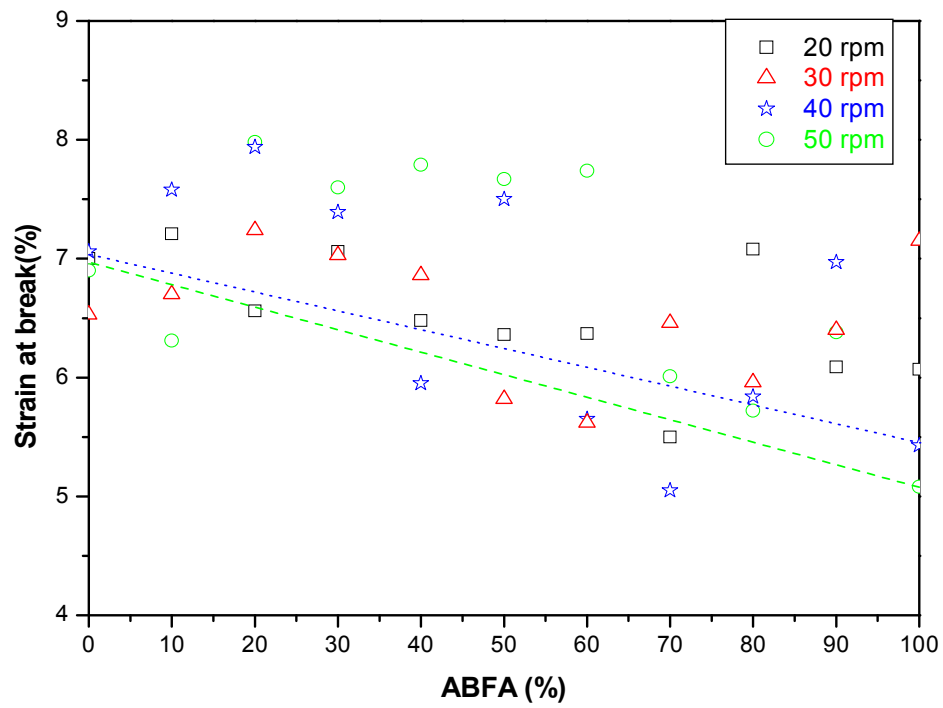


**Figure V.40:** strain at break Strain as a function of ABFA percentage

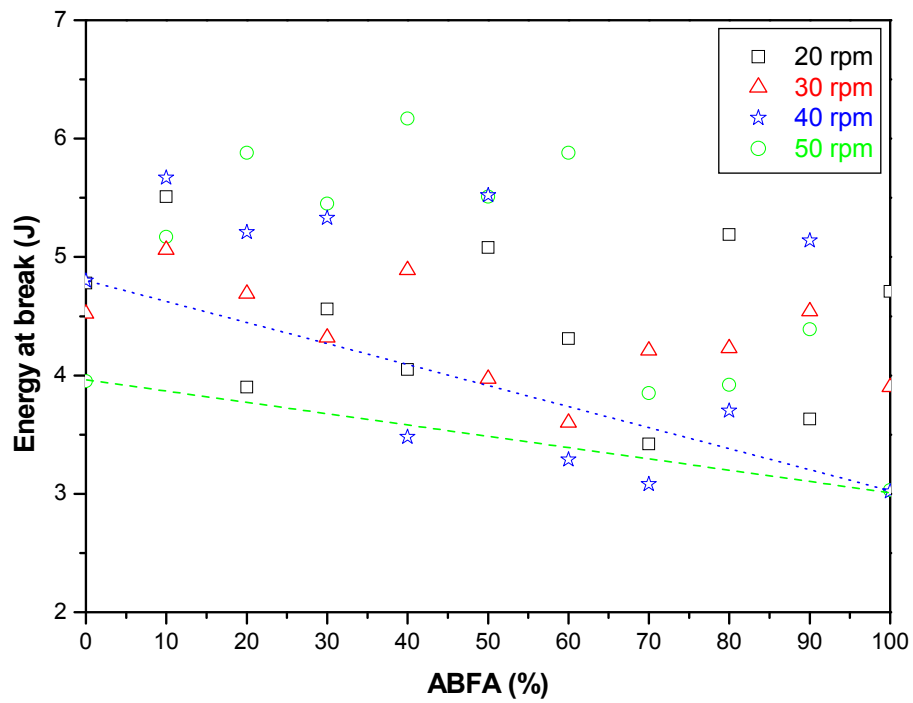


**Figure V.41:** Energy at break as a function of ABFA percentage (%)



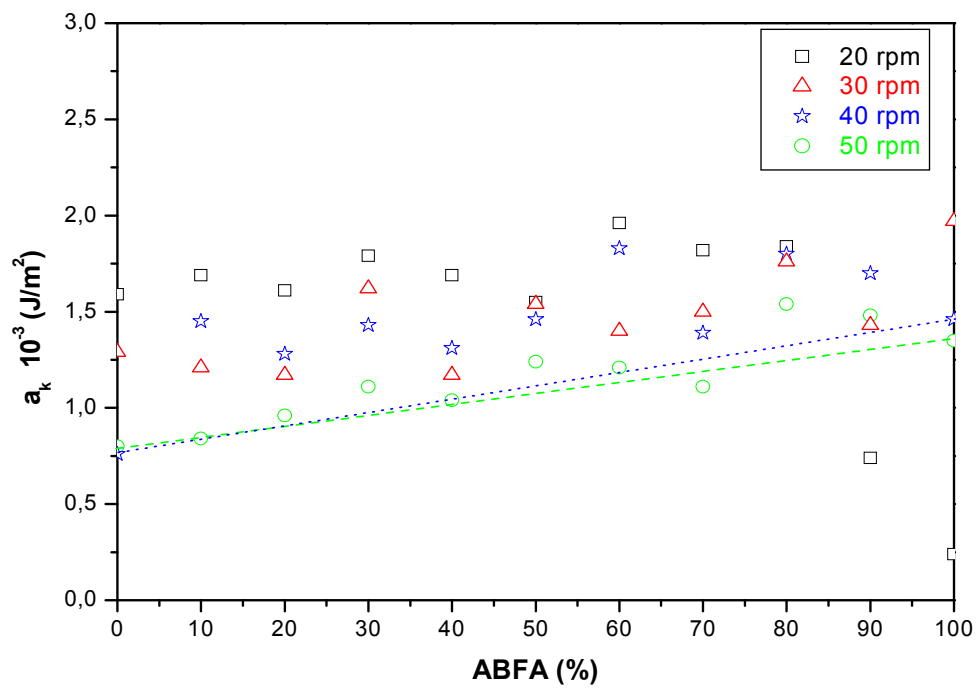


**Figure V.42:** Resilience as a function of ABFA percentage (%)

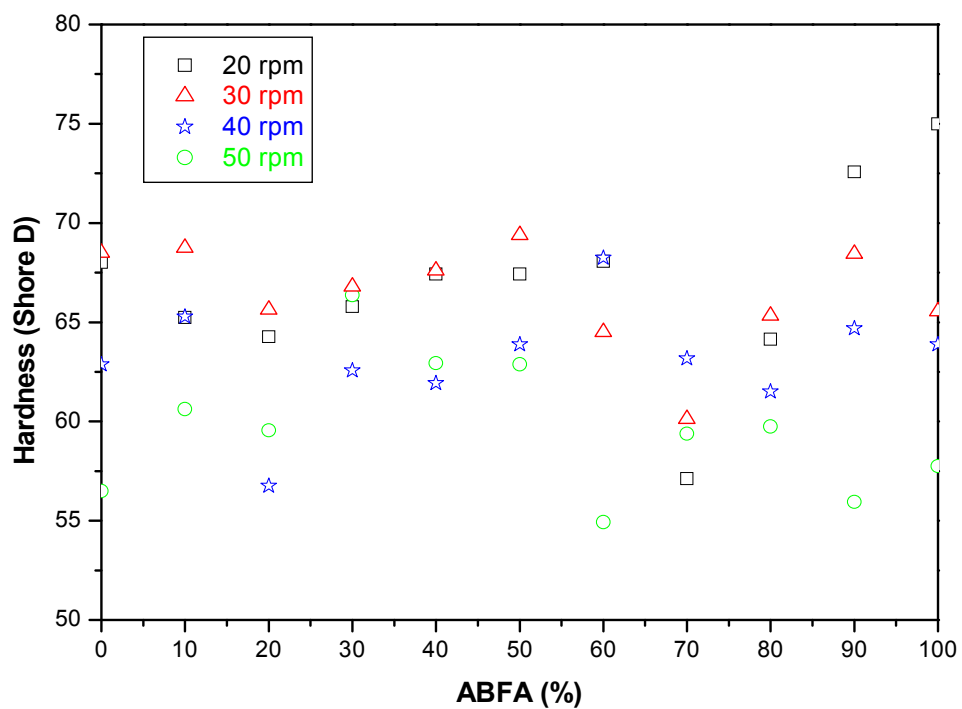


**Figure V.43:** Hardness (Shore D) as a function of ABFA percentage (%) (First lecture)

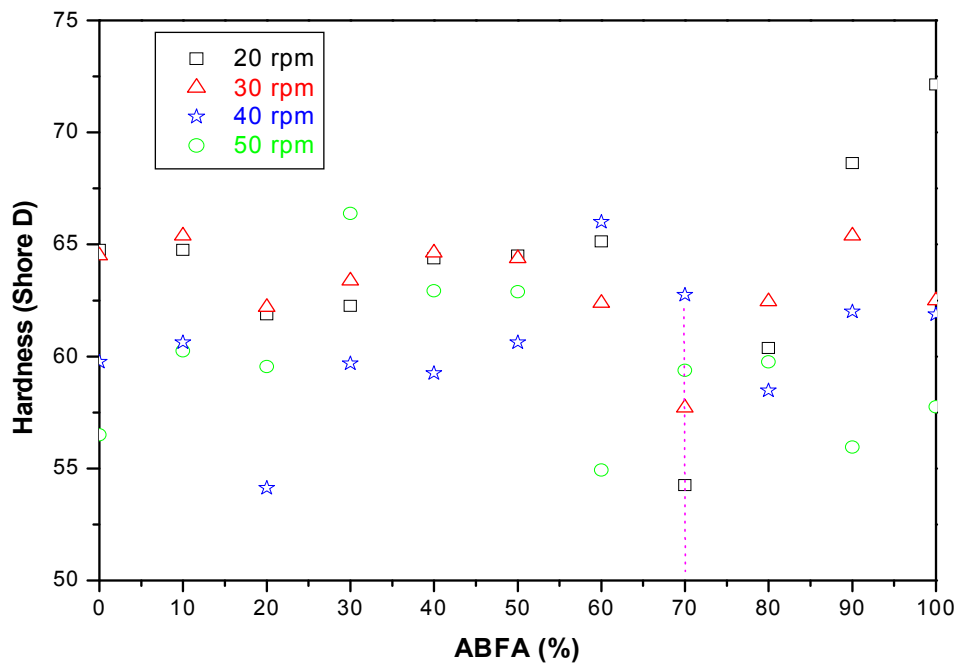


**Figure V.44:** Hardness (Shore D) as a function of ABFA percentage (%) (Second Lecture)

## CONCLUSION

It was concluded that:

- The ABFA exhibits a critical concentration of 0.4 phr while that of SBC is 0.6 phr.
- The optimum expansion corresponds in general to a transition from a smooth surface to a rough one.
- The expression of expansion in terms of percentage allows the elimination of die swell effect and to highlight the expansion.
- The optimum expansion with ABFA gives rise to a closed cellular structure with a better surface state; but SBC forms a structure characterized by a random and partially communicating cells.
- The use of the percentage of the optimum concentration of each BA in the mixture (at a variable total concentration) allows obtaining a better extent of expansion and more economical benefit.
- In general, the increase of the BA concentration results in a decrease of the mechanical properties; namely: strain at break, resilience and hardness.

## **GENERAL CONCLUSIONS**

## GENERAL CONCLUSIONS

- The BRABENDER has proven to be a universal instrument in the vinyl polymers industry. Its use in our study proved that it is a valid tool to help understand the behavior of rigid PVC formulations containing BA through the follow up of the decomposition and the expansion mechanisms
- The addition of ABFA and SBC separately gives rise to a new peak after that of fusion, but the addition of their mixture causes the apparition of two peaks.
- The ABFA exhibits a critical concentration of 0.4 phr while that of SBC is 0.6 phr.
- The optimum expansion corresponds in general to a transition from a smooth surface to a rough one.
- The expression of expansion in terms of percentage allows the elimination of die swell effect and to highlight the expansion.
- The optimum expansion with ABFA gives rise to a closed cellular structure with a better surface state; but SBC forms a structure characterized by a random and partially communicating cells.
- The use of the percentage of the optimum concentration of each BA in the mixture (at a variable total concentration) allows to obtain synergism in terms of extent of expansion and important economical benefit.
- In general, the increase of the BA concentration results in a decrease of the mechanical properties; namely: strain at break, resilience and hardness.

## RECOMMENDATIONS

In the further study, the investigation of other additives has to be carried out for a specific application such as an impact modifier to improve the mechanical properties of this material; and addition of filler (wood flower) to reduce its cost and to give it wood appearance. Then, the following tests have to be performed:

- Chemical resistance;
- Fire resistance (classification);
- Soundproofing and heat insulation.

## REFERENCES

## REFERENCES

- [1]. WENDEL B. C., Cellular Plastics, May / June, p. 178, 1977.
- [2]. THOMAS N. L., EASTUP R. P., Plast. Rubber comps. Process. Appl., 22, p 115, 1994
- [3]. KITAI K. and HOLOSOPPLE p., J. Vinyl technol., 14, p211, 1992
- [4]. REED, R.A., Chemistry of Modern Blowing Agents, Plastics progress, British Plastics Conf., p. 51, 1955.
- [5]. CRAM D. J. and LAVENDER C. M., British Plastics, Sept. 1962
- [6]. ASTM D1715, Method of Test for gas Evolved from Chemical Blowing Agents for Cellular plastics.
- [7]. HANSEN R. H. SPE Journal, 18, p. 80, 1962
- [8]. LALLY R. E. and ALTER L. I., SPE Journal, 23, p. 434, 1967
- [9]. COLLINGTON K. T., Plastics and polymers, Feb. 1973.
- [10]. COLLINGTON K. T., Journ. Cell. Plast. , 7, vol.11, p. 213, 1975.
- [11]. BUCKLEY C. D., J. Vinyl & additives technol., 1, vol.9 , p. 35, 1971
- [12]. TU C. F., Journ. Cell. Plast., 3, vol.14, p. 92, 1978
- [13]. BENNING C., Plastics technology, vol.13, p. 56, 1967.
- [14]. HAWKINS T., Journal of Vinyl Technology, Vol. 4, No. 3, p. 110, Sept. 1982
- [15]. PFENNING J. L. and ROSS M., 4<sup>th</sup> International Conference, Brighton, UK., 24-26, April 1990.
- [16]. BRYDSON J.A., "Plastic materials", Edward E., Third edition, London, p.322, 1975.
- [17]. MASCIA L. "The role of additives in plastics", Arnold E., First edition, London, p. 105. 1974.
- [18]. HEIBERGER C.A., "Encyclopaedia of PVC", Nass L., Second edition, New Jersey, p. 957, 1975.
- [19]. SCHEURLIN H. A., Germ. Plast. Kunsts., 47, p. 165, 1957.
- [20]. LASMAN H. R., "Mod. Plast. Ency.", Mc. Graw Hill Publications, New York, Vol. 43, No.1, p. 394, 1966.
- [21]. F. D. A. REGULATIONS, Subpart F, 121, p. 255, 1977.
- [22]. CURLIS W. B. and HUNTER B. A., U.S. Patent 2, 808, 073, Sept. 10, 1957.
- [23]. BIOS, report 1150, No. 22, P. 21-23, 1980.
- [24]. REED R. A., Brit. Plast., 33, p.249, 1960.
- [25]. REED R. A., Brit. Plast., 33, p.253, 1960

- [26]. LASMAN H. R., "Mod. Plast. Ency.", Mc. Graw Hill Publications, New York, Vol. 43, No.1, p. 397, 1966.
- [27]. NASS L. I., Mod. Plast. ,40, p. 195, 1963
- [28]. Genitron Blowing Agents, Tech. News, Whriffew and Sons, Loughborough, p. 49, 1963.
- [29]. HARRIS E. B, National polychemicals, 1, p. 221, 1965.
- [30]. Advanced Division, Akzo Inerstab Chemicals, New jersey, p. 32, 1966
- [31]. LALLY R. E. and ALTER L. I., SPE Journal, 23, p. 436, 1967
- [32]. NAIRN R. F., HARKINS J. C. and EHRENFELD F. E., U.S. Patent 3, 293, 094, Dec. 20, 1966.
- [33]. HARTMEN T. V. and KOZLOWSKI B. R., "Vinyl dryblend powders", SPE Retec, 10, Accow, Ohio, p. 95, 1965.
- [34]. HACKERT A., Ger. Palst. Kuunsts., 52, p. 321, 1962
- [35]. CONGER R. P., SPE Journal, 24, p. 530, 1968
- [36]. LANTHIER P. V. and LASMAN H R., "Preparation of low density cellular thermoplastics", SPE Retec, 11, New Jersey, p. 35, 1964.
- [37]. ESROVE D. and MEYER. J., Plast. Techn., 5, p. 196, 1959.
- [38]. MEYER. J. and ESROVE D. J., Plast. Techn., 6, p. 271, 1959.
- [39]. RHODES T. J., U.S. Patent 2, 907, 074, Oct. 6, 1959.
- [40]. HANSEN R. H., SPE Journal, 18, p. 88, 1962
- [41]. ASTM. Standarts, Part 35, D-883-75a, Nomenclature relating to plastics.
- [42]. BILLMEYER F.W., "Text Book of Polymer Science", A. Wiley, Third edition, New York, p.326, 1984
- [43]. BRARD F. and KIESLLING G.C., Journ. Cell. Plast. ,11, vol.13, p. 388, 1977
- [44]. KUHLMAN U., U.S. Patent 3, 764, 642, Oct. 9, 1973
- [45]. LASMAN H. R., J. C. Plast. Techn., 9, p. 220, 1963.
- [46]. PFENNING J. L. Kunstsuffe 73, p. 394, 1983.
- [47]. KIM B. C. KIM K. U. and HONG S. I., Poly. Society of Korea, Vol. 10, No.2, p. 178, 1986
- [48]. KIM K. U., PARK T. S. and KIM B. C., J. Poly. Eng., Vol. 7, No.1, p. 5, 1986
- [49]. THOMAS N. L. and HARVEY R.J., "Statistical Experimental design to Optimize Formulations for Foam Vinyl Applications", Foamplas'98, p.55, 1998.
- [50]. LUEBKE G., "Blowing agents and processes", Rapra technology Ltd., Frankfurt, Germany, 13<sup>th</sup>-14<sup>th</sup> March 2001.



- [51]. PATTERRSON. J.R, U.S. Patent 6,784,230, Aug. 31, 2004.
- [52]. PATTERRSON. J.R, U.S. Patent 7,030,179, Apr. 18, 2006.
- [53]. DOUIBI A. and BENACHOUR D., Intern. J. Polym. Mater., Vol.52, N°10, 2003.
- [54]. DEANNIN R. D. AGARWAL P., 4<sup>th</sup> International Conference, Brightoh, UK, 24-26, April 1990.

## **APPENDICES**

**Table 1:** Variation of the extrudate diameter  $D_j$  (mm) as a function of ABFA concentrations

V (tr/min) ABFA (pcr)	20	30	40	50
0.0	7.40*	7.23*	7.39*	7.45*
0.1	7.30*	7.39*	7.50*	7.46*
0.2	8.35*	8.11*	8.13*	8.02*
0.3	8.3*	8.22*	8.12*	8.09*
0.4	8.58***	8.53**	8.87*	8.82*
0.5	7.01***	8.18**	8.37*	8.35*
0.6	7.26***	7.67***	8.35**	8.54*
0.7	7.22***	7.46***	8.25**	8.58**
0.8	7.33***	7.62***	7.67***	8.49**

**Table 2:** Variation of the extrudate diameter  $D_j$  (mm) as a function of SBC concentrations

V (tr/min) ABFA (pcr)	20	30	40	50
0.0	7.04*	7.23*	7.39*	7.45*
0.1	6.8*	6.94*	7.18*	7.55*
0.2	7.03*	7.13*	7.17*	7.34*
0.3	7.04*	7.41*	7.53*	7.49*
0.4	7.30*	7.46*	7.50*	7.47*
0.5	7.43*	7.39*	7.33*	7.36*
0.6	8.18**	8.81**	9.26*	9.00*
0.7	7.64**	7.59**	7.55*	7.62*
0.8	7.95***	7.78**	7.61*	7.49*
0.9	7.67***	6.72***	7.50**	7.32*
1.0	7.88***	7.74***	7.63**	7.57*
1.1	8.10***	8.10***	7.99**	7.89**
1.2	8.12***	8.09***	8.11**	8.04**

\*: Smooth surface

\*\* : Rough surface

\*\*\*: Very rough surface

**Table 3:** Variation of the expansion (%) as a function of ABFA concentrations

V (tr/min) ABFA (pcr)	20	30	40	50
0.0	0.0	0.0	0.0	0.0
0.1	8	4.5	3	0.27
0.2	41	25.82	21.03	15.89
0.3	39	29.26	20.73	17.92
0.4	48.54	39.19	44.06	40.16
0.5	0.0	28	28.28	25.62
0.6	6.34	13.13	27.67	31.4
0.7	5.18	6.46	24.63	32.64
0.8	8.4	11.08	7.72	29.87

**Table 4:** Variation of the expansion (%) as a function of SBC concentrations

V (tr/min) ABFA (pcr)	20	30	40	50
0.0	0.00	0.00	0.00	0.00
0.1	-6.70	-7.86	-5.60	2.70
0.2	-0.30	-2.75	-5.87	-2.93
0.3	0.00	5.04	3.82	1.08
0.4	7.52	6.46	3.00	0.54
0.5	11.39	4.47	-1.60	-2.40
0.6	35.01	48.48	57.01	45.94
0.7	17.77	10.21	4.38	4.62
0.8	27.52	15.79	6.04	1.08
0.9	18.70	-13.61	3.00	-3.46
1.0	25.28	14.61	6.60	3.25
1.1	32.38	25.51	16.90	12.16
1.2	33.04	25.2	20.44	16.47

**Table 5:** Variation of the Elastic Modulus (  $E \cdot 10^{-2}$  ) as a function of ABFA concentrations

V (tr/min) ABFA (pcr)	20	30	40	50
0.0	18.13 ± 3.98	15.01 ± 1.12	18.20 ± 1.01	16.65 ± 1.25
0.1	7.99 ± 1.98	12.95 ± 0.92	15.95 ± 2.59	15.03 ± 1.91
0.2	6.15 ± 1.62	11.23 ± 0.19	9.64 ± 0.92	11.33 ± 0.55
0.3	8.38 ± 0.34	9.13 ± 0.25	9.14 ± 0.37	11.00 ± 0.89
0.4	2.47 ± 0.26	7.06 ± 0.20	7.02 ± 0.54	8.37 ± 0.04
0.5	3.57 ± 0.82	7.91 ± 0.64	6.96 ± 0.50	6.86 ± 0.61
0.6	2.33 ± 0.00	2.05 ± 0.05	5.19 ± 0.65	8.55 ± 0.22
0.7	2.53 ± 0.00	2.18 ± 0.00	3.54 ± 0.63	8.23 ± 0.12
0.8	1.39 ± 0.00	1.74 ± 0.00	1.61 ± 0.63	7.09 ± 0.20

**Table 6:** Variation of the Stress at break (  $\sigma_{\text{break}}$  ) as a function of ABFA concentrations

V (tr/min) ABFA (pcr)	20	30	40	50
0.0	49.83 ± 5.15	47.78 ± 0.82	47.66 ± 2.90	49.04 ± 0.78
0.1	33.99 ± 4.97	39.07 ± 0.11	39.20 ± 1.56	44.05 ± 0.49
0.2	23.08 ± 1.04	26.94 ± 0.78	27.88 ± 0.25	28.82 ± 2.65
0.3	24.32 ± 0.52	24.44 ± 0.34	25.42 ± 0.27	28.30 ± 0.63
0.4	5.19 ± 0.61	1.40 ± 0.40	19.95 ± 0.94	21.36 ± 1.64
0.5	0.52 ± 0.01	23.06 ± 1.28	24.30 ± 0.66	22.82 ± 0.84
0.6	2.13 ± 0.96	1.36 ± 0.33	12.44 ± 3.22	21.70 ± 0.94
0.7	4.07 ± 0.83	3.61 ± 0.39	8.84 ± 0.82	19.10 ± 0.91
0.8	1.77 ± 0.30	3.07 ± 0.27	2.66 ± 0.33	14.76 ± 1.56

**Table 7:** Variation of the Elongation at break ( $\epsilon_{\text{break}}$  %) as a function of ABFA concentrations

V (tr/min) ABFA (pcr)	20	30	40	50
0.0	7.33 ± 0.43	6.21 ± 0.56	6.06 ± 0.64	6.85 ± 0.78
0.1	5.85 ± 0.60	6.19 ± 0.48	6.00 ± 0.55	6.08 ± 0.43
0.2	7.34 ± 0.76	7.32 ± 1.09	5.83 ± 0.91	6.45 ± 0.82
0.3	8.94 ± 0.74	6.38 ± 0.45	7.17 ± 0.49	8.20 ± 0.96
0.4	3.05 ± 0.27	5.77 ± 0.12	5.46 ± 0.37	5.59 ± 0.33
0.5	3.05 ± 0.27	5.06 ± 0.63	6.45 ± 0.50	6.19 ± 0.17
0.6	2.52 ± 0.17	3.69 ± 0.24	3.09 ± 0.32	4.32 ± 0.56
0.7	2.81 ± 0.31	2.62 ± 0.28	2.43 ± 0.24	3.95 ± 0.31
0.8	1.56 ± 0.14	2.39 ± 0.19	2.36 ± 0.43	3.26 ± 0.37

**Table 8:** Variation of the Energy at rupture  $U_r$  (KJ) as a function of ABFA concentrations

V (tr/min) ABFA (pcr)	20	30	40	50
0.0	8.62 ± 1.49	7.79 ± 0.85	6.51 ± 1.03	8.18 ± 1.68
0.1	5.88 ± 0.77	6.47 ± 0.82	6.20 ± 0.76	7.18 ± 0.73
0.2	6.70 ± 0.67	6.61 ± 1.30	5.02 ± 1.04	4.96 ± 0.44
0.3	7.01 ± 0.84	5.04 ± 0.54	5.93 ± 0.52	7.67 ± 1.22
0.4	0.40 ± 0.05	2.30 ± 0.78	3.51 ± 0.28	2.42 ± 0.05
0.5	0.53 ± 0.08	3.46 ± 0.75	4.96 ± 0.21	4.45 ± 0.41
0.6	0.16 ± 0.02	0.34 ± 0.05	0.37 ± 0.08	2.53 ± 0.31
0.7	0.12 ± 0.03	0.23 ± 0.05	0.69 ± 0.02	2.32 ± 0.34
0.8	0.04 ± 0.00	0.17 ± 0.02	0.14 ± 0.03	0.49 ± 0.09

**Table 9:** Variation of the Elastic Modulus ( $E \cdot 10^{-2}$ ) as a function of SBC concentrations

V (tr/min) ABFA (pcr)	20	30	40	50
0.1	13.45 ±	12.24 ± 3.24	15.08 ± 2.61	13,57 ± 3.52
0.2	4.60	11.33 ± 1.68	8.65 ± 3.06	9,63 ± 4.32
0.3	7.44 ± 1.13	14.74 ± 4.25	7.79 ± 2.29	11,53 ± 2.65
0.4	12.63 ± 3.48	9.17 ± 3.67	9.78 ± 1.90	11,33 ± 2.78
0.5	9.35 ± 2.97	8.82 ± 3.82	5.07 ± 1.93	12,67 ± 2.60
0.6	4.35 ± 0.77	7.18 ± 0.25	5.08 ± 0.32	8,26 ± 0.55
0.7	8.38 ± 0.30	12.14 ± 0.21	12.28 ± 0.13	13,64 ± 0.59
0.8	9.96 ± 0.24	10.38 ± 0.50	11.52 ± 0.72	14,64 ± 0.01
0.9	9.04 ± 0.44	12.26 ± 0.54	12.38 ± 0.64	14,36 ± 0.39
1.0	10.60 ± 0.11	9.57 ± 0.33	10.21 ± 0.79	10,21 ± 0.79
1.1	14.36 ± 0.39	8.44 ± 0.34	9.72 ± 0.07	10,40 ± 0.36
1.2	8.79 ± 0.34	9.13 ± 0.87	8.43 ± 0.73	9,27 ± 0.44
	8.26 ± 0.63			

**Table 10:** Variation of the Stress at break ( $E \cdot 10^{-2}$ ) as a function of SBC concentrations

V (tr/min) ABFA (pcr)	20	30	40	50
0.1	34,14 ± 7.74	44,2 ± 1.87	54,74 ± 3.17	33,98 ± 7.71
0.2	44,76 ± 0.93	46,98 ± 0.78	43,64 ± 1.27	41,88 ± 3.03
0.3	44,52 ± 0.99	43,88 ± 0.37	42,52 ± 0.61	41,2 ± 2.53
0.4	39,1 ± 0.80	38,4 ± 0.78	39,64 ± 0.87	41,16 ± 0.92
0.5	30,02 ± 3.94	35,88 ± 0.63	39,58 ± 0.66	35,72 ± 8.76
0.6	23,18 ± 0.60	18,26 ± 0.30	17,54 ± 0.24	22,56 ± 1.45
0.7	34,24 ± 8.63	30,26 ± 0.50	32,16 ± 0.41	36,06 ± 0.58
0.8	23,76 ± 0.64	26,74 ± 1.82	28,36 ± 3.03	31,46 ± 2.64
0.9	29,18 ± 0.76	34,18 ± 0.59	30,1 ± 2.52	35,86 ± 1.60
1.0	26,4 ± 1.34	26,66 ± 0.32	29,32 ± 0.62	31,96 ± 1.64
1.1	23,22 ± 0.36	22,62 ± 0.42	24,3 ± 0.43	27,42 ± 0.58
1.2	21,4 ± 0.83	23,64 ± 0.22	23,42 ± 0.40	26,78 ± 0.72

**Table 11:** Variation of the Strain at break ( $\epsilon_{\text{break}}$  %) as a function of SBC concentrations

V (tr/min) ABFA (pcr)	20	30	40	50
0.1	6,97 ± 0.32	6,65 ± 0.75	6,37 ± 0.20	5,18 ± 1.11
0.2	6,20 ± 0.14	6,07 ± 0.13	6,46 ± 0.16	6,33 ± 0.23
0.3	5,24 ± 0.49	6,09 ± 0.15	5,77 ± 0.20	5,06 ± 0.42
0.4	6,53 ± 0.59	5,63 ± 0.08	5,06 ± 0.34	5,41 ± 0.46
0.5	4,86 ± 0.72	5,41 ± 0.37	6,15 ± 0.29	5,31 ± 0.79
0.6	5,46 ± 0.43	7,13 ± 0.71	7,15 ± 1.05	6,81 ± 0.54
0.7	6,67 ± 0.36	5,77 ± 0.39	6,93 ± 0.75	8,1 ± 0.62
0.8	5,96 ± 0.37	7,28 ± 0.72	5,63 ± 0.66	6,82 ± 0.92
0.9	5,03 ± 0.57	6,29 ± 0.67	5,3 ± 1.16	6,89 ± 0.75
1.0	5,75 ± 0.25	4,96 ± 0.39	4,69 ± 0.29	4,25 ± 0.47
1.1	5,72 ± 0.54	6,20 ± 0.80	5,98 ± 0.75	5,05 ± 0.55
1.2	6,04 ± 0.76	7.00 ± 0.42	6,39 ± 0.37	5,73 ± 0.48

**Table 12:** Variation of the Energy at rupture  $U_r$  (KJ) as a function of SBC concentrations

V (tr/min) ABFA (pcr)	20	30	40	50
0.1	7.33 ± 0.84	7.55 ± 1.10	8.70 ± 0.62	8.83 ± 1.51
0.2	6.88 ± 0.36	7.21 ± 0.20	7.43 ± 0.13	7.59 ± 0.19
0.3	6.30 ± 0.71	7.17 ± 0.30	6.51 ± 0.27	5.37 ± 0.82
0.4	7.38 ± 0.25	5.59 ± 0.19	5.07 ± 0.49	6.31 ± 0.74
0.5	4.93 ± 0.28	4.84 ± 0.53	6.36 ± 0.45	5.37 ± 1.22
0.6	3.96 ± 0.46	5.14 ± 0.66	5.81 ± 0.42	5.17 ± 0.46
0.7	4.28 ± 0.74	4.74 ± 0.44	6.52 ± 0.92	7.92 ± 0.93
0.8	4.21 ± 0.41	6.01 ± 0.75	5.38 ± 0.51	6.16 ± 0.76
0.9	3.88 ± 0.65	4.66 ± 0.62	3.23 ± 0.72	6.38 ± 0.68
1.0	4.41 ± 0.27	3.93 ± 0.45	3.82 ± 0.21	3.78 ± 0.43
1.1	4.01 ± 0.55	4.74 ± 0.84	4.48 ± 0.79	3.88 ± 0.62
1.2	4.08 ± 0.74	5.29 ± 0.40	4.71 ± 0.38	4.08 ± 0.66



**Table 13:** Variation of the Resilience  $a_k$  (KJ/m<sup>2</sup>) as a function of ABFA concentrations

V (tr/min) ABFA (pcr)	20	30	40	50
0.0	7,19 ± 0.30	7,96 ± 0.96	7,57 ± 0.95	6,08 ± 0.93
0.1	6,14 ± 0.24	3,88 ± 0.19	3,64 ± 0.13	3,54 ± 0.96
0.2	2,17 ± 0.55	2,86 ± 0.22	2,7 ± 0.65	2,73 ± 0.44
0.3	2,04 ± 0.35	2,39 ± 0.24	2,38 ± 0.48	2,26 ± 0.43
0.4	0,38 ± 0.08	1,25 ± 0.52	1,61 ± 0.41	1,68 ± 0.48
0.5	0,21 ± 0.06	1,86 ± 0.43	1,63 ± 0.28	2,25 ± 0.34
0.6	0,11 ± 0.03	0,19 ± 0.08	0,46 ± 0.09	0,74 ± 0.24
0.7	0,13 ± 0.03	0,16 ± 0.02	0,15 ± 0.02	0,39 ± 0.08
0.8	0,09 ± 0.01	0,07 ± 0.00	0,06 ± 0.00	0,28 ± 0.09

**Table 14:** Variation of the Resilience  $a_k$  (KJ/m<sup>2</sup>) as a function of SBC concentrations

V (tr/min) ABFA (pcr)	20	30	40	50
0.0	7,19 ± 0.30	7,96 ± 0.96	7,57 ± 0.95	6,08 ± 0.93
0.1	7,99 ± 0.74	8,22 ± 0.08	4,31 ± 0.50	3,86 ± 0.80
0.2	3,89 ± 0.45	2,68 ± 0.63	3,81 ± 0.93	2,70 ± 0.23
0.3	2,75 ± 0.43	2,65 ± 0.18	2,65 ± 0.72	3,16 ± 0.36
0.4	2,00 ± 0.33	2,53 ± 0.29	1,95 ± 0.29	2,44 ± 0.27
0.5	1,73 ± 0.27	1,55 ± 0.05	2,11 ± 0.26	2,19 ± 0.30
0.6	1,26 ± 0.13	0,88 ± 0.12	0,85 ± 0.16	0,76 ± 0.12
0.7	1,23 ± 0.29	1,34 ± 0.15	1,55 ± 0.21	1,80 ± 0.17
0.8	1,23 ± 0.16	1,17 ± 0.31	1,32 ± 0.27	2,15 ± 0.29
0.9	0,91 ± 0.16	1,56 ± 0.15	1,73 ± 0.09	1,17 ± 0.67
1.0	0,77 ± 0.13	1,08 ± 0.17	1,52 ± 0.48	1,45 ± 0.17
1.1	0,89 ± 0.07	0,86 ± 0.09	1,00 ± 0.18	1,07 ± 0.16
1.2	1,24 ± 0.25	0,78 ± 0.09	0,83 ± 0.08	0,83 ± 0.12

**Table 15:** Variation of the Hardness Shore D (first lecture) as a function of ABFA concentrations

V (tr/min) ABFA (pcr)	20	30	40	50
0.0	83.00 ± 1.23	82,13 ± 4.73	84,63 ± 2.46	83,75 ± 3.18
0.1	81,75 ± 0.72	80,50 ± 1.31	78.00 ± 2.69	81,50 ± 3.52
0.2	71,63 ± 1.43	73,88 ± 2.16	74,50 ± 1.31	70.00 ± 5.69
0.3	66,75 ± 4.80	65,63 ± 5.34	74,80 ± 2.03	73,38 ± 4.51
0.4	--	61,50 ± 3.80	69,38 ± 2.88	68,75 ± 6.03
0.5	--	71,50 ± 3.19	72.00 ± 4.14	69,63 ± 2.66
0.6	--	--	--	67,63 ± 2.03
0.7	--	--	--	--
0.8	--	--	--	--

**Table 16:** Variation of the Hardness Shore D (Second lecture) as a function of ABFA concentrations

V (tr/min) ABFA (pcr)	20	30	40	50
0.0	80,88 ± 1.25	77,63 ± 6.58	82,50 ± 2.33	81,63 ± 2.92
0.1	78,50 ± 0.44	77,63 ± 0.84	75,50 ± 1.99	79.00 ± 3.34
0.2	68,38 ± 1.46	70,63 ± 2.17	71,63 ± 1.25	66,88 ± 5.21
0.3	63,75 ± 5.37	63,75 ± 4.50	72,25 ± 1.68	69,25 ± 4.42
0.4	--	61,50 ± 2.07	66,63 ± 1.86	66.00 ± 6.05
0.5	--	71,50 ± 3.54	68,63 ± 1.04	66,63 ± 2.53
0.6	--	--	--	65,63 ± 2.32
0.7	--	--	--	--
0.8	--	--	--	--

**Table 17:** Variation of the Hardness Shore D (First lecture) as a function of SBC concentrations

V (tr/min) ABFA (pgr)	20	30	40	50
0.0	83.00 ± 1.23	82,13 ± 4.73	84,63 ± 2.46	83,75 ± 3.18
0.1	81,38 ± 3.75	83,43 ± 2.27	83,13 ± 2.15	80,38 ± 0.94
0.2	81,63 ± 1.98	82,93 ± 2.05	81.00 ± 0.31	86,80 ± 1.20
0.3	81,83 ± 4.57	81,70 ± 4.44	81,25 ± 5.31	82,88 ± 2.08
0.4	85.00 ± 2.65	79,25 ± 2.66	80,13 ± 2.44	81,63 ± 6.74
0.5	77.00 ± 9.13	79,88 ± 2.48	76,50 ± 6.12	80.00 ± 4.45
0.6	64,88 ± 7.51	59,45 ± 7.70	60,75 ± 3.32	60,75 ± 4.48
0.7	78,38 ± 2.17	79,50 ± 5.33	61,63 ± 1.06	75,63 ± 6.95
0.8	68,63 ± 1.70	75,50 ± 8.08	76,75 ± 5.03	79,25 ± 5.25
0.9	75,75 ± 2.66	75,25 ± 6.83	74.00 ± 7.33	80,25 ± 2.62
1.0	--	75,25 ± 1.81	73,25 ± 1.79	77,13 ± 4.12
1.1	--	74,25 ± 1.13	70,75 ± 0.72	76,50 ± 4.73
1.2	--	62.00 ± 4.22	72.00 ± 2.53	69,75 ± 1.40

**Table 18:** Variation of the Hardness Shore D (Second lecture) as a function of SBC concentrations

V (tr/min) ABFA (pgr)	20	30	40	50
0.0	80,88 ± 1.25	77,63 ± 6.58	82,50 ± 2.33	81,63 ± 2.92
0.1	78,88 ± 2.71	80,88 ± 3.23	80,88 ± 2.10	78,13 ± 1.36
0.2	79,38 ± 1.89	81.00 ± 2.29	79,75 ± 2.70	78,75 ± 3.87
0.3	79,25 ± 4.29	79,38 ± 4.34	78,50 ± 5.60	80,88 ± 1.86
0.4	82,13 ± 2.77	77,25 ± 2.26	76,13 ± 3.00	76.00 ± 8.73
0.5	73,75 ± 8.52	78,25 ± 2.70	74,63 ± 6.48	78.00 ± 3.75
0.6	62,13 ± 7.25	57,85 ± 6.83	58,50 ± 3.29	58,88 ± 8.92
0.7	76,13 ± 1.70	77.00 ± 4.29	69,75 ± 9.17	73,75 ± 6.18
0.8	65,88 ± 2.10	72,13 ± 8.13	74,38 ± 4.71	77,50 ± 4.96
0.9	71,50 ± 4.68	73,50 ± 6.77	72,50 ± 7.55	78,38 ± 1.94
1.0	--	76,13 ± 5.45	70,50 ± 2.07	74,75 ± 3.87
1.1	--	71,25 ± 0.72	71,25 ± 4.42	73,75 ± 4.82
1.2	--	62,50 ± 5.56	68,13 ± 1.73	67,05 ± 1.67

**Table 19:** Variation of the Extrudate diameter Dj as a function of (ABFA/SBC: 0.4/0.6) concentrations

V (tr/min) ABFA (pcr)	20	30	40	50
0	8,31**	8,70**	9,08*	9,22*
10	8,53**	8,57*	8,65*	8,99*
20	8,39*	8,66*	8,63*	8,89*
30	8,37*	8,63*	8,68*	8,74*
40	8,34*	8,67*	8,94*	9,07*
50	8,40*	8,70*	8,92*	9,26*
60	8,60*	8,60*	8,86*	9,80*
70	8,49**	8,71*	9,15*	9,94*
80	8,22**	8,70*	8,87*	9,42*
90	8,42***	8,48*	8,75*	9,08*
100	7,83***	8,53*	8,73*	9,32*

**Table 20:** Variation of the Expansion (%) as a function of (ABFA/SBC: 0.4/0.6) concentrations

V (tr/min) ABFA (pcr)	20	30	40	50
0	39,33	44,80	50,97	50,84
10	46,81	40,50	37,01	45,62
20	42,03	43,47	36,37	42,39
30	41,35	42,48	37,96	37,63
40	40,34	43,80	46,35	48,22
50	42,37	44,80	45,96	54,49
60	49,23	41,49	43,74	73,04
70	45,44	45,13	53,30	78,02
80	36,33	44,80	44,06	59,88
90	43,05	37,57	40,19	48,55
100	23,70	39,19	39,55	56,50

**Table 21:** Variation of the Elastic Modulus ( $E \cdot 10^{-2}$ ) as a function of (ABFA/SBC: 0.4/0.6) concentrations.

V (tr/min) ABFA (pcr)	20	30	40	50
0.0	8,41 ± 0.29	7,14 ± 0.40	6,60 ± 0.10	6,27 ± 0.3125
0.1	8,28 ± 0.22	7,95 ± 0.22	7,72 ± 0.30	6,96 ± 0.23
0.2	6,64 ± 0.45	6,45 ± 0.25	6,74 ± 0.19	7,03 ± 0.05
0.3	6,63 ± 0.26	6,61 ± 0.50	7,20 ± 0.08	7,32 ± 0.17
0.4	6,83 ± 0.40	6,87 ± 0.14	6,18 ± 0.38	6,39 ± 0.38
0.5	6,41 ± 0.33	6,29 ± 0.31	6,08 ± 0.20	5,88 ± 0.38
0.6	5,01 ± 1.41	4,89 ± 0.65	5,50 ± 0.74	4,85 ± 0.28
0.7	7,24 ± 0.33	4,68 ± 0.88	5,24 ± 0.69	5,02 ± 0.19
0.8	5,73 ± 0.80	6,27 ± 1.35	6,28 ± 0.08	3,93 ± 0.48
0.9	5,80 ± 0.50	5,46 ± 0.56	5,77 ± 0.55	4,65 ± 0.71
1.0	5,12 ± 1.40	4,78 ± 1.31	5,83 ± 0.40	4,41 ± 0.71

**Table 22:** Variation of the stress at break ( $\sigma_{\text{break}}$ ) as a function of of (ABFA/SBC: 0.4/0.6) concentrations.

V (tr/min) ABFA (pcr)	20	30	40	50
0.0	20,82 ± 0.64	16,42 ± 1.81	16,56 ± 0.99	15,50 ± 0.72
0.1	16,78 ± 2.36	20,00 ± 0.35	18,98 ± 0.34	18,10 ± 0.48
0.2	18,40 ± 0.27	18,10 ± 0.37	18,02 ± 0.24	15,50 ± 1.04
0.3	18,18 ± 0.79	17,82 ± 0.86	17,78 ± 0.54	18,98 ± 0.46
0.4	19,44 ± 0.71	18,22 ± 0.41	16,78 ± 0.69	16,62 ± 0.62
0.5	18,70 ± 0.61	16,88 ± 0.49	16,62 ± 0.27	14,94 ± 0.44
0.6	12,12 ± 0.39	18,80 ± 0.30	16,82 ± 0.45	13,98 ± 0.58
0.7	17,60 ± 0.52	18,80 ± 0.66	14,90 ± 0.91	13,22 ± 0.39
0.8	21,52 ± 0.50	17,74 ± 1.16	18,20 ± 1.25	15,77 ± 0.27
0.9	20,80 ± 0.44	19,88 ± 0.50	18,82 ± 0.76	16,98 ± 0.39
1.0	23,68 ± 0.38	17,85 ± 0.64	17,18 ± 0.74	15,44 ± 0.28

**Table 23:** Strain at break ( $\epsilon_{\text{break}}$  %) variation as a function of of (ABFA/SBC: 0.4/0.6) concentrations

V (tr/min) ABFA (pcr)	20	30	40	50
0.0	7.00 ± 0.68	6,53 ± 0.47	7,06 ± 0.40	6,90 ± 0.96
0.1	7,21 ± 0.59	6,70 ± 0.76	7,58 ± 0.67	6,31 ± 0.54
0.2	6,56 ± 0.33	7,24 ± 0.18	7,94 ± 0.65	7,98 ± 0.50
0.3	7,06 ± 0.83	7,03 ± 0.47	7,39 ± 0.55	7,60 ± 0.33
0.4	6,48 ± 0.53	6,86 ± 0.51	5,95 ± 0.41	7,79 ± 0.80
0.5	6,36 ± 0.68	5,82 ± 0.72	7,50 ± 0.64	7,67 ± 0.62
0.6	6,37 ± 0.63	5,62 ± 0.15	5,65 ± 0.54	7,74 ± 0.40
0.7	5,50 ± 0.66	6,46 ± 0.80	5,05 ± 0.36	6,01 ± 0.31
0.8	7,08 ± 0.98	5,96 ± 0.53	5,84 ± 0.64	5,72 ± 0.66
0.9	6,09 ± 0.63	6,40 ± 0.63	6,97 ± 0.32	6,38 ± 0.25
1.0	6,07 ± 0.25	7,15 ± 0.69	5,43 ± 0.51	5,08 ± 0.53

**Table24:** Energy at rupture  $U_r$  (KJ) variation as a function of of (ABFA/SBC: 0.4/0.6) concentrations

V (tr/min) ABFA (pcr)	20	30	40	50
0.0	4,78 ± 0.71	4,52 ± 0.50	4,80 ± 0.32	3,95 ± 0.46
0.1	5,51 ± 0.71	5,06 ± 0.76	5,67 ± 0.63	5,17 ± 0.82
0.2	3,90 ± 0.25	4,69 ± 0.46	5,21 ± 0.63	5,88 ± 0.50
0.3	4,56 ± 0.65	4,32 ± 0.30	5,33 ± 0.49	5,45 ± 0.26
0.4	4,05 ± 0.56	4,89 ± 0.38	3,48 ± 0.32	6,17 ± 0.42
0.5	5,08 ± 0.96	3,97 ± 0.77	5,52 ± 0.27	5,51 ± 0.40
0.6	4,31 ± 0.64	3,60 ± 0.18	3,29 ± 0.42	5,88 ± 0.60
0.7	3,42 ± 0.64	4,21 ± 0.73	3,08 ± 0.29	3,85 ± 0.25
0.8	5,19 ± 0.92	4,23 ± 0.51	3,70 ± 0.73	3,92 ± 0.52
0.9	3,63 ± 0.54	4,54 ± 0.61	5,14 ± 0.26	4,39 ± 0.20
1.0	4,71 ± 0.76	3,90 ± 0.45	3,02 ± 0.33	3,03 ± 0.51

**Table 25:** Variation of the Resilience  $a_k$  (KJ/m<sup>2</sup>) as a function of of (ABFA/SBC: 0.4/0.6) concentrations

V (tr/min) ABFA (pcr)	20	30	40	50
0.0	1,59 ± 0.29	1,29 ± 0.14	0,76 ± 0.06	0,80 ± 0.09
0.1	1,69 ± 0.19	1,21 ± 0.07	1,45 ± 0.19	0,84 ± 0.06
0.2	1,61 ± 0.18	1,17 ± 0.07	1,28 ± 0.11	0,96 ± 0.16
0.3	1,79 ± 0.31	1,62 ± 0.19	1,43 ± 0.23	1,11 ± 0.10
0.4	1,69 ± 0.30	1,17 ± 0.03	1,31 ± 0.09	1,04 ± 0.07
0.5	1,55 ± 0.22	1,54 ± 0.05	1,46 ± 0.11	1,24 ± 0.10
0.6	1,96 ± 0.29	1,40 ± 0.09	1,83 ± 0.33	1,21 ± 0.13
0.7	1,82 ± 0.11	1,50 ± 0.09	1,39 ± 0.10	1,11 ± 0.11
0.8	1,84 ± 0.15	1,76 ± 0.14	1,80 ± 0.25	1,54 ± 0.28
0.9	0,74 ± 0.07	1,43 ± 0.20	1,70 ± 0.11	1,48 ± 0.23
1.0	0,24 ± 0.05	1,97 ± 0.06	1,46 ± 0.18	1,35 ± 0.15

**Table 26:** Variation of the Hardness Shore D (first lecture) as a function of (ABFA/SBC: 0.4/0.6) concentrations at various extrusion speeds

V (tr/min) ABFA (pcr)	20	30	40	50
0	68.00 ± 5.59	68,50 ± 3.29	62,87 ± 6.18	56,50 ± 3.80
10	65,25 ± 3.77	68,75 ± 2.65	65,27 ± 4.45	60,63 ± 6.63
20	64,26 ± 1.64	65,63 ± 2.88	56,75 ± 6.51	59,55 ± 2.70
30	65,78 ± 3.27	66,80 ± 3.26	62,57 ± 5.90	66,38 ± 4.38
40	67,43 ± 1.96	67,60 ± 2.55	61,93 ± 2.09	62,93 ± 2.14
50	67,43 ± 3.48	69,38 ± 1.36	63,88 ± 2.80	62,88 ± 2.59
60	68,08 ± 3.29	64,50 ± 1.72	68,25 ± 6.64	54,94 ± 1.67
70	57,13 ± 5.11	60,13 ± 5.19	63,18 ± 4.46	59,38 ± 3.68
80	64,15 ± 1.25	65,33 ± 5.27	61,50 ± 3.86	59,75 ± 5.50
90	72,58 ± 2.04	68,45 ± 1.77	64,68 ± 5.00	55,95 ± 3.40
100	75.00 ± 2.33	65,55 ± 4.13	63,88 ± 3.39	57,75 ± 1.70

**Table 27:** Variation of the Hardness Shore D (Second lecture) as a function of (ABFA/SBC: 0.4/0.6) concentrations

V (tr/min) ABFA (pcr)	20	30	40	50
0	64,75 ± 5.43	64,50 ± 2.90	59,75 ± 6.42	56,50 ± 2.51
10	64,75 ± 3.87	65,3 ± 2.34	60,63 ± 5.62	60,25 ± 5.56
20	61,88 ± 2.10	62,20 ± 2.75	54,13 ± 6.10	59,55 ± 2.82
30	62,25 ± 3.09	63,38 ± 2.87	59,68 ± 5.18	66,38 ± 4.22
40	64,38 ± 2.38	64,63 ± 1.55	59,25 ± 0.49	62,93 ± 2.02
50	64,50 ± 2.94	64,38 ± 3.79	60,63 ± 2.30	62,88 ± 2.40
60	65,13 ± 3.60	62,38 ± 1.36	66.00 ± 4.91	54,93 ± 1.34
70	54,25 ± 4.38	57,70 ± 3.71	62,75 ± 2.63	59,38 ± 3.48
80	60,38 ± 1.17	62,45 ± 4.79	58,48 ± 2.78	59,75 ± 4.51
90	68,63 ± 2.23	65,38 ± 1.96	62.00 ± 4.71	55,95 ± 2.81
100	72,13 ± 2.01	62,5 ± 3.35	61,88 ± 3.00	57,75 ± 1.46